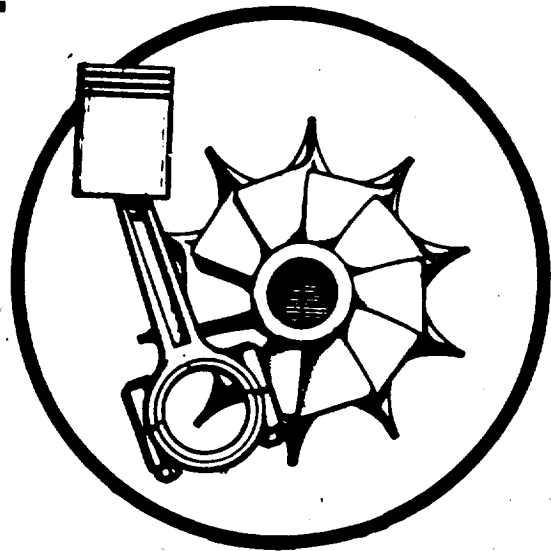


P-188-1  
AVSCOM-TR-87-C-30

NASA CR-180824

475128

# COMPOUND CYCLE ENGINE FOR HELICOPTER APPLICATION



ORIGINAL PAGE IS  
OF POOR QUALITY

Date for general release October 31, 1992



**GARRETT TURBINE ENGINE COMPANY**  
A DIVISION OF THE GARRETT CORPORATION  
PHOENIX, ARIZONA



**NASA**  
National  
Aeronautics and  
Space  
Administration

**FINAL REPORT**  
**CONTRACT NO. NAS3-24346**  
**21-5854-1**

Prepared For:  
National Aeronautics & Space Administration  
Lewis Research Center  
Cleveland, Ohio 44135

(NASA-CR-180824) COMPOUND CYCLE  
ENGINE FOR HELICOPTER APPLICATION  
Final Report (Garrett Turbine  
Engine Co.) 188 p

N93-10348

Unclass

63/07 0116856



|   |  |  |  |  |  |
|---|--|--|--|--|--|
| 1. Report No. AVSCOM TR-87-C-30<br>NASA CR-1808 24  |  | 2. Government Accession No.                          |  | 3. Recipient's Catalog No.                                 |  |
| 4. Title and Subtitle<br>Compound Cycle Engine for Helicopter Application   |  |  |  | 5. Report Date<br>09-30-87                                 |  |
|   |  |  |  | 6. Performing Organization Code                            |  |
| 7. Author(s)<br>Jere Castor, John Martin and Curtiss Bradley  |  |  |  | 8. Performing Organization Report No.<br>21-5854-1         |  |
| 9. Performing Organization Name and Address<br>Garrett Turbine Engine Co.<br>111 S. 34th Street<br>P.O. Box 5217<br>Phoenix, AZ 85010   |  |  |  | 10. Work Unit No.  |  |
|   |  |  |  | 11. Contract or Grant No.<br>NAS3-24346                    |  |
| 12. Sponsoring Agency Name and Address<br>U.S. Army Aviation Research & Technology Activity -<br>AVSCOM, Propulsion Directorate,<br>Lewis Research Center<br>Cleveland, OH 44135-3127   |  |  |  | 13. Type of Report and Period Covered<br>Contractor Report |  |
|   |  |  |  | 14. Sponsoring Agency Code<br>1L16110AH45                  |  |
| 15. Supplementary Notes<br>John Acurio, Program Manager - Propulsion Directorate<br>U.S. Army Aviation Research & Technology Activity - AVSCOM<br>William Wintucky, Project Manager<br>NASA Lewis Research Center, Cleveland, OH 44135  |  |  |  |  |  |
| 16. Abstract<br>The compound cycle engine (CCE) is a highly turbocharged, power-compounded, ultra-high-power-density, lightweight diesel engine. The turbomachinery is similar to a moderate-pressure-ratio, free-power-turbine gas turbine engine and the diesel core is high speed and a low compression ratio. This engine is considered a potential candidate for future military helicopter applications.<br><br>This final report presents cycle thermodynamic specific fuel consumption (SFC) and engine weight analyses performed to establish general engine operating parameters and configurations. An extensive performance and weight analysis based on a typical 2-hour helicopter (+30 minute reserve) mission determined final conceptual engine design. With this mission, CCE performance was compared to that of a contemporary gas turbine engine. The CCE had a 31 percent lower-fuel consumption and resulted in a 16 percent reduction in engine plus fuel and fuel tank weight. Design SFC of the CCE is 0.33 lb/hp-hr and installed wet weight is 0.43 lb/hp.<br><br>The major technology development areas required for the CCE are identified and briefly discussed. |  |  |  |  |  |
| Date for general release <u>October 31, 1992.</u>   |  |  |  |  |  |
| 17. Key Words (Suggested by Author(s))<br>Compound Cycle, Diesel, Turbine/Diesel,<br>Light-weight Diesel, High Performance Diesel,<br>Helicopter Engine, Low Heat Rejection Engine  |  |  |  | 18. Distribution Statement<br>See Above                    |  |
| 19. Security Classif. (of this report)<br>Unclassified  |  | 20. Security Classif. (of this page)<br>Unclassified |  | 21. No. of Pages<br>181                                    |  |
| 22. Price*  |  |  |  |  |  |

\_\_\_\_\_

## PREFACE

Recent studies by the U.S. Army have shown that fuel constitutes 70 percent of the tonnage required to supply and support its forces under battlefield conditions. The search for a more fuel efficient engine has led some investigators to the Compound Cycle Engine (CCE). The engine combines the airflow capacity and lightweight features of a gas turbine with the highly efficient but heavier diesel.

This report covers the thermodynamic cycle analysis, component arrangement, weight, and configuration layout of a CCE for a light helicopter application. The study was funded by the Army Aviation Systems Command (AVSCOM) and has been conducted jointly with NASA. This effort has been underway since mid-1984 with the Garrett Turbine Engine Company (GTEC), under Contract NAS3-24346.

These efforts have been conducted under the direction of:

John Acurio - AVSCOM

William Wintucky - NASA

Jere Castor - GTEC

The authors wish to acknowledge the valuable technical contribution of associates in the performance of the design studies by the following individual:

K.E. Boyd

C.E. Bradley

J.H. Brooks

Dr. R.T. Caldwell

L.G. Cruse

E.J. Eckelberg

I.G. Fowkes

T.A. Kincheloe

E.A. Mack

J.J. Martin

R.W. Rencenberger

J.R. Stoll

## TABLE OF CONTENTS

|  | <u>Page</u> |
|--|-------------|
| PREFACE  | iii         |
| 1.0 EXECUTIVE SUMMARY  | 1           |
| 1.1 Introduction   | 1           |
| 1.2 Helicopter Engine Configuration Study Results                  | 4           |
| 1.3 Selected Engine Configuration                                  | 9           |
| 1.4 Mission Comparison With Gas Turbines                           | 14          |
| 1.5 Altitude Performance   | 15          |
| 1.6 Major Technology Development Areas                             | 18          |
| 1.6.1 Piston Ring/Liner Interface Wear Life                        | 18          |
| 1.6.2 Exhaust Valve Life   | 19          |
| 1.6.3 Fuel Injection/Combustion                                    | 19          |
| 1.7 Mission Payoff Sensitivity                                     | 21          |
| 1.8 Conclusions  | 21          |
| 1.9 Recommendations  | 21          |
| 2.0 INTRODUCTION   | 23          |
| 2.1 Historical Background  | 25          |
| 2.1.1 Aircraft Diesel Engines                                      | 25          |
| 2.1.2 Aircraft Compound Cycle Engines                              | 27          |
| 2.2 Helicopter Engine Study Goals, Objectives,<br>and Requirements | 29          |
| 2.2.1 Engine Performance Goals                                     | 30          |
| 2.2.2 Engine Design Priorities                                     | 31          |
| 2.3 Study Techniques and Technologies                              | 32          |
| 2.3.1 Diesel Performance Model                                     | 32          |
| 2.3.2 Current Technology Turbomachinery                            | 38          |
| 2.3.3 CCE Performance Model  | 38          |
| 2.3.4 Cycle Boundary Conditions                                    | 40          |
| 2.3.5 Design Point Calculations                                    | 44          |
| 2.3.6 Weight Prediction  | 44          |
| 2.3.7 Off-Design Performance                                       | 51          |

## TABLE OF CONTENTS (Contd)

|  | <u>Page</u> |
|--|-------------|
| 3.0 CANDIDATE SCREENING AND SELECTION OF THE BEST CONFIGURATION          | 52          |
| 3.1 Candidate Engines and Selection Criteria                             | 52          |
| 3.2 Scavenging Arrangements  | 52          |
| 3.3 Candidate Compound Engines   | 55          |
| 3.4 CCE Selection  | 55          |
| 3.4.1 Selection of Engine Type   | 58          |
| 3.4.2 Turbomachinery Configuration Selection                             | 58          |
| 3.5 Other Thermodynamic Studies  | 63          |
| 3.6 Best Candidate Engine Selection                                      | 65          |
| 4.0 FURTHER DEFINITION AND OPTIMIZATION OF THE BEST CANDIDATE            | 67          |
| 4.1 The 1-1/2-Spool Uniflow Engine                                       | 67          |
| 4.2 Design-Point Performance   | 67          |
| 4.3 Part-Power Performance   | 78          |
| 4.4 Engine Flat Rating   | 78          |
| 4.5 Contingency and Emergency Power Requirements                         | 86          |
| 4.5.1 Power Increase by Fumigation                                       | 86          |
| 5.0 MISSION COMPARISON BETWEEN A COMPOUND CYCLE ENGINE AND A GAS TURBINE | 93          |
| 5.1 Gas Turbine Description  | 93          |
| 5.2 Results of Comparison  | 93          |
| 5.3 Infrared Signature   | 98          |
| 6.0 CONCEPTUAL ENGINE DESIGN   | 100         |
| 6.1 CCE Configuration  | 100         |
| 6.2 Conceptual Details and Materials                                     | 100         |
| 6.2.1 Diesel Core  | 100         |
| 6.2.2 Candidate High-Temperature Materials                               | 106         |
| 6.2.3 Turbomachinery   | 107         |
| 6.2.4 Gearbox  | 112         |
| 6.2.5 Engine Controls and Accessories                                    | 118         |
| 6.3 Operation With Failed Turbomachinery                                 | 125         |
| 7.0 CCE ENGINE SCALING   | 126         |

## TABLE OF CONTENTS (Contd)

|   | <u>Page</u> |
|---|-------------|
| 8.0 ENGINE LIFE AND MAJOR TECHNOLOGY DEVELOPMENTS | 129         |
| 8.1 Piston Ring/Liner Interface Wear Life         | 129         |
| 8.1.1 Piston Ring/Liner Geometries                | 129         |
| 8.1.2 Surface Topography                          | 130         |
| 8.1.3 Material Chemistry and Properties           | 130         |
| 8.1.4 Piston Velocity and Physical Speed          | 130         |
| 8.1.5 Oil Type and Film Thickness                 | 133         |
| 8.1.6 Operating Pressure and Temperature          | 133         |
| 8.1.7 Contamination                               | 135         |
| 8.1.8 Time Between Oil Changes                    | 138         |
| 8.2 Exhaust Valve Life                            | 139         |
| 8.3 Fuel Injection and Combustion Requirements    | 140         |
| 9.0 MISSION PAYOFF SENSITIVITIES                  | 143         |
| 9.1 Diesel Engine Speed                           | 143         |
| 9.2 Exhaust Gas Temperature                       | 145         |
| 9.3 Trapped Equivalence Ratio                     | 145         |
| 9.4 Mission Payoff Recapitulation                 | 147         |
| 10.0 CCE POTENTIALS BEYOND THE YEAR 2000          | 149         |
| 10.1 Assumptions Used in the Year-2000 Study      | 149         |
| 10.2 Year-2000 Mission Predictions                | 150         |
| 11.0 CONCLUSIONS AND RECOMMENDATIONS              | 152         |
| 11.1 Conclusions                                  | 152         |
| 11.2 Recommendations                              | 153         |
| APPENDIXES  |             |
| A - NAPIER NOMAD AIRCRAFT DIESEL ENGINE           |             |
| B - METRIC CONVERSION FACTORS                     |             |
| REFERENCES  |             |



# COMPOUND CYCLE ENGINE FOR HELICOPTER APPLICATION

## 1.0 EXECUTIVE SUMMARY

### 1.1 Introduction

This report presents the results of a study funded by the U.S. Army Aviation Systems Command (AVSCOM) on the subject of compound cycle engines for helicopter applications. This effort, conducted jointly with NASA and under contract with the Garrett Turbine Engine Company (GTEC), has been underway since mid-1984 (Contract NAS3-24346).

As shown in Figure 1, a compound cycle engine (CCE) combines the airflow capacity and lightweight features of a gas turbine with the highly efficient but heavier diesel. The compressor of the gas turbine module delivers high-pressure air to the diesel core, where further compression takes place in the cylinders (as with a conventional reciprocating compressor). Fuel is introduced and burned at very high pressure and temperature, and power is extracted in the downstroke of the diesel piston. With its remaining energy, the discharge gas is then ducted to turbines that drive the compressor and also augment the output of the diesel core. Therefore, the term compound cycle is an expression used to describe the process where excess power is extracted from the turbomachinery and compounded through gearing to add to the output of the diesel core.

Recent studies by the Army have revealed that fuel constitutes 70 percent of the tonnage required to supply and support its forces under battlefield conditions. Other preliminary studies by AVSCOM supported by Compound Cycle Turbofan Engine

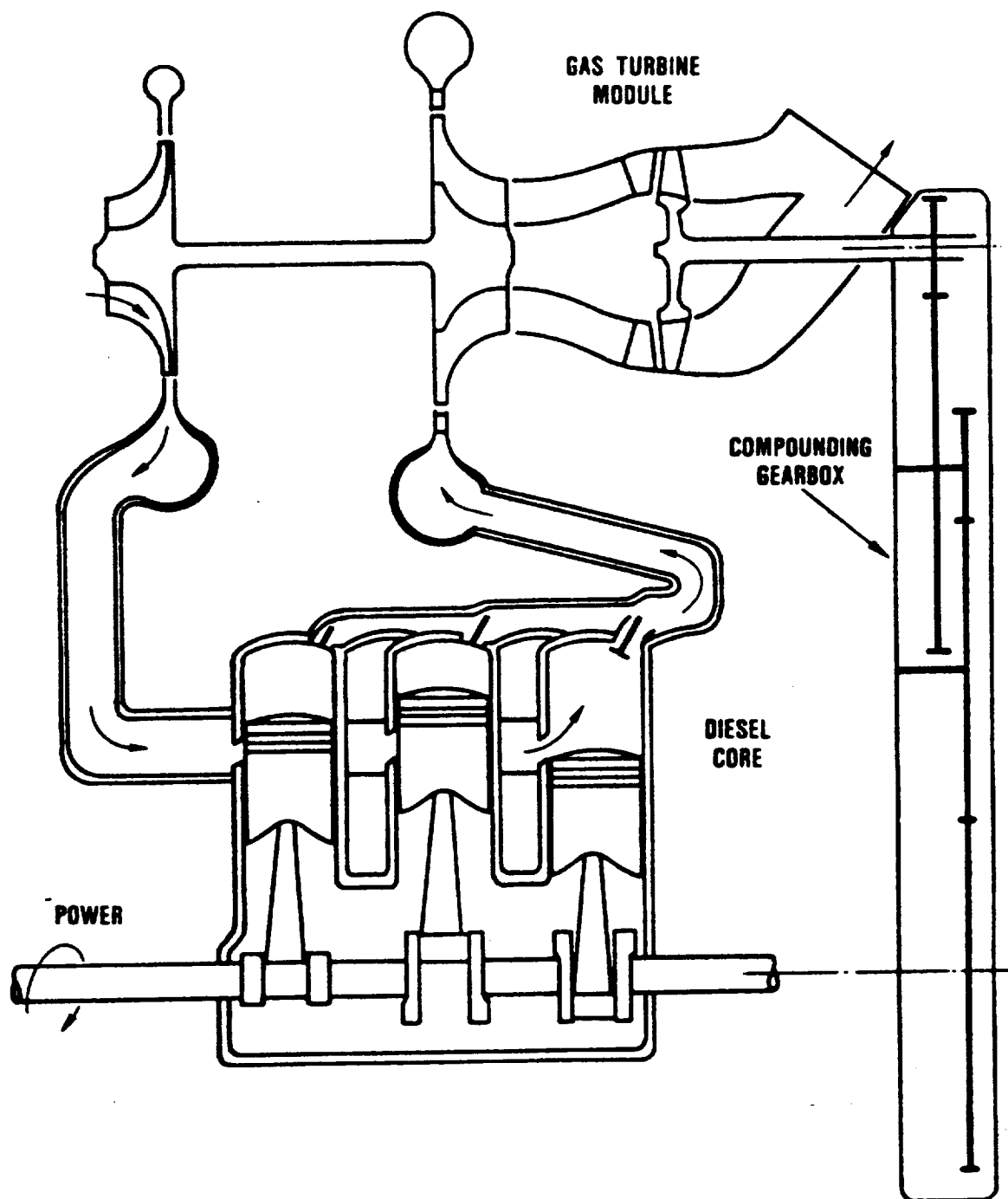


Figure 1. Arrangment of CCE.

(CCTE) information obtained under Defense Advanced Research Project Agency (DARPA)/U.S. Air Force \Contract F33657-77-C-0391, indicated that a 40 percent fuel savings potential exists for compound-cycle-engine-powered helicopters. A 23 percent reduction in required engine power (installed) was also estimated for the same mission when compared with a contemporary simple-cycle gas turbine. This reduction in required power was translated into a smaller helicopter for the same payload and mission.<sup>1</sup>

Earlier estimates that used the Blackhawk helicopter, showed that the allowable specific weight of a CCE could be as high as 0.76 lb/hp and still be competitive with the gas turbine because of the large fuel savings. The computation was based on the allowable engine weight increase that would offset reduced fuel and tank weight, so that the take-off gross weight of the helicopter remained the same.<sup>2</sup>

The most fuel-efficient aircraft engine ever flown (1952) was the Napier Nomad (3000+ horsepower) compound cycle engine.<sup>3</sup> The Nomad's operating conditions were:

|   |                               |                |
|---|-------------------------------|----------------|
| o | Shaft Horsepower              | 3000+ shp      |
| o | Diesel Core Speed             | 2050 rpm       |
| o | Compressor Pressure Ratio     | 6.5:1          |
| o | Diesel Inlet Air Temperature  | 475F           |
| o | Diesel Compression Ratio      | 8:1            |
| o | Fuel Injection Pressure       | 15,000 psi     |
| o | Maximum Firing Pressure       | 2200 psi       |
| o | Brake Mean Effective Pressure | 205 psi        |
| o | Equivalence Ratio             | 0.65           |
| o | Diesel Exhaust Temperature    | 1250F          |
| o | Specific Weight               | 1.0 lb/hp      |
| o | BSFC                          | 0.345 lb/hp-hr |

During the 1950s, all development effort was directed toward gas turbines. Therefore, the Nomad never reached full-scale production, but represented the pinnacle of diesel aircraft engine technology. Applying today's technologies and designs to the Nomad, could result in an engine having a specific weight under 0.60 lb/hp.

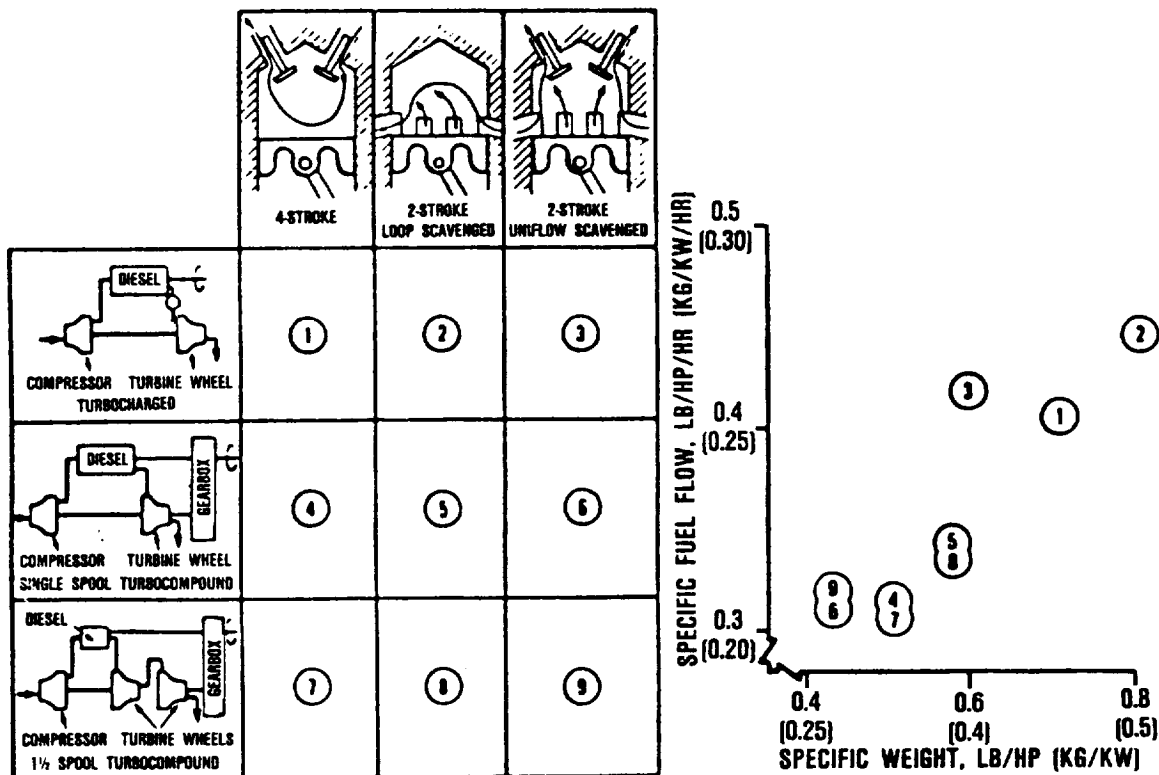
Based on preliminary studies and the significant advancements in technology demonstrated under the GTEC/Air Force CCE program,<sup>4,5</sup> the Army undertook a detailed engine analysis for a light helicopter application to establish CCE parameters that would best meet overall program objectives of fuel savings and system payoffs.

This summary presents an overview of the thermodynamic cycle analysis, component arrangement, weight, and configuration layout. CCE payoffs are compared with a contemporary gas turbine for a typical 2-hour (30+ minute reserve) mission. In addition, major technology development areas are identified and discussed.

## **1.2 Helicopter Engine Configuration Study Results**

As shown in Figure 2, nine different diesel-turbine combinations were investigated during the initial screening phase of the study. The factors considered in making the selection were SFC, engine weight, and aircraft mission range/payload.

The objective was to identify the combination that would provide a maximum saving in mission fuel with the lightest-weight engine, so as to achieve a maximum gain in range payload for the vehicle. Turbocharged diesels (Designs 1, 2, and 3 on Figure 2) were eliminated early, because their fuel consumption and weights were not competitive. Another general conclusion is that 4-stroke diesels Designs 4 and 7 will be much heavier than their



67-004-20

**Figure 2. Nine Configurations Design Point (1000 HP) Diesel/Turbine Thermodynamic (SFC) and Weight Analysis.**

2-stroke counterparts 6 and 9, but their fuel efficiency, although best, was not significantly better than a 2-stroke design. A third conclusion is that a 2-stroke, uniflow-scavenged Designs 6 and 9 is much more efficient and lighter than a loop-scavenged Designs 5 and 8. Therefore, Designs 6 and 9 were carried into the next step of the studies.

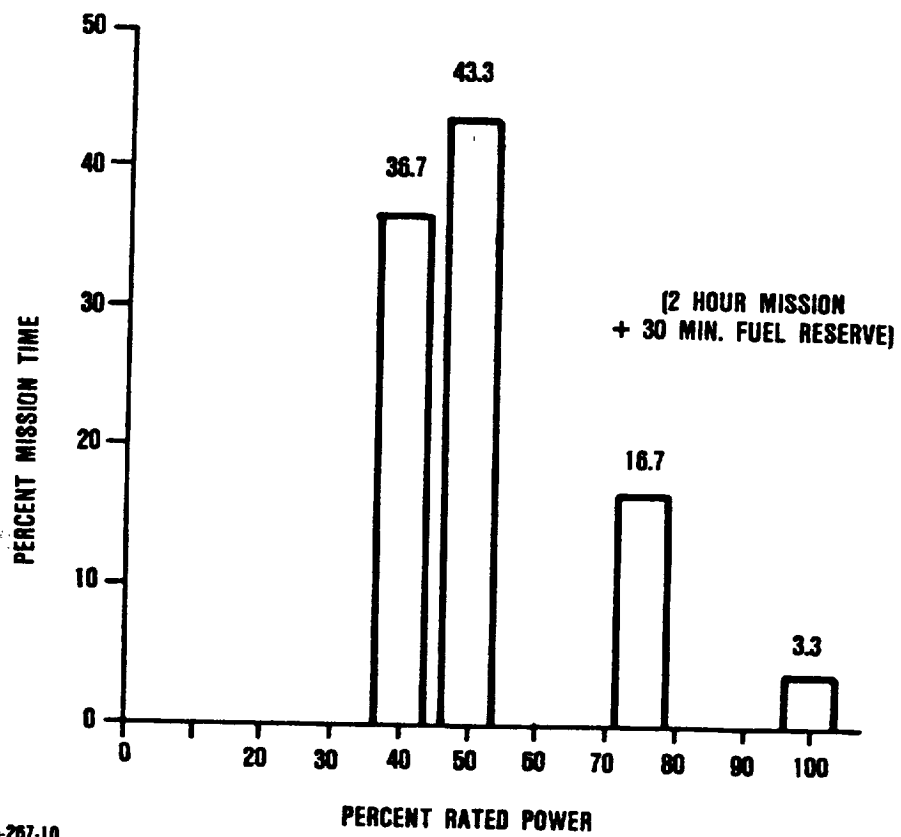
In the final analysis, the choice between Designs 6 and 9 was based on considerations other than operation at full design power. The added turbine stage in Design 9 provided the needed flexibility to avoid variable geometry in the turbomachinery or variable ratio gearing to match the speeds of the diesel and turbine modules. Therefore, this 1-1/2 spool module arrangement offered a better gain in fuel consumption in the 50 percent power range where most of the mission is flown. The mission-power profile used to estimate the magnitude of the gains is shown in Figure 3.

The resulting comparison of SFC as a function of shaft power for Designs 6 and 9 is shown in Figure 4.

As reflected in Figure 2, installed engine weights include:

- o Diesel core
- o Basic CCE engine
- o Installation items

Previous methods for estimating internal combustion engine core weights were considered inadequate for this study. To develop an approach, five key engine design parameters (bore, stroke, number of cylinders, speed, and maximum firing pressure) were identified and their sensitivities quantified. Sensitivities were derived by least squares regression analysis of data from 21 different turbocharged or supercharged reciprocating air-



65-267-10

Figure 3. Mission Power/Time Profile.

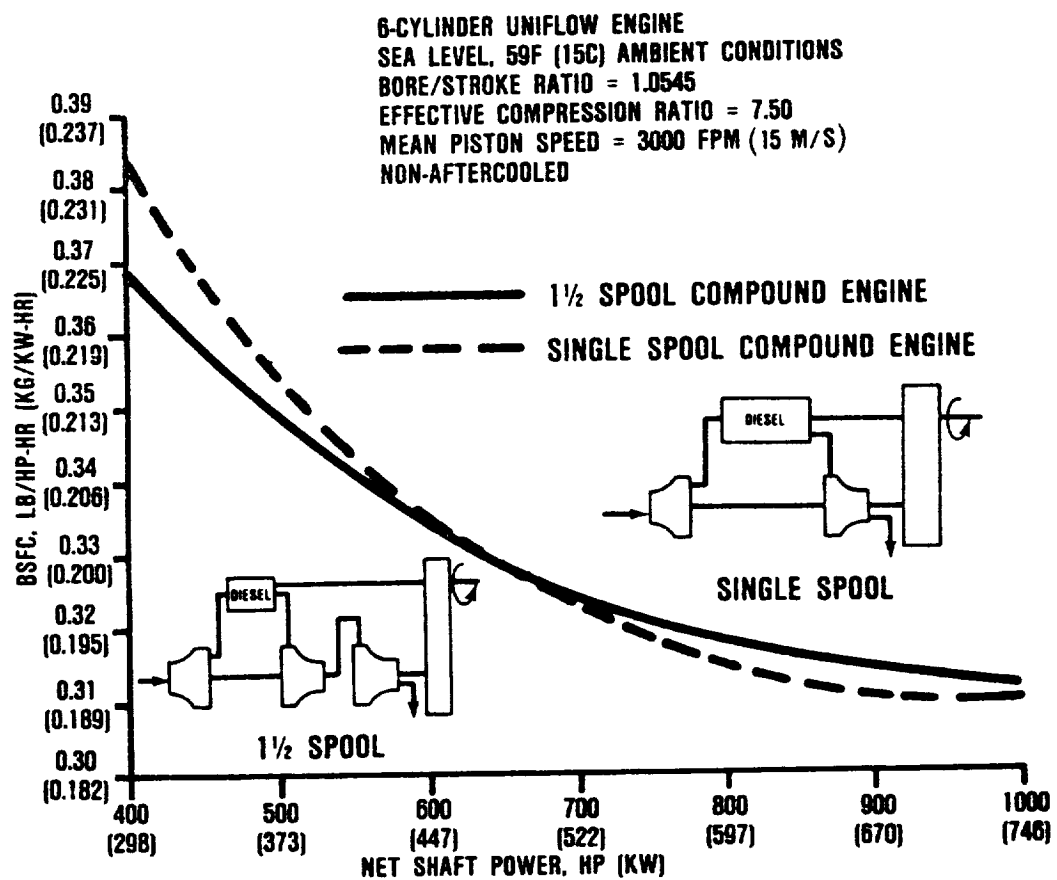


Figure 4. SFC as a Function of Power.



craft engines. All weight estimates for the remaining items were based on data available from NASA and GTEC.

The resulting weight equation is shown in Figure 5.

### 1.3 Selected Engine Configuration

Parametric design point and off-design trade offs were conducted to evaluate the effects of cycle variants, such as cylinder compression ratio, compressor pressure ratio, aftercooler effectiveness, and pressure drop across the cylinder. These trade offs resulted in a 1-1/2 spool, aftercooled, 2-stroke uniflow scavenged CCE, with a thermodynamic cycle as shown in Figure 6.

An aftercooler was introduced to reduce cylinder inlet air temperature, so as to reduce combustion, ring reversal, and exhaust valve temperatures. Addition of the aftercooler and its weight was offset by reduced cylinder size and a lighter diesel core because of higher charge air density. More importantly, it will enhance engine life. However, a small SFC increase (0.02 lb/hp-hr) (12gm/kw-hr) will be incurred.

The best SFC and engine weight balance was found to exist at high compressor pressure ratios (over 10). The diesel core effective compression ratio was limited to 7.5 in order to keep peak firing pressure below 3400 psia (234 bar), which was considered a safe limit. A diesel flow pressure drop of 10 percent across the cylinder achieved the best compromise between overall cycle efficiency and weight.

Core design parameters are shown in Table 1. The established rpm and  $P_{max}$  levels were reduced from those demonstrated during the CCTE program, primarily to enhance life. The design

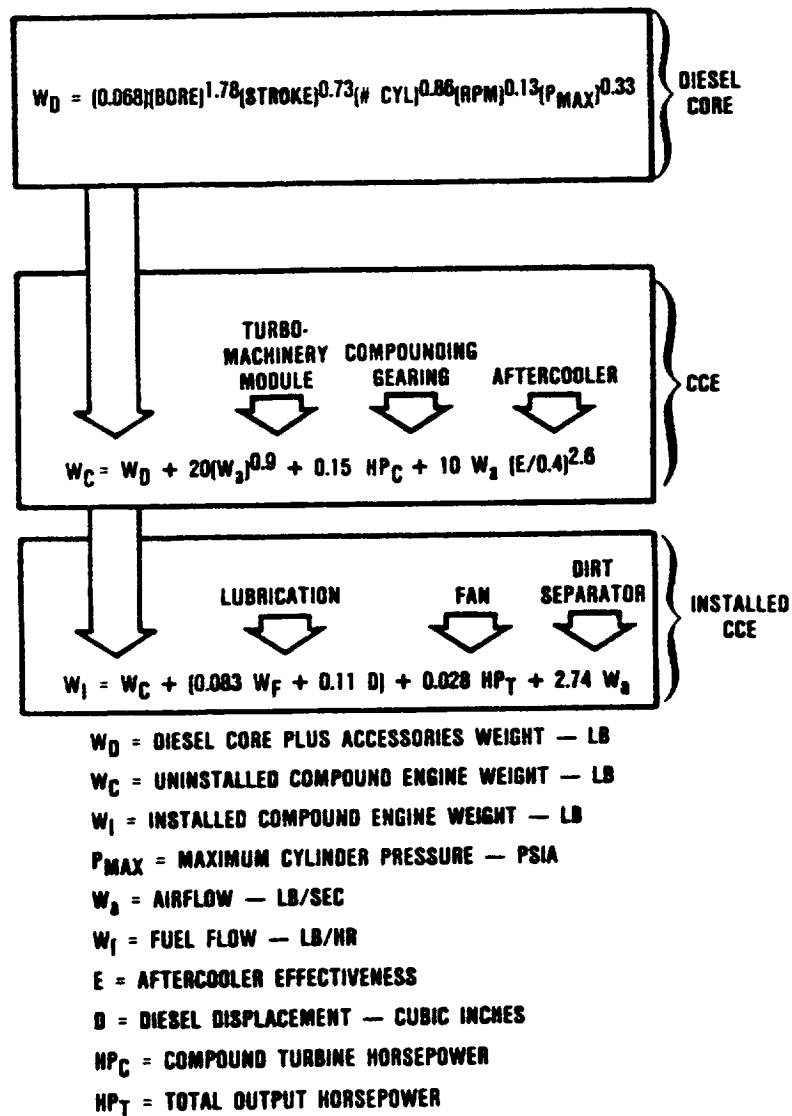


Figure 5. Engine Weight Functions.

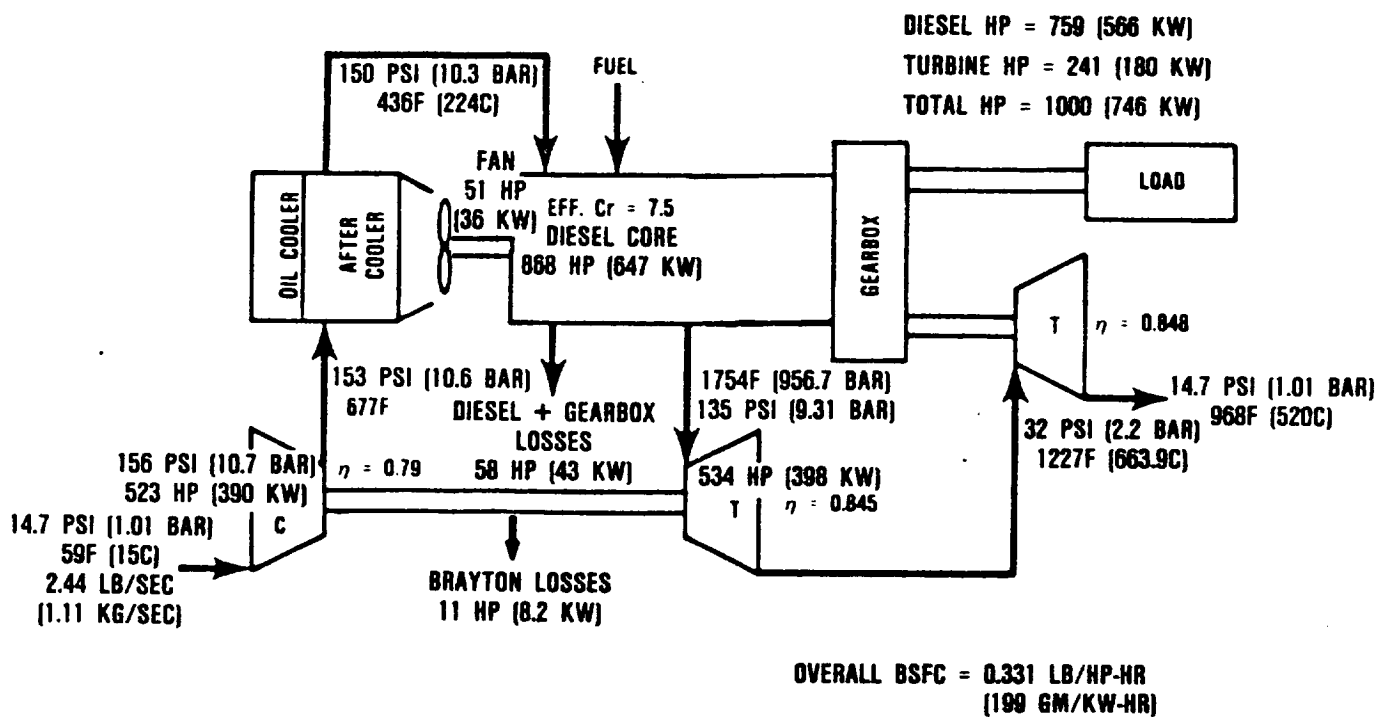


Figure 6. Sea-Level, Standard Day, Design Point Operating Conditions of Selected 1-1/2 Spool CCE.

Table 1. Diesel Core Description.

|  |                    |
|--|--------------------|
| o Engine, rpm  | 6122               |
| o Airflow Rate, lb/sec (kg/sec)<br>at 6122 rpm         | 2.44 (1.11 kg/sec) |
| o Bore, in. (cm)                                       | 3.10 (7.87)        |
| o Stroke, in. (cm)                                     | 2.95 (7.47)        |
| o Number of Cylinders                                  | 6                  |
| o Displacement, in <sup>3</sup> (liters)               | 133.2 (2.2)        |
| o Equivalence Ratio                                    | 0.68               |
| o Peak Firing Pressure,<br>P <sub>max</sub> psia (bar) | 3362 (231.9)       |
| o Effective Compression Ratio                          | 7.5                |
| o BMEP, psi (bar)                                      | 393 (27.1)         |

point equivalence ratio\* of 0.68 was selected because it is an industry-accepted value for nonvisible smoke. A six cylinder configuration was chosen for simplicity.

A conceptual design layout of the selected CCE is shown in Figure 7. The figure shows two major modules, i.e., turbomachinery and diesel core. The turbomachinery module is similar to the more familiar turboshaft engine. It has a typical gas generator spool with a two-stage, backward-curved, broad-range, high-pressure ratio centrifugal compressor, driven by a single-stage, radial-inflow turbine. The half-spool axial power turbine is geared into the compounding gearbox. The turbomachinery is mounted into the V-form of the diesel core so as to minimize overall box volumes to less than 14 cubic feet (0.39 m<sup>3</sup>), including oil cooler and aftercooler. The 2-stroke diesel module has six cylinders, is uniflow scavenged, and has four exhaust valves

---


$$\text{*Equivalence Ratio} = \frac{\text{Actual Fuel/Air Ratio}}{\text{Stoich Fuel/Air Ratio}}$$

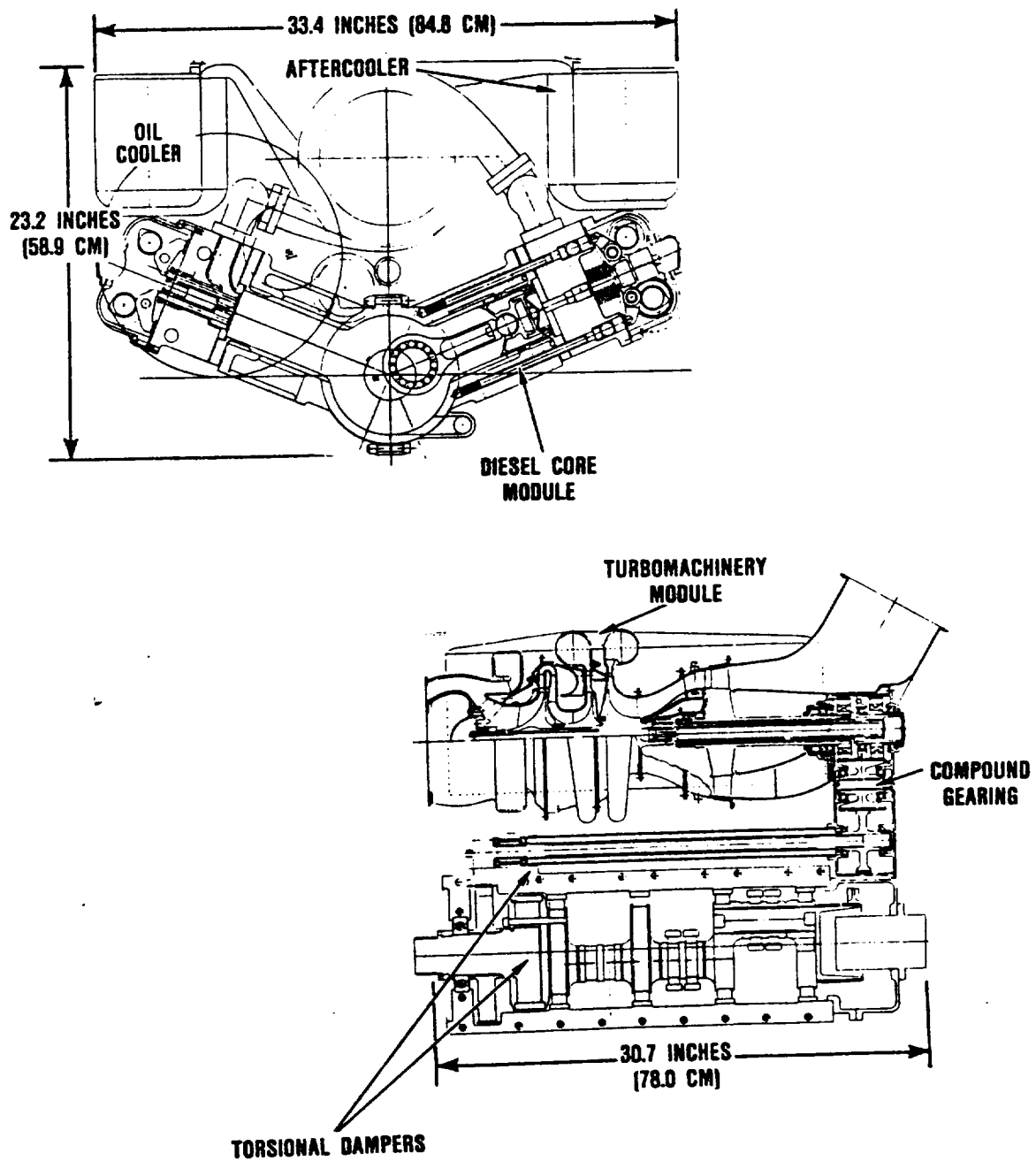


Figure 7. Conceptual Design of 1-1/2 Spool, CCE.

per cylinder that are activated with overhead cams. Fuel injectors are located centrally in the cylinder heads. A low heat loss combustion chamber with thermally isolated and preferentially cooled cylinder liner/head and piston dome are used. The engine is oil cooled and fully self-contained with all engine required-to-run controls and accessories. Total installed weight including oil, oil cooler, fan, and inlet air particle separator is 432 pounds (196 kg) for a specific weight of 0.43 lb/hp (0.15 kg/kw).

#### 1.4 Mission Comparison with Gas Turbines

The CCE configuration selected for this study resulted from an analysis of many engine design and performance parameters to minimize the sum of engine plus fuel weight for the mission. This engine meets the major study objectives of at least a 30 percent savings in fuel.

The mission used in preliminary design is the Army's standard of 2 hours plus 30 minutes fuel reserve and is typical for a twin-engine light helicopter. The mission is flown at 4000 feet (1.22 km) on a 95F (35C) day, and the engine is designed to be flat-rated at 1000 shp (746 kW) to the hot-day, altitude conditions. For comparison, the simple-cycle gas turbine was sized for 1400 shp at sea-level, standard day so that it could produce the same 1000 horsepower (746 kW) at 4000 feet, 95F (1.22 km, 35C).

On the other hand, flat rating of the CCE is accomplished by increasing the turbocompressor spool speed 4 percent and increasing the trapped equivalence ratio from 0.68 to 0.80 for the short duration of rated-power conditions at 4000 ft, 95F (1.22 km, 35C).

The results of the mission comparison study are shown in Table 2. Total fuel, tank, and engine weights have been calculated under static operating conditions for a twin-engine application. These results show a potential for:

- o 31.4 percent fuel consumption savings
- o 15.8 percent engine plus fuel weight savings
- o 8.5 percent engine plus fuel volume savings
- o One-third more missions for a given quantity of fuel

These savings may also be translated into more range or more payload for the same gross-weight vehicles:

- o 36.5 percent increase in payload, or
- o 40.7 percent increase in range

### 1.5 Altitude Performance

Shaft horsepower and SFC as a function of altitude, for the selected CCE are shown in Figure 8 for hot, standard, and cold-day conditions. Flat rating at 1000 shp (746 kW) for the various conditions is achieved by allowing the equivalence ratio to increase to a value of 0.80. This condition is reached at 4,000, 7,000, and 9,600 feet (1.22, 2.31, 2.91 km) for hot, standard, and cold days respectively. The cold-day SFC curve below 9,600 feet is affected by changes in fuel injection timing and trapped air equivalence ratio. On a standard day, engine operation at  $\theta = 0.68$  is about equal to the hot-day performance at  $\theta = 0.80$ .

Table 2. CCE/GAS Turbine Weight Comparison at 4000 Feet,  
95F, (1.22 km, 35C) Static Conditions.\*\*\*

|                                 |             | CCE                          |                          | Gas Turbine                  |                          |
|---------------------------------|-------------|------------------------------|--------------------------|------------------------------|--------------------------|
| Percent Power                   | Time, hours | BSFC, lb/hp-hr<br>(Kg/kw-hr) | Weight Fuel, lbs<br>(Kg) | BSFC, lb/hp-hr<br>(Kg/kw-hr) | Weight Fuel, lbs<br>(Kg) |
| 100                             | 0.08        | 0.342<br>(0.208)             | 28.6<br>(13.0)           | 0.457<br>(0.278)             | 38.1<br>(17.3)           |
| 75                              | 0.42        | 0.349<br>(0.212)             | 109.2<br>(49.6)          | 0.490<br>(0.298)             | 153.3<br>(69.6)          |
| 50                              | 0.58        | 0.377<br>(0.229)             | 110.0<br>(49.9)          | 0.553<br>(0.336)             | 161.5<br>(73.3)          |
| 40                              | 0.92        | 0.400<br>(0.243)             | 146.1<br>(66.3)          | 0.603<br>(0.367)             | 221.4<br>(100.5)         |
| 50 (reserve)                    | <u>0.50</u> | 0.377<br>(0.229)             | <u>94.3</u><br>(42.8)    | 0.553<br>(0.336)             | <u>138.5</u><br>(62.9)   |
| Totals                          | 2.50        |                              | **488.7<br>(221.6)       |                              | **712.8<br>(323.6)       |
| Fuel =                          |             |                              | 488.7<br>(221.6)         | 712.8<br>(323.6)             |                          |
| Fuel Tank Weight =              |             |                              | 83.0<br>(37.7)           | 121.1<br>(55.0)              |                          |
| Installed Engine Weight =       |             |                              | 432.4<br>(196.3)         | 358.0<br>(162.5)             |                          |
| Total: Fuel, Tank, and Engine = |             |                              | * 1004.1<br>(455.6)      | *1191.9<br>(541.1)           |                          |
| For Two Engines =               |             |                              | 2008.3<br>(911.8)        | 2383.9<br>(1082.3)           |                          |

\*Percent Weight Savings:  $1.0 - \frac{\text{CCE Total Weight}}{\text{Gas Turbine Weight}} = 15.8$

\*\*Percent Fuel Savings:  $1.0 - \frac{\text{CCE Total Fuel Weight}}{\text{Gas Turbine Fuel Weight}} = 31.4$

\*\*\*Reference Figure 3 Mission Power/Time Profile



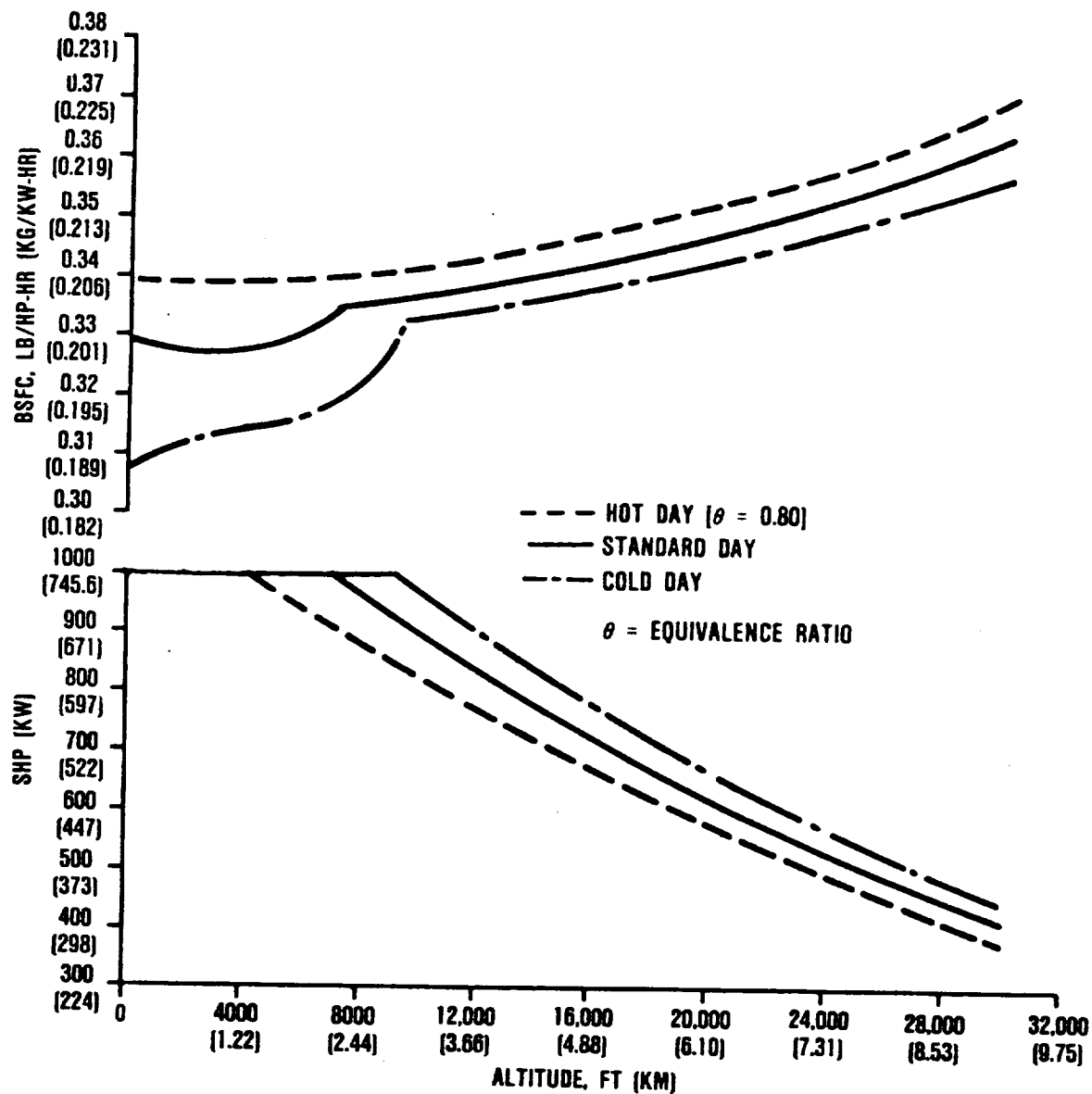


Figure 8. SHP and BSFC Performance of CCE Versus Altitude.

## 1.6 Major Technology Development Areas

The turbomachinery module consists of state-of-the-art technology components. The diesel core configuration follows somewhat conventional design practices for 2-stroke engines, but the cycle pressure, temperatures, and speeds are somewhat higher and therefore, beyond today's demonstrated diesel engine technologies.

Three major technology development areas have been identified for the diesel core. They are in order of considered importance:

- o Piston ring/liner interface wear life
- o Exhaust valve life
- o Fuel injection with high-heat-release combustion

### 1.6.1 Piston Ring/Liner Interface Wear Life

Because a main objective is long engine life, the first development challenge or life-limiting factor of most concern is the wear rate of the piston ring/liner interface materials. Factors that influence wear are:

- o Piston velocity and engine speed
- o Piston ring/liner geometries
- o Surface topography
- o Material chemistry and properties
- o Oil film type and thickness
- o Operating pressures and temperatures
- o Contamination - foreign and self-generated

- o Lubricant type and additives
- o Time between oil changes

Complex interactions between the different factors make it difficult to quantify overall effects on engine life. However, the qualitative effects are well understood. A great deal of experience is available on low-power-density diesel engines, but it is quite limited in its extension into the design regions of the CCE discussed. Total system (single cylinder) testing under controlled-environment conditions using best lubricant formulations and tribological couples is necessary to establish a technology baseline for CCE wear-life predictions.

#### 1.6.2 Exhaust Valve Life

The exhaust valve life is the second most important item for CCE development. Exhaust gas valve temperature at full power on a hot day is several hundred degrees hotter than current engines. High temperature creep and fatigue resistant materials that also have high oxidation corrosion resistance will be required. Means to thermally isolate, insulate, and preferentially cool the valves and seats will be required.

#### 1.6.3 Fuel Injection/Combustion

Fuel injection with high-heat-release combustion is considered to be the third area for development. The primary requirement for the fuel injection equipment for a direct-injected diesel is to distribute a uniform, finely atomized charge of fuel throughout the combustion chamber, at the right time and in the right quantity. If not, excessive peak cylinder pressure could occur, exhaust smoke would increase, and engine life could be shortened. High speed requires high injection pressures for increased heat-release-rate combustion. A high-

pressure [ $>20,000$  psi (1380 bar)], electronically controlled hydromechanical type fuel injection system is considered the prime candidate.

### 1.7 Mission Payoff Sensitivity

Figure 9 shows projected improvements over a contemporary gas turbine in engine SFC (mission fuel weight), and range or payload as a function of diesel core speed. As diesel core rpm is increased, the required technology levels in the three major development areas are also increased for the improved performance.

An engine based on application of current technologies could provide a 20 percent savings in mission fuel. However, its weight would be unacceptable. Near-term (moderate) development could produce 25 percent fuel savings at an acceptable engine weight, but with no gain in range or payload. However, with an aggressive concentrated thrust, the selected CCE offers a 31.4 percent savings in fuel and about a 40 percent improvement in range or payload for the same vehicle gross weight. It should be again noted that the CCTE engine was run at 8000 rpm, under the Air Force/DARPA program and that the targeted speed for the CCE is well under that value.

### 1.8 Conclusions

Based on the standard two-hour design mission for helicopters, the compound cycle engine offers significant payoffs when compared with a contemporary gas turbine:

- o 31 percent less fuel consumption
- o 36 percent more payload (or 42 percent more range)
- o One-third more missions per unit fuel

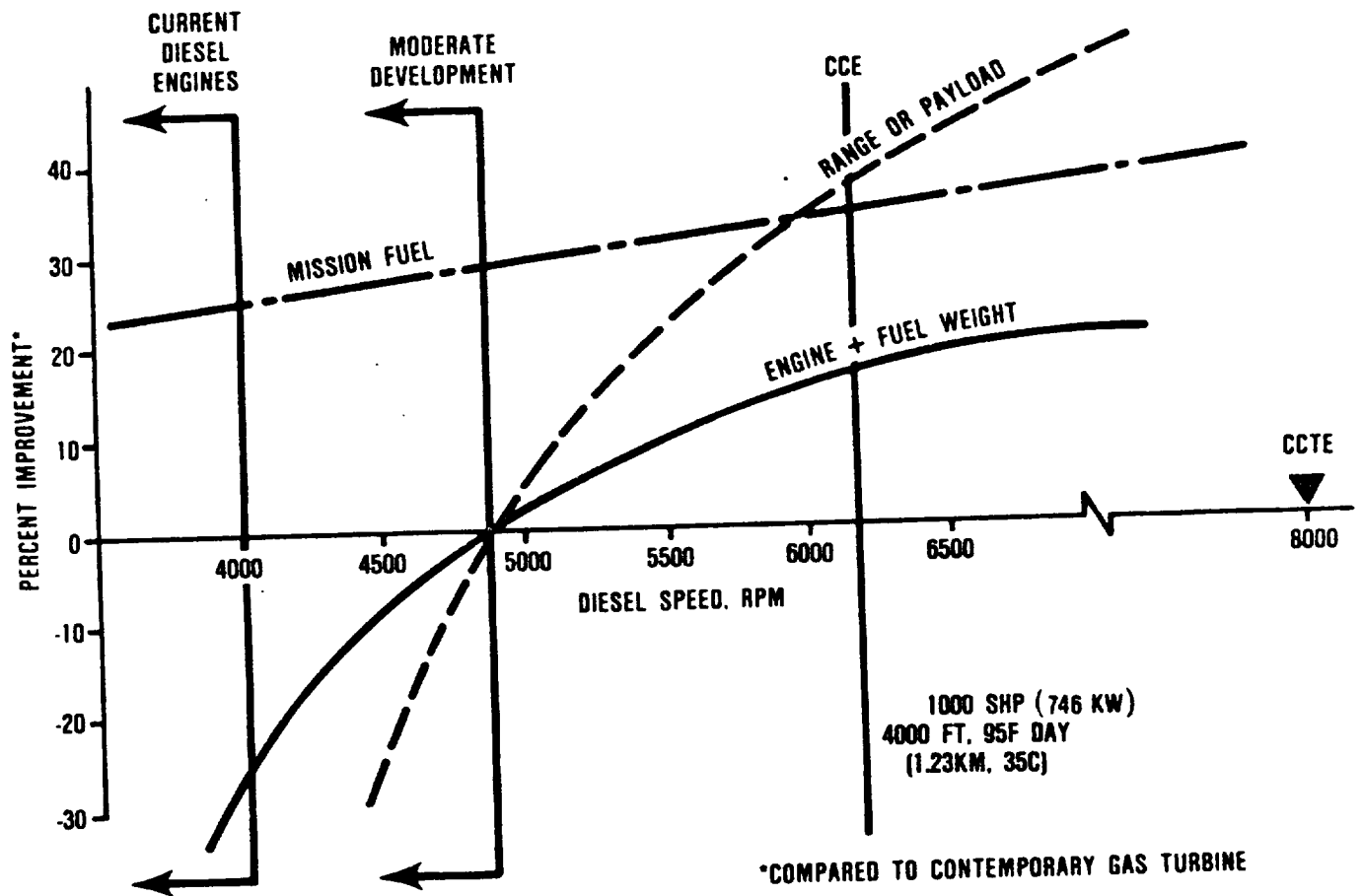


Figure 9. Potential Improvements As a Function of Diesel Engine Speed.

For longer missions, the CCE payoffs increase, which is consistent with the savings in fuel consumption.

## 1.9 Recommendations

Because the potential mission payoffs are so significant, it is recommended that the following activities be pursued vigorously:

### o Piston Ring/Liner Interface Wear Life

Expand lubricant formulation, advance tribology and uniflow scavenged single cylinder R&D activities currently underway on the ADEPT program.

### o Exhaust Valve Life

Demonstrate high-power-density, uniflow scavenged performance, and evaluate alternate valving schemes.

### o Fuel Injection/Combustion

Expand the fuel injector/combustion effort started under CCTE on electronically-controlled, hydromechanical injectors.

### o Overall CCE

To demonstrate the overall viability of the diesel core, tests should be performed on a multicylinder engine/rig to confirm integration of technologies, core performance, and life and weight prediction methodologies.

## 2.0 INTRODUCTION

This report presents the results of a Compound Cycle Engine (CCE) study for a helicopter application. The work was conducted with AVSCOM funds under Contract NAS3-24346 from NASA-Lewis Research Center. This contract continued some of the work begun in late 1977 for the design and development of a Compound Cycle Turbofan Engine (CCTE) conducted under DARPA funding and USAF Contract F33657-77-C-0391.<sup>6</sup>

The Army is being restructured for greater mobility over extended battlefields and, therefore, must operate in areas where the supporting infrastructure could be limited or nonexistent. Recent studies by the Army have revealed that fuel constitutes 70 percent of the tonnage required to supply and support its rapid deployment forces under battlefield conditions. These conditions mandate the need for reliable, fuel-efficient, and lightweight engines to increase the range-payload product of volume-limited vehicles.

The purpose of this study was to characterize and determine the potential of a 1000-shp (746 kW), CCE engine for a helicopter application that is competitive with a contemporary gas turbine engine on a 2-hour mission with a 30 minute reserve.

A CCE (Figure 10) combines the airflow capacity and lightweight features of a gas turbine with the highly efficient but heavier diesel. The compressor of the gas turbine module delivers high-pressure air to the diesel core where further compression takes place in the cylinders (as with a conventional reciprocating compressor). Fuel is introduced and burned at very high pressure and temperature, and power is extracted in the downstroke of the diesel piston. The discharged gas, with its

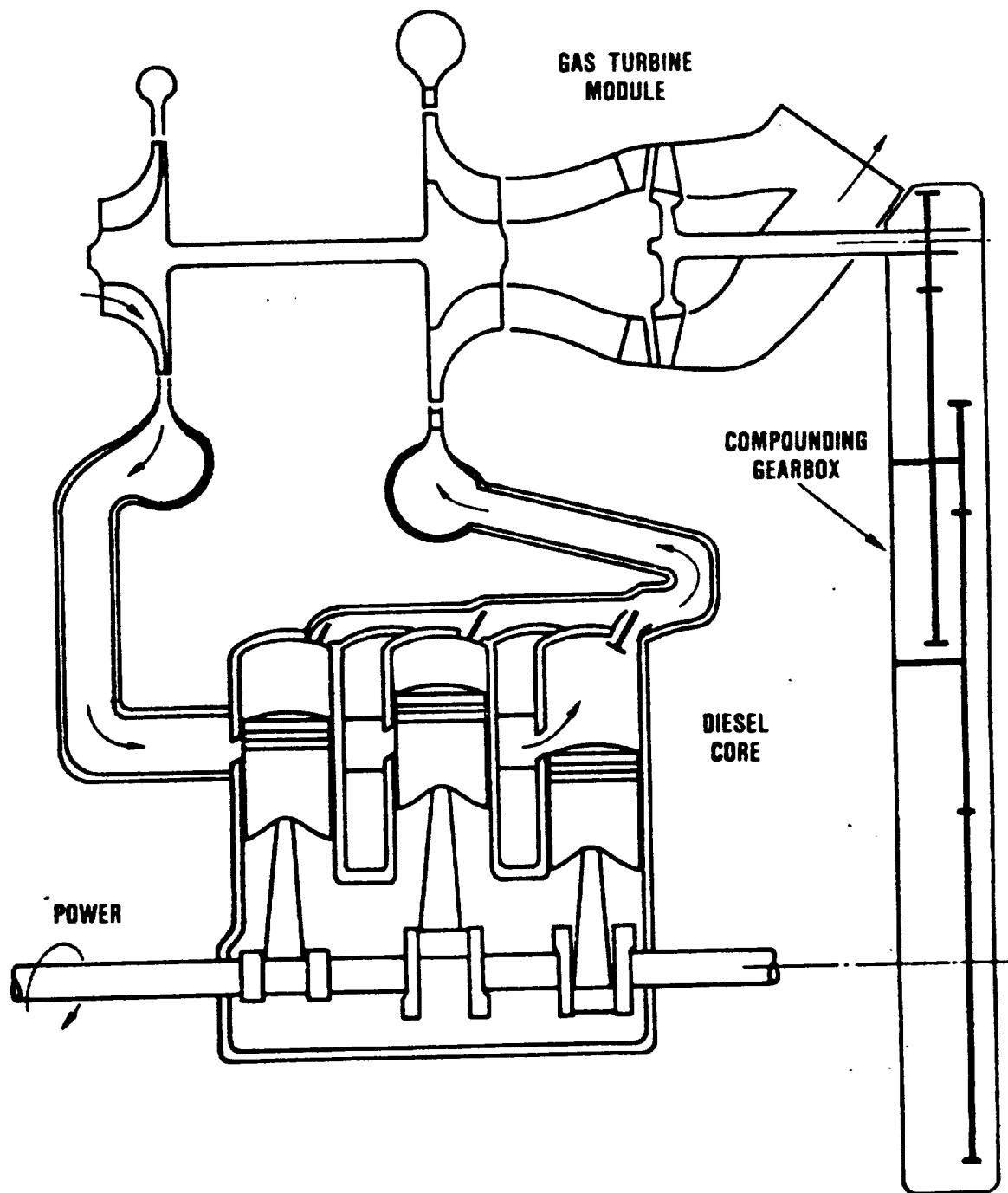


Figure 10. Arrangement of CCE.



remaining energy, is then ducted to turbines that drive the compressor but also augment the output of the diesel core. Therefore, the term compound cycle is an expression used to describe the process where excess power is extracted from the turbomachinery and compounded through gearing to add to the output of the diesel core.

## 2.1 Historical Background

### 2.1.1 Aircraft Diesel Engines

Over the past 50 years, there have been a series of diesel engines made for aircraft applications. For proper perspective of this current study, a survey of these previous engines is shown in the Table 3. Some observations can be made from a review of these engines.

The Junkers 200<sup>7</sup> series diesel engines started out as a fairly lightweight ( $1.0 \text{ lb/in}^3$  [ $27.67 \text{ kg/l}$ ]) design, based on gasoline engine structure. The power was low (700 hp [ $522 \text{ kW}$ ]) and the specific weight was therefore quite high ( $1.44 \text{ lb/hp}$  [ $0.876 \text{ kg/kW}$ ]). This engine was used in some commercial aircraft because its cruise brake specific fuel consumption (BSFC) was two-thirds that of contemporary gasoline engines. The engine was redesigned and weight increased from 1144 pounds ( $518.9 \text{ kg}$ ) to 1903 pounds ( $863.2 \text{ kg}$ ) as seen for the 1943 vintage turbocharged engine. The final version of this engine (1945)<sup>8</sup> was series supercharged/turbocharged and had a specific weight of  $0.95 \text{ lb/hp}$  ( $0.578 \text{ kg/kW}$ ), which was comparable to contemporary gasoline engines. This drastic reduction in specific weight was made possible because of the high (for that time) supercharging pressure of 43.5 psia (3.0 bar), which provided a brake mean effective pressure (BMEP) of 225 psi (15.5 bar) for the engine. The BSFC was  $0.330 \text{ lb/hp-hr}$  ( $198 \text{ gm/kW-hr}$ ) at takeoff power and 0.336 at

Table 3. Aircraft Engines.

| Engine                                | Displacement<br>in <sup>3</sup> (l) | Weight<br>lb,<br>kg | Takeoff<br>BHP at rpm,<br>kW at rpm     | Specific<br>Weight<br>lb/hp<br>kg/kW | Specific<br>Power<br>HP/in <sup>3</sup><br>kW/l | Takeoff<br>BMEP<br>psi<br>bar | Cruise<br>BSFC<br>lb/hp-hr,<br>kg/kW-hr | Remarks                   |
|---------------------------------------|-------------------------------------|---------------------|---|--------------------------------------|---|-------------------------------|---|---------------------------|
| Wankers<br>105 (1939)                 | 1024<br>(16.8)                      | 1144<br>(518.9)     | 700 at 2600<br>(522 at 2600)            | 1.44<br>(0.876)                      | 0.69<br>(31.4)                                  | 105<br>(7.2)                  | 0.336<br>(202)                          | Centrifugal compressor    |
| Wankers<br>107 (1943)                 | 1024<br>(16.8)                      | 1903<br>(863.2)     | 1000 at 3000<br>(745.7 at 3000)         | 1.90<br>(1.16)                       | 0.99<br>(45.0)                                  | 130<br>(9.0)                  | 0.336<br>(202)                          | Early design turbocharger |
| Wankers<br>107 (1945)                 | 1124<br>(18.4)                      | 1903<br>(863.2)     | 2000 at 3200<br>(1491 at 3200)          | 0.95<br>(0.578)                      | 2.14<br>(97.3)                                  | 210<br>(14.5)                 | 0.336<br>(202)                          | Improved turbocharger     |
| HD<br>12710                           | 3142<br>(51.5)                      | 3190<br>(1447)      | 2700 at 2700<br>(2013 at 2700)          | 1.18<br>(0.718)                      | 0.86<br>(39.1)                                  | 126<br>(8.7)                  | 0.350<br>(210)                          | Turbocharged              |
| Capier<br>11040                       | 2502<br>(41.0)                      | 3580<br>(1624)      | 3046 at 2050<br>(2271 at 2050)          | 1.18<br>(0.718)                      | 1.22<br>(55.5)                                  | 204<br>(14.1)                 | 0.340<br>(204)                          | Turbocompound             |
| Illison*<br>1-1710                    | 1710<br>(28.0)                      | 1950<br>(884.5)     | 2050 at 3200<br>(1529 at 3200)          | 1.14<br>(0.693)                      | 1.20<br>(54.6)                                  | 304<br>(21.0)                 | 0.45<br>(270)                           | Turbocompound             |
| Curtis<br>Bright*<br>R-3350           | 3350<br>(54.9)                      | 3675<br>(1667)      | 3600 at 2900<br>(2685 at 2900)          | 1.02<br>(0.620)                      | 1.07<br>(48.7)                                  | 252<br>(19.4)                 | 0.38<br>(228)                           | Turbocompound             |
| Holls<br>Royce*<br>Grey<br>(2-stroke) | 1169<br>(19.2)                      | 1800<br>(816.5)     | 4000 at 4000<br>(est)<br>(3132 at 4000) | 0.43<br>(0.262)                      | 3.43<br>(156.0)                                 | 338<br>(25.0)                 | 0.42<br>(252)                           | Turbocompound             |

\*Gasoline

26,000-feet (7.92-km) altitude. Some applications operated at 40,000-feet (12.19-km) altitude with a BSFC of 0.375 lb/hp-hr (225 gm/kW-hr).

The German KHD DZ-710<sup>9</sup> World War II diesel aircraft engine, was a loop-scavenged, 2-stroke cycle of 16 cylinder horizontally opposed construction. The early development engines were supercharged to produce 2300 hp (1715 kW) at 2700 rpm and weighed 2600 pounds (1180 kg). Toward the end of the war, these engines had been redesigned with a turbosupercharger flowing into a gear-driven centrifugal compressor and then into the engine. The overall weight increased to 3190 pounds (1447 kg) (1.02 lb/in<sup>3</sup> [28.2 kg/l]) with a take-off rating of 2700 brake horsepower (bhp) (2013 kW) at 2700 rpm (0.86 hp/in<sup>3</sup> [39.1 kW/l]), which was close to that of contemporary gasoline engines<sup>10</sup>.

For their time, these engines had BSFCs that were 25 to 35 percent less than that of contemporary gasoline engines, but there was a considerable weight penalty because of the nonavailability of high-performance turbochargers. The diesel engine service life time between overhaul (TBO) was equivalent to, or longer than, that of the gasoline engines of that period (300 hours for transport service).

#### 2.1.2 Aircraft Compound Cycle Engines

The CCE for aircraft use was investigated at NACA and the Allison Division of GMC during World War II. An Allison V-1710<sup>11</sup> engine was modified to be mechanically supercharged through two compressors in series, and have the exhaust gases ducted through a bottoming turbine that was geared to the engine. This arrangement was somewhat complex, but tests made in an altitude chamber showed a reduction in fuel consumption of 21 percent and a power increase of 36 percent for cruise condition at 25,000 feet (7.62

km) altitude. The combination of the war's end and the great interest in turboprop engines brought this development program to an end in 1945.

Another turbocompound engine was the Curtiss-Wright R-3350<sup>12</sup>, which was the only one to be in production for both military and commercial applications over a 10-year period. Turbocompounding of this engine was started in 1946. It was mechanically supercharged through two series compressors. Power recovery was achieved with three blow-down turbines geared to the crankshaft through fluid couplings. Commercial versions of this engine had a 20 percent increase in takeoff power over that of the standard engine and, at cruise, a reduction in BSFC of up to 21 percent. The military versions of this engine produced up to 3600 bhp (2685 kW), 33 percent over that of the standard, non-compounded engine.

Rolls-Royce and others did a study during World War II concerning 2-stroke cycle, sleeve valve, gasoline aircraft engines, which used several forms of turbocompounding.<sup>13</sup> The "Crecy" by Rolls-Royce had been tested both as a single-cylinder and a 12-cylinder engine. The performance was remarkable. In 1944 it had a power density of 3 bhp/in<sup>3</sup> (136.5 kW/l), when at the time the norm was only 1 bhp/in<sup>3</sup> (45.5 kW/l). Computed performance at 25,000-feet (7.6-km) altitude and cruise conditions showed a 26-percent reduction in BSFC over that of a comparable 4-stroke cycle, supercharged engine. Again, the advent of the turbine and turboprop engines after World War II ended all research on these reciprocating engines.

The most famous experimental aircraft diesel compounded engine was the Napier "Nomad" of the 1950 to 1954 period. Several technical papers<sup>14,15</sup> have been written on this engine, which is described in Appendix A. This engine, which was

designed for the long-range transport aircraft business, showed impressive (as much as 35 percent) reductions in direct operating cost (DOC) over the same aircraft equipped with a turboprop engine for a 4000-mile (2486-km) stage distance. The Nomad was a 2-stroke cycle, loop-scavenged engine that had a 12-stage axial compressor, a three-stage axial turbine, and an infinitely variable speed drive between the engine and its turbomachinery. The specific weight was between 1.18 and 0.93 pounds per equivalent horsepower (0.718 and 0.566 kg/kW), depending on the extent of power augmentation through water injection and auxiliary combustion. These values were comparable to those of spark ignition engines at that time, and the BSFC was up to 24 percent lower than that of supercharged engines and 15 percent lower than the turbocompounded Curtiss Wright R-3350 engine. The 10 to 20 cents-per-gallon fuel available in the 1950s, coupled with the desire to fly faster, brought this innovative venture to an early end.

## 2.2 Helicopter Engine Study Goals, Objectives, and Requirements

The goal of this investigation was to identify a 2000-hour MTBO CCE design that could be scaled over the 500 to 2000 hp (373 to 1491 kW) range. For this study, the nominal engine rated power (sea-level, standard day) was set at 1000 hp (746 kW), which is compatible with a future twin engine light helicopter application.

The major objectives of this study were:

- o Identify and configure an engine that has the potential for 30 to 40 percent savings in mission fuel when compared with a contemporary gas turbine engine

- o Minimize overall system weight (engine plus fuel) to increase mission range-payload product
- o Determine diesel core and turbomachinery operating parameters commensurate with performance and weight
- o Identify major diesel core technology development areas for required 2000-hour initial MTBO

The following engine configurations and factors were evaluated in the study:

- o 2-stroke versus 4-stroke
- o Loop and uniflow scavenge systems
- o Turbocharging and turbocompounding
- o Aftercooled and nonaftercooled
- o Cylinder arrangement
- o Fuel injection
- o Insulated components
- o Lubrication
- o Power augmentation or boosting
- o Engine starting
- o Engine operation without its turbocharger

#### 2.2.1 Engine Performance Goals

It was necessary to establish those preliminary performance goals that would define the boundaries of this study.

They were:

- o Nominal replacement for a gas turbine
- o Engine operating life: 2000 hours MTBO

- o Rated net engine power: 1000 hp (746 kW) (sea level, standard day), scalable from 500 to 2000 hp (373 to 1491 kW)
- o Engine specific weight: less than 0.6 lb/hp (0.447 kg/kW)
- o Rated engine speed: approximately 6000 rpm
- o Rated engine piston speed: approximately 3000 ft/min (15 m/sec)
- o Engine configuration specific fuel consumption (SFC): approximately 0.3 lb/hp-hr (0.182 kg/kW-hr) at cruise conditions
- o Power boost investigations: up to 140 percent
- o Specific power: approximately 5 hp/in<sup>3</sup> (227.5 kW/l) displacement

### 2.2.2 Engine Design Priorities

The study was based on the following list of technical requirements shown in order of priority:

- (1) Performance
- (2) Fuel economy
- (3) Specific weight
- (4) Volume
- (5) Reliability and durability
- (6) Fuel tolerance
- (7) Maintainability

Reliability and durability (Item 5) is further defined to require a MTBO life of 2000 hours.

## 2.3 Study Techniques and Technologies

This investigation was based on "all metal" engines, i.e., no monolithic ceramics or composites are required to achieve these performances. However, certain diesel core metallic components (cylinder heads, pistons, and valves) have been designed with thermal barrier coatings (TBC) or insulators in order to reduce overall heat transfer and decrease metal temperatures.

### 2.3.1 Diesel Performance Model

Diesel core engine performance was generated with a modified version of the Benson Mark 12 computer program from the University of Manchester Institute of Science and Technology. The Mark 12 program assumes instant and complete mixing of cylinder contents during gas exchange and a homogenous condition during compression, combustion, and expansion. The computation is initiated by making an assumption of trapped pressure and temperature prior to compression. Indicated work and heat loss are calculated in a step-wise manner using one-degree crank angle increments during the power stroke and user-defined step size during gas exchange. Required program inputs include:

- (1) Cycle designation (2- or 4-stroke)
- (2) Crankshaft speed
- (3) Inlet and exhaust pressure
- (4) Inlet air temperature
- (5) Nominal compression ratio
- (6) Bore, stroke, and connecting rod length
- (7) Port and/or valve timing



- (8) Mean cycle temperature of cylinder head, piston dome, and cylinder liner.
- (9) Fuel injection rate per cylinder per cycle
- (10) Start of combustion
- (11) Heat transfer constants
- (12) Heat release schedule
- (13) Fuel lower heating value and carbon fraction
- (14) Port and/or valve area schedule with crank angle

The parent Mark 12 program required additional input data that defines dimensions and layout for multicylinder engines. The model was designed for exhaust tuning analysis and as a consequence, required the assumption of a constant mean exhaust gas heat capacity (specific heat) in the calculations. Use of the multicylinder model along with the CCE study would have required excessive computer time and, hence, led to the development at GTEC of a single-cylinder model that uses constant intake and exhaust manifold pressures.

The resulting performance does not include possible exhaust pulse energy recovery which if included at the high-pressure ratios used, is not considered to be a significant contributor to performance. Therefore, the performance predicted may be slightly understated by the omission of any pulse energy potential.

The step-wise diesel cylinder calculations were repeated for a few cycles until all variables agreed closely with their respective values at the same crank angle from the preceding cycle. Convergence was obtained quickly when manifold pressures remain constant.

The fuel heat release schedule is an important factor in determining the engine output and thermal efficiency. The one

used in the Benson program was obtained from AVL,\* an internationally known combustion engine research and design firm, for the CCTE program, funded by DARPA in 1977-1981. As shown in Figure 11, this predicted schedule was found to provide good agreement with the actual data obtained on the CCTE engine at comparable speeds and power outputs.

The heat-release duration was assumed to vary linearly with trapped equivalence ratio at constant engine speed. The heat release model in the computer program could be readily adjusted to accommodate future test data and to improve the correlation between predicted and actual engine performances. For consistency, the AVL combustion model was used in all CCE calculations.

The basic Benson Model 12 computer program used a constant heat capacity (specific heat) term, which caused errors and discontinuities in the calculated exhaust gas temperature. GTEC modified the program to incorporate the more realistic variable heat capacity expression, which then predicts exhaust gas temperatures more accurately.

Another parameter that greatly influences the output and efficiency of 2-stroke cycle diesel engines is "scavenge efficiency." This also impacts the correlation between predicted and actual engine performance data. Scavenge efficiency is defined as the mass of fresh charge trapped, divided by the total mass of charge trapped in the cylinder. Schweitzer<sup>16</sup> and others have developed the following expression for perfect mixing scavenge efficiency:

---

\*AVL Prof. List GmbH, Graz, Austria

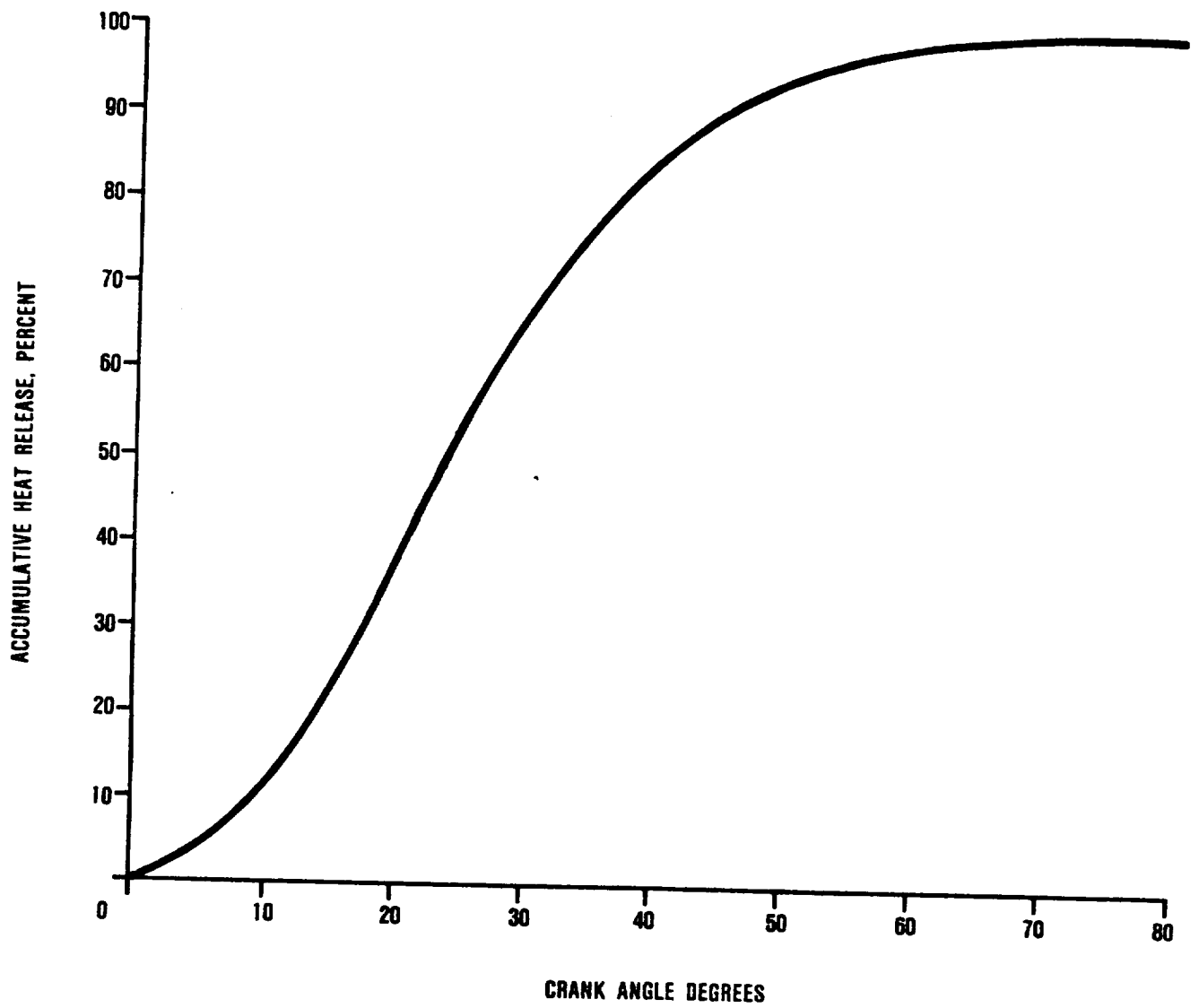


Figure 11. AVL Heat Release Schedule.

$$\eta_s = 1 - e^{-R_s}$$

where:  $\eta_s$  is scavenge efficiency

"e" is the natural logarithm (2.718)

$R_s$  is the mass of air delivered to the cylinder, divided by the total mass of air filling the swept volume at inlet density

This equation is based on the assumptions that the piston remains at bottom center during scavenging, and that the cylinder pressure is equal to the exhaust pressure during the scavenging process.

Neither of these assumptions apply rigorously to the Benson diesel model. In fact, the model predicts somewhat higher scavenge efficiencies, which are in close agreement with test data for loop-scavenged engines. The original Benson program tended to underpredict scavenge efficiency for uniflow cylinders because of the assumed gas mixing process. Recent increased charging efficiency data for uniflow engines reported in SAE Paper 850317<sup>17</sup> is plotted in Figure 12 for comparison with the unmodified Benson simulation. Charging efficiency is defined as the mass of air trapped at port closure divided by the total mass of air contained in the swept volume at inlet density. The trapped mass was determined experimentally by gas sampling techniques. The scavenge ratio was altered mathematically in the program by varying either crankshaft speed or cylinder pressure drop. The DDAD charging efficiency data is about 10 percent higher than the computed efficiency throughout the entire range of scavenge ratios. All uniflow engine runs were subsequently made with a scavenge efficiency multiplier to obtain better agreement with experimental measurements.

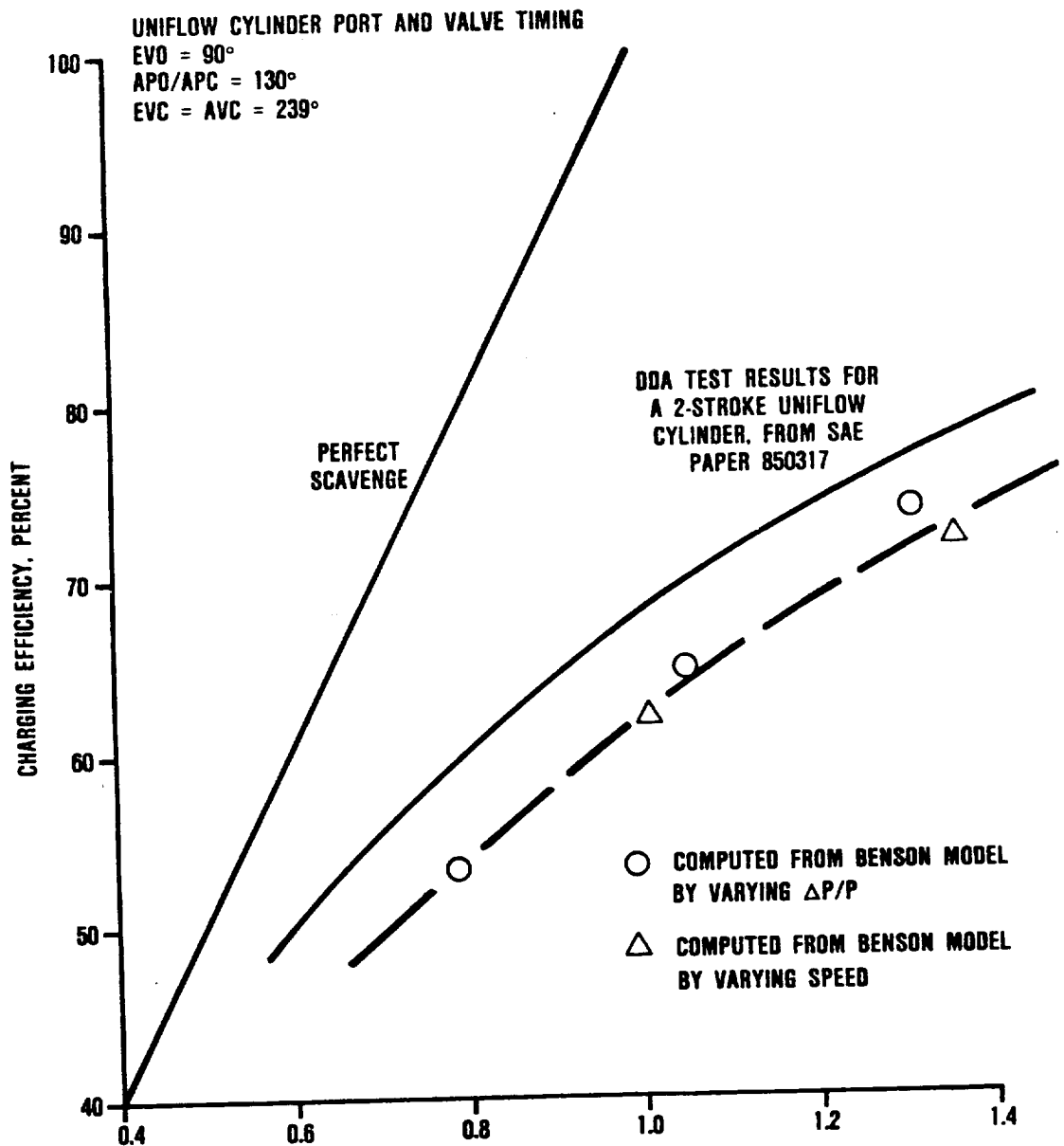


Figure 12. Effect of Scavenge Ratio on Uniflow Engine Charging Efficiency.

The heat lost during the cycle also has a large effect on the computed power and thermal efficiency of the engine. It also provides a measure of the correlation between predicted and actual performance. The Benson program requires cylinder wall, piston dome, and combustion chamber mean cycle temperatures as inputs so that cycle heat losses can be determined. Heat transfer across these boundaries is determined by the Annand<sup>18</sup> heat transfer model. A fundamental part of this investigation was the design of a low heat loss (LHL) engine, so the increased exhaust energy could be recovered in the turbomachinery for increased thermal efficiency. The nominal heat loss chosen for this study was 6 percent of the fuel input, (which is a very low value) based on data obtained from an engine of approximately the same size and speed.

A major factor in determining the power output and efficiency of the theoretical engine is the trapped equivalence ratio. This is defined as the ratio of the actual fuel-to-air ratio inside the cylinder, divided by the stoichiometric (chemically correct) fuel-to-air ratio.

### **2.3.2 Current Technology Turbomachinery**

A proprietary GTEC gas turbine computer program was employed for the study, while compressor and turbine performance maps were selected from state-of-the-art turbomachinery components.

### **2.3.3 CCE Performance Model**

The GTEC general purpose turbomachinery performance model and the Benson Mark 12 cycle analysis programs were combined, and an aftercooler subroutine added. The program logic is shown in Figure 13. The main program searched for match-point solutions

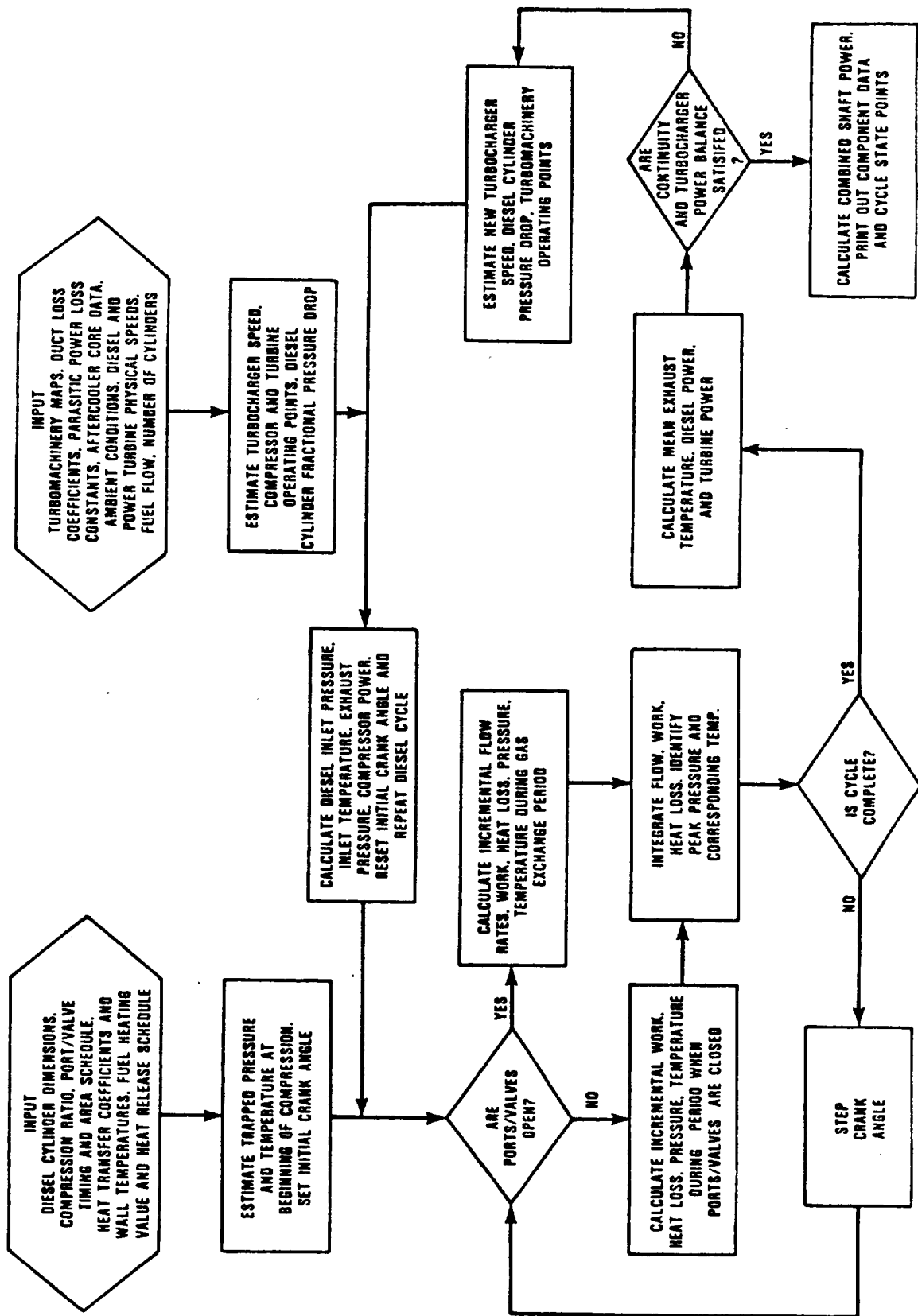


Figure 13. CCE Performance Model Flow Chart.

that satisfy conservation of energy and continuity. Additional provisions were made for variable geometry on the turbomachinery.

#### 2.3.4 Cycle Boundary Conditions

Cycle boundary conditions were specified in order to reduce the number of engine permutations and possibilities. The following nominal boundary conditions and reasons for their selection are shown in the following:

- o Piston velocity, maximum ft/min: 3000 (15.2 m/sec)

The maximum piston velocity of 3000 ft/min (15.2 m/sec) was selected because the friction mean effective pressure (FMEP) increases rapidly with piston speed and this adversely affects mechanical efficiency and BSFC. The 3000 ft/min (15.2 m/sec) value is a compromise between high specific output and the required engine life and thermal efficiency. World War II aircraft engines were designed to obtain maximum power at 3000 ft/min (15.2 m/sec).

The CCTE engine was rated at 4000 ft/min (20.2 m/sec) because weight was more critical than in the helicopter application and the mission life was relatively short, (five hours) so that the high piston speed was not critical.

- o Engine speed, approximate rpm: 6000

The combination of engine speed and piston velocity helps to establish the engine stroke, size, and weight, thereby optimizing these parameters and with high BMEP result in a high specific output engine. In addition,



higher rotation speeds tend to increase piston ring/liner wear and cause problems with fuel injection systems because of the short cycle times available for it to function.

The helicopter engine speed was reduced to the 6000 rpm arena rather than employing the 8000 rpm speed of the CCTE.

- o Peak firing pressure, maximum psi: 3500 (241 bar)

The firing pressure has a strong influence on engine weight because of the mechanical loads on the structure and power producing components. However, the thermal efficiency and specific power benefit from higher firing pressure. Therefore, more compromises were made.

- o Trapped equivalence ratio at sea level, static: 0.4 to 0.7

The usual range of equivalence ratio at full load for commercial engines is 0.4 to 0.7 with the upper limit for smoke-free operation being 0.68 for nonfumigated engines.<sup>19</sup> The trapped equivalence ratio strongly influences the in-cylinder mean gas temperature, combustion efficiency, and heat transfer so that practical limit compromises again were made.

- o Bore/stroke ratio: 0.9 to 1.10

Most commercial diesel engines operate between this range for reasons of engine weight, height, and thermal efficiency. A too low bore/stroke ratio ( $<0.8$ ) adversely

effects the heat transfer (surface/volume ratio) and air available for combustion.

- o Connecting rod length/stroke ratio: 2.4:1

The connecting rod angularity relationship imposes a side thrust on the piston, which tends to increase the FMEP and likelihood of scuffing. The l/r ratio of 2.4:1 is a compromise between engine height, weight, and acceptable friction forces and represents good engine design practice.

- o Bore size, inches: 2.5 to 4.5 (6.3 to 11.4 cm)

Bore sizes smaller than 2 inches (5.1 cm) are usually not employed because of high heat transfer, poorer thermal efficiency, and usually greater friction (20). The bore range of 2.5 to 4.5 inches (6.3 to 11.4 cm) provides engine speeds between 4000 and 6800 rpm, which is compatible with the boundary conditions of piston and rotation speed.

- o Boost pressure ratio: 7 to 11:1

GTEC has considerable experience in this range of compressor pressure ratios because of its TPE331 turbo-shaft engine. Higher boost pressure ratios result in greater specific output (shp/in<sup>3</sup>) and lighter specific weight (lb/shp) engines. However, a compromise must be reached because of the limit set peak for firing pressure 3500 psi (241 bar) which is accomplished via the route of adjusting the boost pressures and the cylinder compression ratios.

- o Compression ratio: 6 to 10:1

Along with boost pressure ratio, the compression ratio is used to control the peak firing pressure and reach compromises with thermal efficiency and ease of starting. The range of 6 to 10:1 compression ratio is compatible with the selected boost pressure ratios, so that optimum engine weight and BSFC are attained.

- o Aftercooler effectiveness: 35 to 80 percent

This range of aftercooler effectiveness is found in commercial engine installations and results from studies interrelating, after cooler size, weight, plus engine efficiency and life.

- o Number of cylinders: 4 to 12

This range of cylinder numbers is typical of commercial engines and permits compromises between low specific weight and volume, tolerable vibration levels, costs of manufacture and maintenance, life expectancy, and overall shape of the engine package.

- o Engine output (rated, design point, shp): 1000 (745.7 kW)

The engine requirement for this helicopter application is 1000 shp (745.7 kW), flat rated from sea-level, standard day to 4000 feet 95F (1.2 km, 35C) day, both cases being static.

### 2.3.5 Design Point Calculations

For a CCE design-point calculation, the computer program determined the required number of diesel cylinders for a specified power output when bore, stroke, and crankshaft speed were specified. Another design option allowed the user to fix the number of cylinders, as well as the bore/stroke ratio and mean piston speed. In the latter case, cylinder dimensions and crankshaft speed were calculated. Diesel core pressure drop, aftercooler effectiveness, and aftercooler pressure drop also were specified for a design-point run. Engine installed weight (including the aftercooler) was computed and displayed in the output, along with aftercooler dimensions. Either trapped equivalence or fuel flow per cylinder may be designated.

Diesel engine friction horsepower was computed in a subroutine containing a relationship between friction mean effective pressure (MEP) and mean piston speed, based on engine survey data. The cooling fan is driven by the diesel engine at a fixed gear ratio and was independent of load. For these cycle calculations, the aftercooler was located upstream from the oil cooler in the cooling air flowpath. However, these could be reversed if it proved advantageous to do so.

### 2.3.6 Weight Prediction

Installed CCE weight is a critical factor when selecting engine type/configuration for short mission durations. Therefore, a weight estimating formula was devised and incorporated into the CCE engines performance program. The element of this equation are shown in Figure 14.

Weight predictions for all components except the diesel core were calculated from validated component data available at GTEC

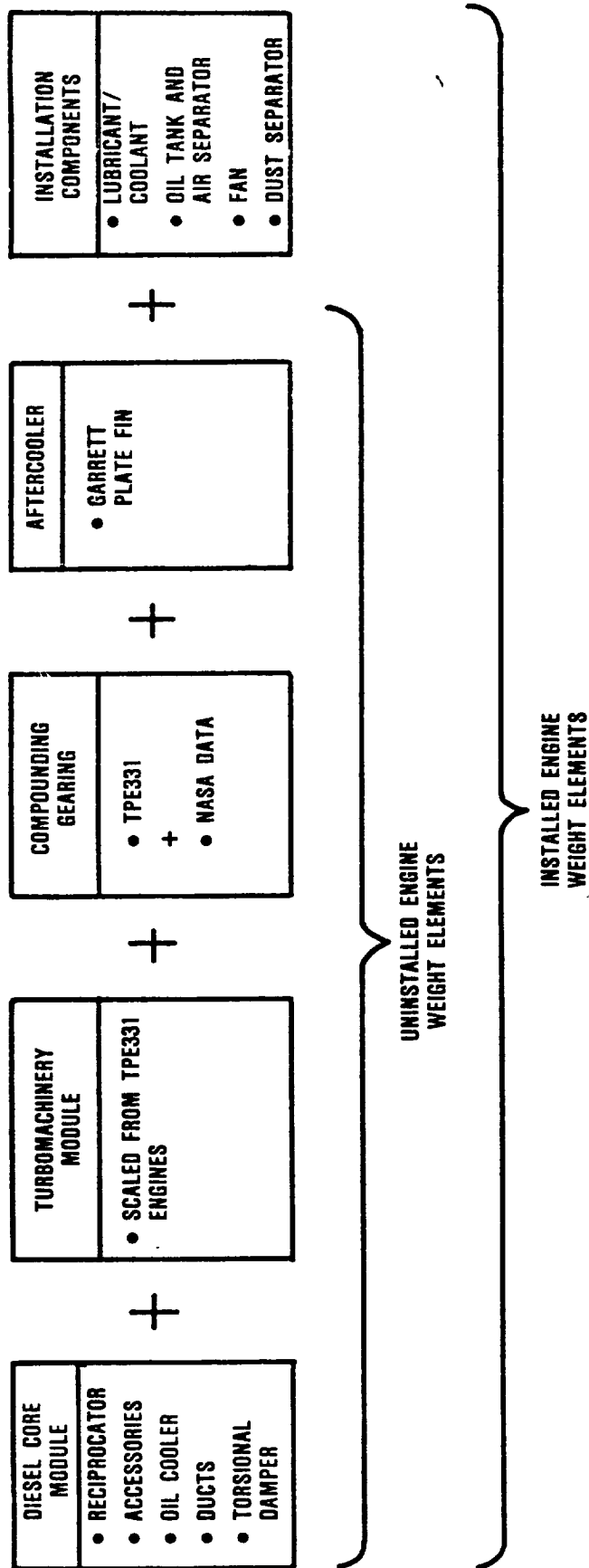


Figure 14. Weight Prediction Elements Used for CCE Study.

and NASA. However, an expression for diesel core weights had to be derived by detailed analysis of available data from aircraft piston engines and subsequent computations could then be made to approximate a flight-weight diesel engine. These calculations involve a maximum firing pressure term in the equation that reflects the higher firing pressure of a diesel engine as compared with a gasoline engine [3362 psi (232 bar) versus 1200 psi (83 bar)].

The diesel engine core weight model was defined to have the form:

$$WT = K \times B^{C1} \times S^{C2} \times N_{CYL}^{C3} \times N^{C4} \times P_{MAX}^{C5}$$

Where:

|                  |   |                               |
|------------------|---|-------------------------------|
| K                | = | Constant                      |
| B                | = | Piston bore diameter, inches  |
| S                | = | Piston stroke length, inches  |
| N <sub>CYL</sub> | = | Number of cylinders           |
| N                | = | Diesel shaft speed, rpm       |
| P <sub>MAX</sub> | = | Maximum firing pressure, psia |

The constant, K, and exponents C1 through C5 were determined by using a least-squares curve fit of the turbocharged or supercharged engine data displayed in Table 4. The resulting constant and exponents for the basic weight equation were established as:

|    |   |       |
|----|---|-------|
| K  | = | 0.068 |
| C1 | = | 1.78  |
| C2 | = | 0.73  |
| C3 | = | 0.86  |
| C4 | = | 0.13  |
| C5 | = | 0.33  |

Table 4. Data Base for Derivation of Diesel Core Weight Polynomial.

| Military/Civil, Gasoline, Liquid Cooled, Aircraft Engines           |                                |      |        |       |      |                  |                    |      |            |                      |               |
|---|--------------------------------|------|--------|-------|------|------------------|--------------------|------|------------|----------------------|---------------|
|   | Cycle                          | Bore | Stroke | CID   | RPM  | P <sub>MAX</sub> | HP <sub>core</sub> | BMEP | Dry Weight | Geared Super Charged | Turbo-Charged |
| 1   | RR Merlin V-12                 | 4    | 5.4    | 6.0   | 1650 | 3000             | 2100               | 420  | 1740       | x                    |               |
| 2   | RR Griffon V-12                | 4    | 6.0    | 6.6   | 2240 | 2750             | 1605               | 321  | 2100       | x                    |               |
| 3   | DB 603 V-12                    | 4    | 6.38   | 7.09  | 2720 | 3000             | 1300               | 260  | 2145       | x                    |               |
| 4   | DB 604 X-24                    | 4    | 5.3    | 5.3   | 2837 | 3200             | 1160               | 232  | 2376       | x                    |               |
| 5   | DB 605 V-12                    | 4    | 6.1    | 6.3   | 2177 | 2600             | 960                | 192  | 1663       | x                    |               |
| 6   | DB 609 V-16                    | 4    | 6.4    | 7.1   | 3770 | 2800             | 1000               | 200  | 3800       | x                    |               |
| 7   | JUMO 211 V-12                  | 4    | 5.9    | 6.5   | 2136 | 3700             | 1300               | 260  | 2024       | x                    |               |
| 8   | JUMO 222 R-24                  | 4    | 5.3    | 5.3   | 2837 | 2900             | 1200               | 240  | 2464       | x                    |               |
| 9   | Allison V-12                   | 4    | 5.5    | 6.0   | 1710 | 3000             | 1135               | 227  | 1395       | x                    |               |
| 10  | Thunder V-8                    | 4    | 4.43   | 4.0   | 495  | 4400             | 1270               | 254  | 681        |                      | x             |
| Military/Civil, Gasoline, Air Cooled, Aircraft Engines              |                                |      |        |       |      |                  |                    |      |            |                      |               |
|   | Cycle                          | Bore | Stroke | CID   | RPM  | P <sub>MAX</sub> | HP <sub>core</sub> | BMEP | Dry Weight | Geared Super Charged | Turbo-Charged |
| 11  | P&W R-2000 R-14                | 4    | 5.75   | 5.5   | 2004 | 2700             | 1055               | 211  | 1605       | x                    |               |
| 12  | P&W R-2800 R-18                | 4    | 5.75   | 6.0   | 2804 | 2800             | 1445               | 289  | 2686       | x                    |               |
| 13  | Wright R-3350 R-18             | 4    | 6.13   | 6.3   | 3347 | 2800             | 1105               | 187  | 2780       | x                    |               |
| 14  | P&W R-4360 R-28                | 4    | 5.75   | 6.0   | 4363 | 2800             | 1800               | 259  | 3780       | x                    |               |
| Civil, Air Cooled, Gasoline, Horizontally Opposed, Aircraft Engines |                                |      |        |       |      |                  |                    |      |            |                      |               |
|   | Cycle                          | Bore | Stroke | CID   | RPM  | P <sub>MAX</sub> | HP <sub>core</sub> | BMEP | Dry Weight | Geared Super Charged | Turbo-Charged |
| 15  | LYC IO-780 F-8                 | 4    | 5.125  | 4.375 | 722  | 2650             | 1080               | 216  | 728        |                      | x             |
| 16  | LYC TIGO-541 F-6               | 4    | 5.125  | 4.375 | 541  | 3200             | 1135               | 227  | 701        |                      | x             |
| 17  | LYC IGSO-540 F-6               | 4    | 5.125  | 4.375 | 541  | 3400             | 820                | 164  | 532        | x                    |               |
| 18  | LYC IGSO-480 F-6               | 4    | 5.125  | 3.875 | 480  | 3400             | 830                | 165  | 497        | x                    |               |
| 19  | Cont GT310-520 F-6 Aftercooled | 4    | 5.25   | 4.0   | 520  | 3400             | 950                | 190  | 590        |                      | x             |
| 20  | Cont T8450 F-8 Aftercooled     | 4    | 4.875  | 3.625 | 542  | 4500             | 730                | 146  | 513        |                      | x             |
| 21  | Cont T6320 F-6 Aftercooled     | 4    | 4.875  | 3.625 | 406  | 4400             | 730                | 146  | 412        |                      | x             |

After the constant and exponents of the weight equation were defined, the equation was used to calculate the weight of existing naturally aspirated engines (i.e., core plus accessories only). It was found to predict high by an average of 11 percent. Therefore, to use the equation to predict the weight of a naturally aspirated engine, the value of K had to be multiplied by 0.89. This scaling was desirable for the CCE application because the level of turbocharging is very high (when compared to conventional turbocharged engines) and the turbocharging equipment weight is already accounted for by separate components of the overall equation shown in Figure 15. Therefore, the constant K was revised to 0.068.

Engines within the final data base typically had bore diameters from 4.5 to 6.0 inches (11.4 to 15.2 cm). The least-squares curve fit weight equation predicted within  $\pm 10$  percent for the majority of these engines. (See "original data base" in Table 4). The weight equation was then used to predict the weight of engines with smaller bores, ranging from 0.495 to 2.83 inches (1.26 to 7.19 cm) (See "Model Aircraft" and "Ultralight Aircraft" engines in Figure 16). The average of these engine weights were predicted within  $\pm 20$  percent, which suggests that the resulting equation can be used over the range of bore diameters under consideration.

The final installed weight equation that was used in the screening process and for the range-payload analyses is shown in Figure 15.

The engine weight equation may be conservative since there have been advancements in strong, lightweight materials developed since the 1950s, when most of the original data-base engines were designed. Ultimately, a new weight prediction equation will need



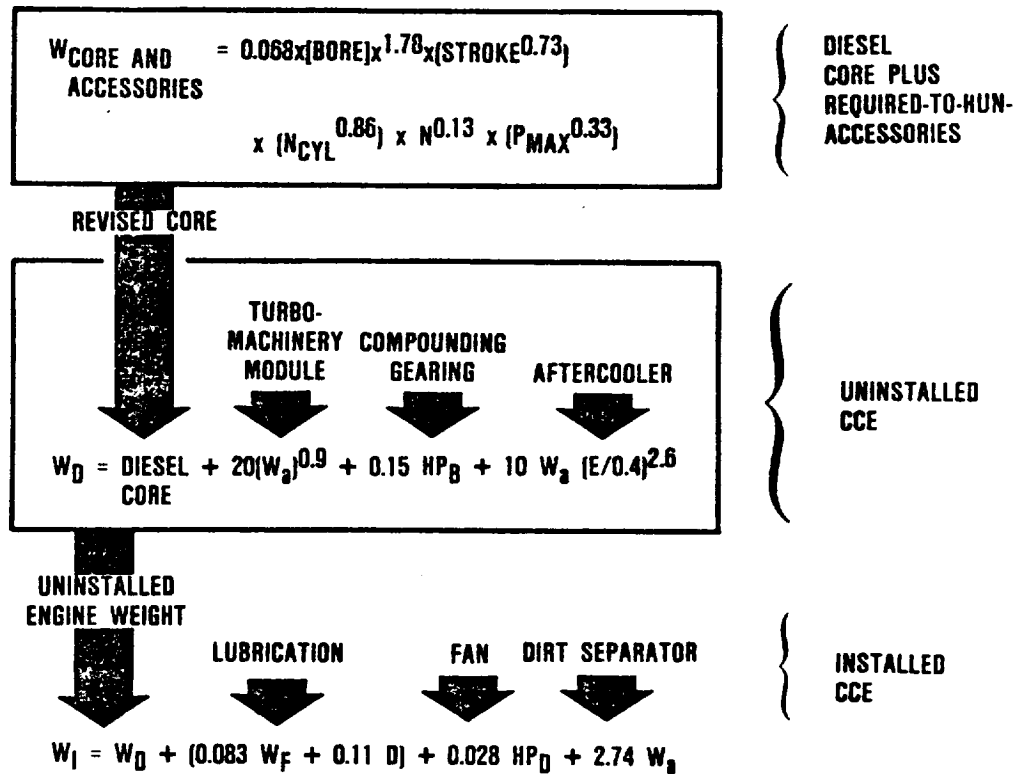


Figure 15. Final Equations and Elements Used to Estimate CCE Installed Weight.

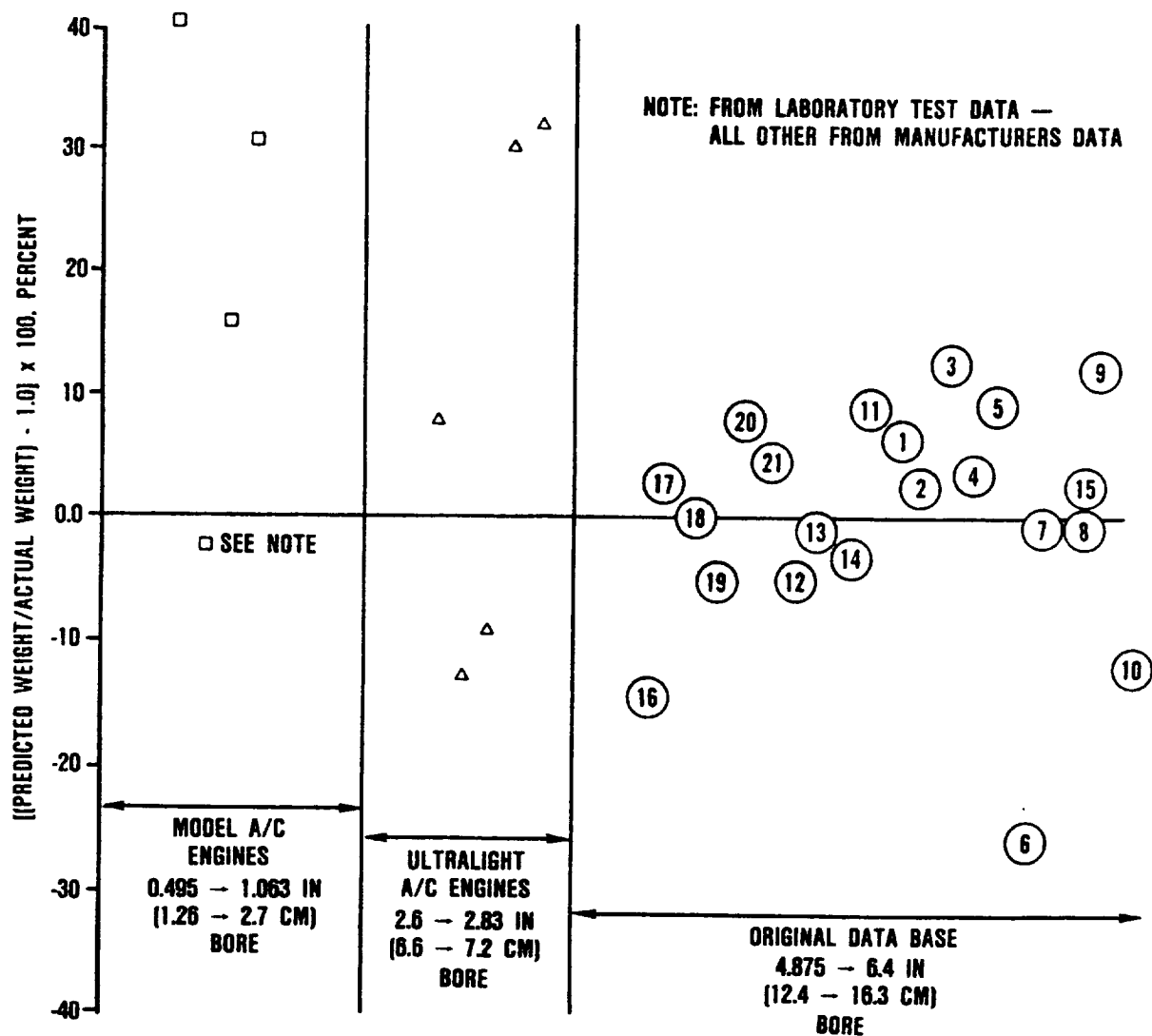


Figure 16. Predicted Versus Actual Engine Core Weight.

to be developed to predict the weight of engines using the new materials when they are applied to advanced designs.

#### **2.3.7 Off-Design Engine Performance**

For an off-design performance run, the number of cylinders, aftercooler dimensions, and fuel flow were specified. Cylinder pressure drop varied as required to satisfy flow continuity, and turbocharger speed was computed to obtain balanced power on the turbocharger shaft when the latter was not mechanically coupled to the diesel engine. Off-design aftercooler effectiveness and pressure drop also were calculated where applicable.

### 3.0 CANDIDATE SCREENING AND SELECTION OF THE BEST CONFIGURATION

#### 3.1 Candidate Engines and Selection Criteria

Nine different diesel-turbomachinery combinations were investigated during the initial screening phase of the study. These will be described in detail later. Both 2-stroke and 4-stroke engines were "designed" with the same bore, stroke, and crankshaft speed limits. The boundary conditions or limits shown in paragraph 2.3.4 were applied to the GTEC compound cycle engine performance model; these engines were then "operated" with each of the three turbomachinery configurations. The required engine displacement that was then calculated, would deliver 1000 shp (746 kW) total, from both the reciprocating and rotating machinery. The installed engine weights were computed using the derived formula, and the 1000-shp (746-kW) BSFC was then computed.

The factors considered in making the CCE selection were:

- o Specific fuel consumption
- o Engine weight
- o Aircraft mission range/payload

The objective was to identify the combination of factors that would provide a maximum savings in mission fuel with the lightest weight engine, in order to achieve a maximum gain in range-payload for the vehicle.

#### 3.2 Scavenging Arrangements

The following diesel engine scavenging arrangements (Figure 17) were evaluated in the preliminary screening:

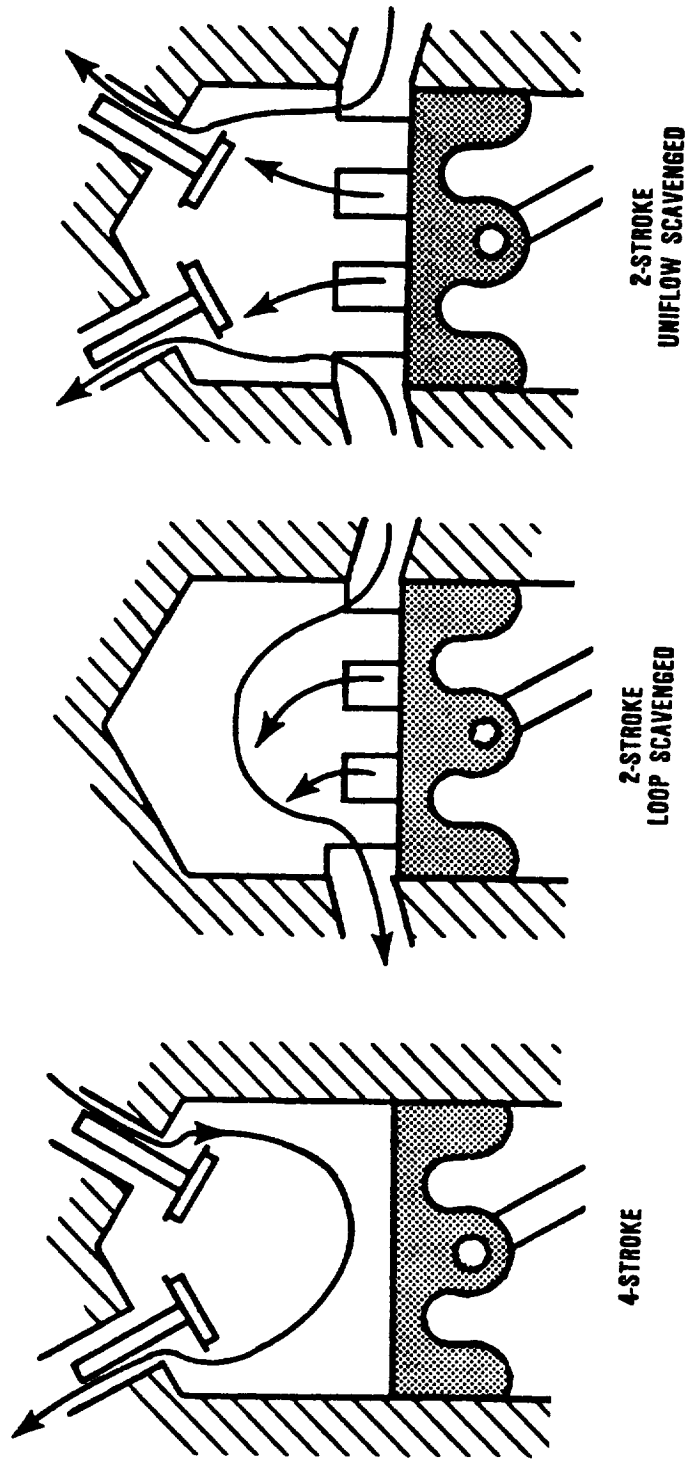


Figure 17. Diesel Engine Designs.

- o Loop Scavenged - Intake and exhaust ports are located on opposite sides of the cylinder. These are uncovered/covered by the piston to effect scavenging and charging of the cylinder. Therefore, port timing is symmetrical with respect to bottom dead center (BDC). The exhaust interval, as measured by crank angle, is longer than the intake duration.
- o Uniflow - This arrangement uses radially and axially symmetric intake ports at the BDC location of the cylinder liner. Poppet exhaust valves are located in the cylinder head. Scavenging is more effective than in a loop-scavenged engine, and circumferential temperature gradients are reduced with the one-way flow path.
- o Four-Stroke - This engine has two intake and two exhaust valves located in the cylinder head, which when coupled with actual intake and exhaust strokes, provide more complete and predictable scavenging. However, it delivers only one power stroke in two crankshaft revolutions.

Air consumption tends to be highest for the loop-scavenged cylinder and least for the 4-stroke version. The latter also is self-breathing and capable of running with a zero or negative pressure drop across the cylinders, although at reduced output.

Port timing and flow area for the loop-scavenged engine were selected to be identical to those of the CCTE studied earlier. The CCTE intake port timing was also used for the uniflow, with exhaust valve timing selected to obtain a good compromise between expansion work and blowback. Maximum effective exhaust flow area was set equal to 20 percent of bore area, consistent with current production engine design.

Valve timing, less critical for a four-stroke engine, was made similar to that of a current truck engine. Maximum flow area can be smaller because longer open periods allow the same time-area product to be obtained. Effective compression ratio was adjusted to yield nearly the same maximum firing pressure for each type of diesel core, regardless of boost pressure. Cylinder bore, stroke, and crankshaft speed were kept constant during the preliminary screening studies.

### 3.3 Candidate Compound Engines

The following three Brayton/diesel engine configurations or types (Figure 18) were evaluated during this study:

- o Turbocharged - The turbomachinery is used to increase the manifold densities, thereby increasing the specific output. There is no mechanical connection between the reciprocator and the turbomachinery.
- o Single-Spool Turbocompound - The turbomachinery is used to supercharge the engine. Surplus turbine power is supplied to the crankshaft via a gearbox.
- o One- and One-Half Spool Turbocompound - The turbosupercharger is used to provide high-pressure air to the engine. Surplus exhaust energy from its turbine is then routed through a bottoming or power-recovery turbine, which is geared to the reciprocator crankshaft.

### 3.4 CCE Selection

The results of the initial screening study are shown in Figure 19 where in the matrix of the nine different diesel-turbine combinations are identified. A plot of the engine specific

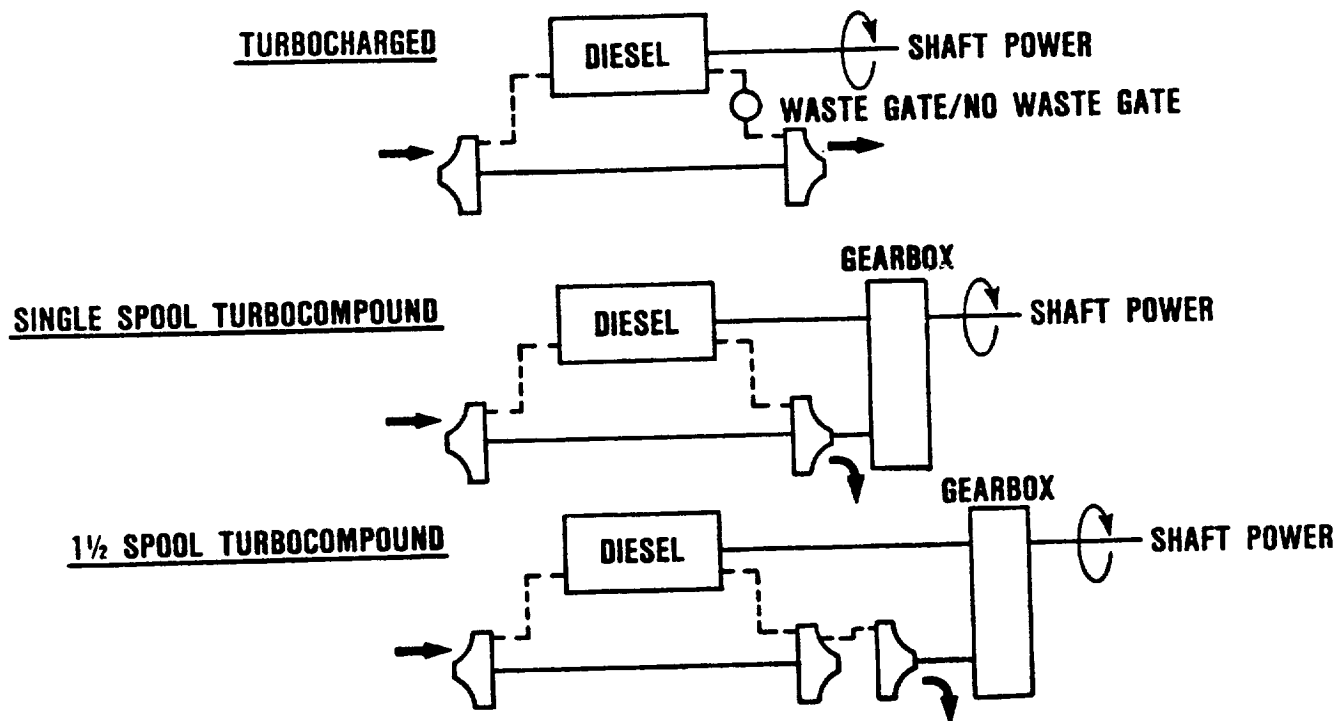
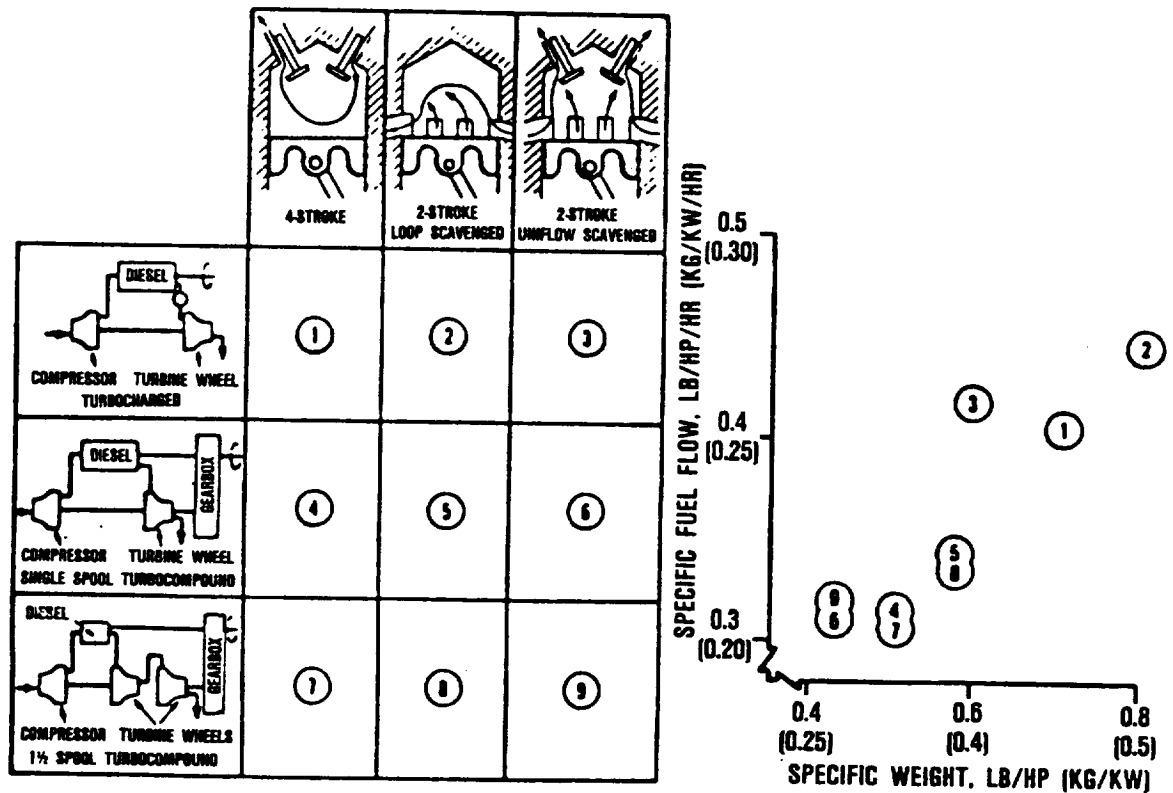


**Figure 18. Brayton/Diesel Engines Examined.**





67-004-20

**Figure 19. Nine Configurations Design Point [1000 HP (746 kW)] Diesel/Diesel/Turbine Thermodynamic (SFC) and Weight Analysis.**

weight [lb/hp (kg/kW)] and SFC [lb/hp-hr (gm/kW-hr)] for each engine is shown at the right and a more complete analysis of these results is presented in the following text.

#### 3.4.1 Selection of Engine Type

The three engine types at 1000 shp (746 kW) net output were matched one at a time with each of the turbomachinery systems. The complete engine weight and fuel consumption was then computed using the CCE Performance Model Program.

#### 3.4.2 Turbomachinery Configuration Selection

The turbocharged cycle (Numbers 1, 2 and 3 on Figure 20), which was included in the study because it was thought to offer better altitude off-design performance, was inferior to the others in terms of both weight and BSFC. When optimized at part power, the turbocharged cycle is not able to make effective use of diesel exhaust energy at full power. Minimum design-point BSFC calls for high compression ratio and low boost pressure, due to maximum cylinder pressure limitations, while minimum weight is achieved with lower compression ratio, higher manifold pressure ratios, and a resultant increase in SFC. After it was found that the turbocharged cycle required much higher mission fuel consumption than the other candidates, it was dropped from further study.

The single-spool turbocompound cycle, (Numbers 4, 5, and 6 Figure 19), which is capable of achieving good thermodynamic efficiency at rated power, requires simpler turbine stages. However, a high gear ratio is needed to transmit power between the turbomachinery and the load. Also, both off-design and altitude performance is adversely affected when the compressor and turbine continue to run at constant speed. The 4-stroke (4) and loop-

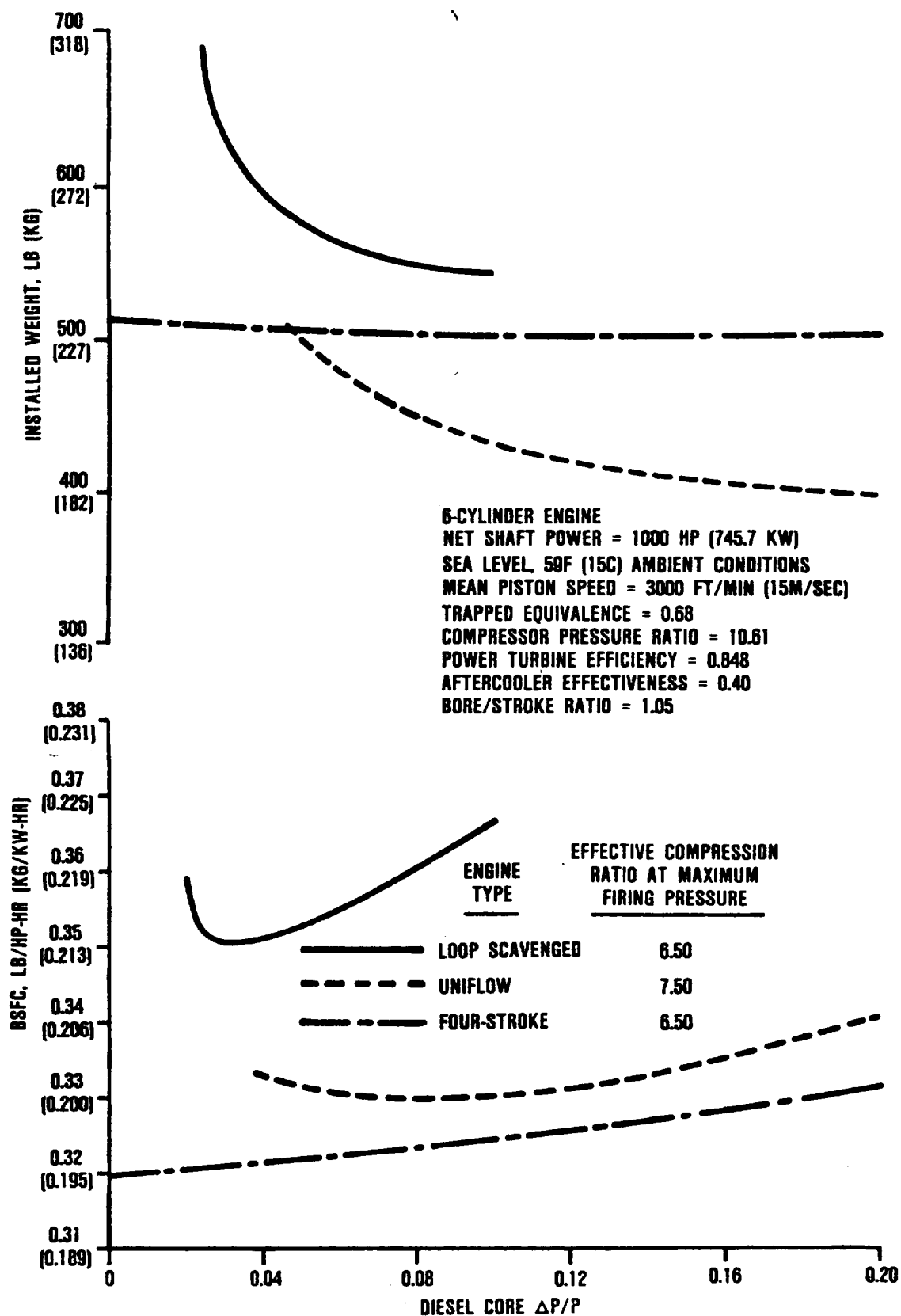


Figure 20. Diesel Engine Design Point Comparison.

scavenged (5) engines were eliminated from further study because of specific weight and/or BSFC.

Typical results for the 1-1/2-spool turbocompound system on the three engine types (Numbers 7, 8 and 9 on Figure 19) are shown in Figure 20 plotted at various diesel core manifold pressure drops. The loop-scavenged engine (8) was thermodynamically inferior in terms of both BSFC and weight due to its relatively high air consumption and low exhaust temperature. The 4-stroke engine (7) was the most efficient, but it was also much heavier than an uniflow 2-stroke engine. The uniflow engine (6) and (9) was selected from the screening studies as the most probable candidate for meeting the specific goals. Therefore, the single and 1-1/2-spool arrangements were carried into the next stage of the studies.

The 1-1/2-spool configuration was identified as the best arrangement, due to superior part-power and altitude performance. A comparison between the 1-1/2-spool and single-spool compound engines is shown in Figure 21 for sea-level, standard-day conditions. The large proportion of mission time (80 percent) flown at 50 percent power or less makes the choice of the 1-1/2-spool engine even more important. The difference between the two systems is even more pronounced at altitude as shown in Figure 22, with the 1-1/2-spool engine clearly superior in BSFC over the single-spool compound engine. The additional turbine weight is effectively offset by reduced gearbox weight because the power turbine runs at a lower speed than the turbocompressor and provides the needed flexibility to avoid variable geometry in the turbomachinery or variable ratio gearing to match the speeds of the diesel and turbine modules.

A disadvantage of the 1-1/2-spool cycle, along with a 2-stroke diesel engine is the need to include either an engine-

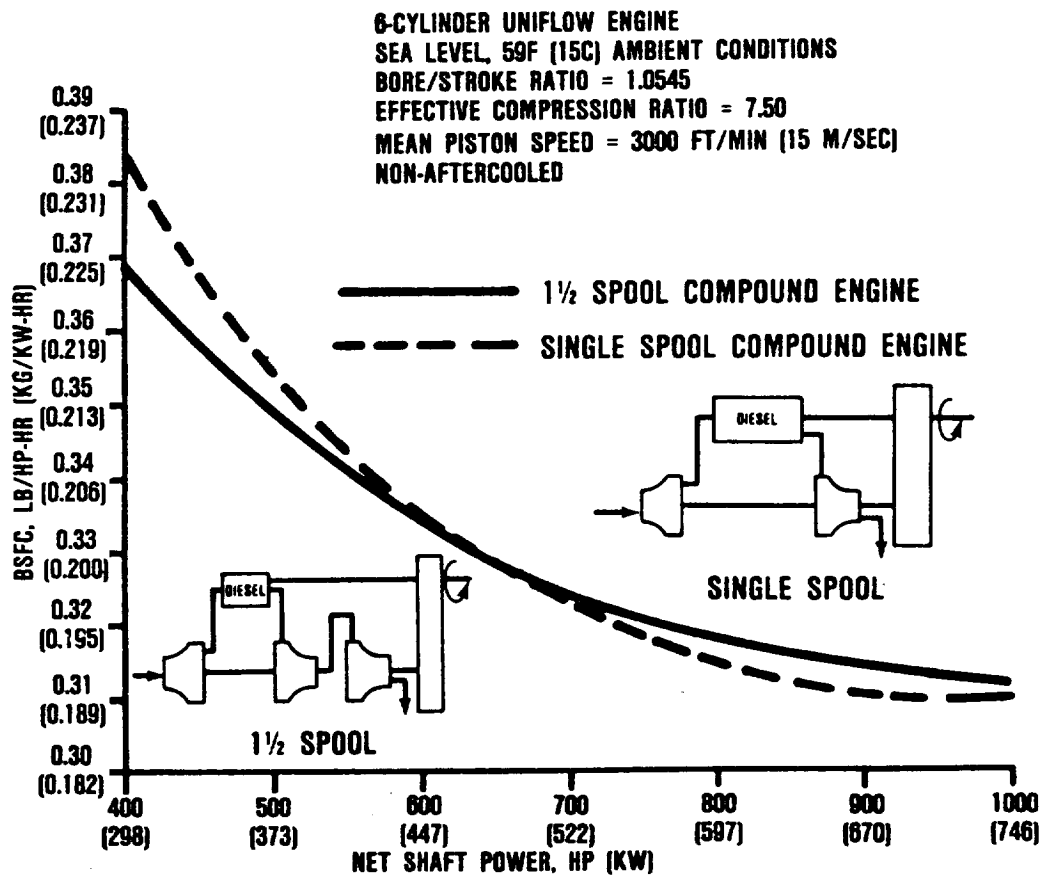


**Figure 21. Specific Fuel Consumption of Single and 1-1/2-Spool Engines as a Function of Power at Sea Level.**

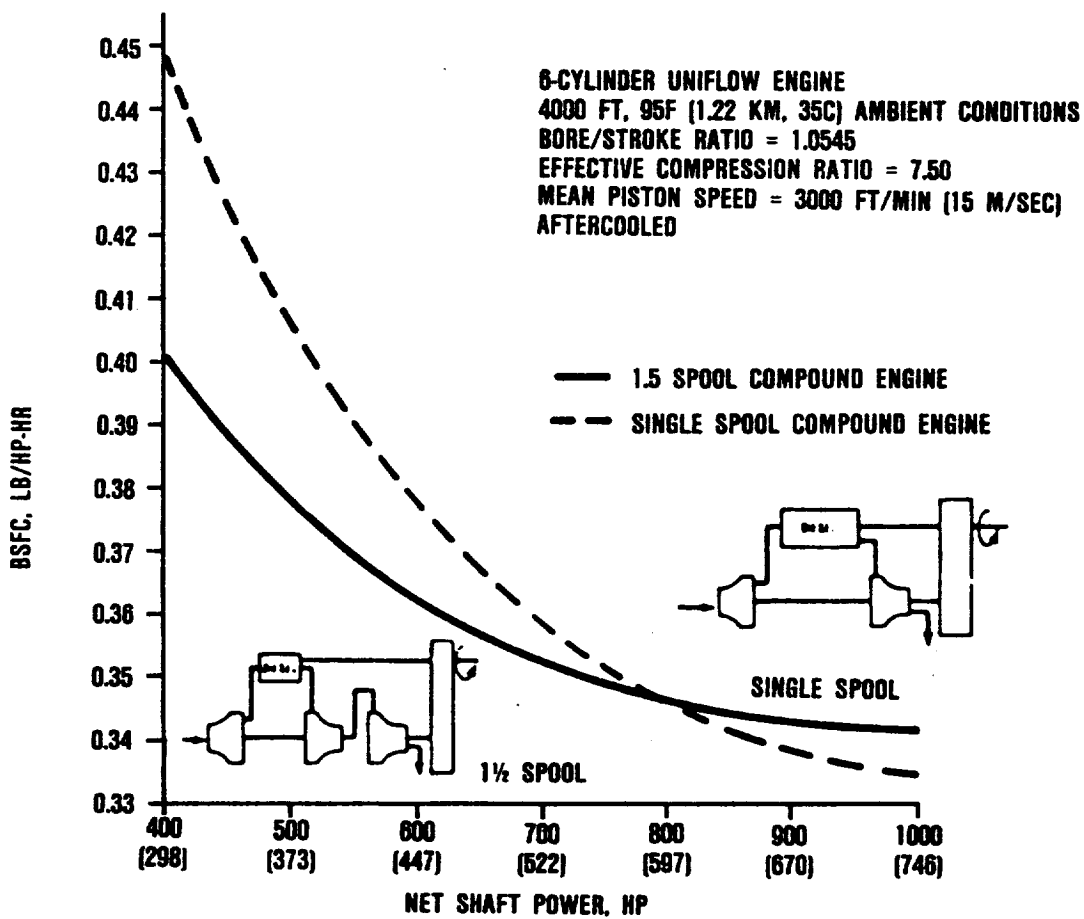


Figure 22. SFC of Single and 1-1/2-Spool Engines as a Function of Power at 4000 ft (1.22 km).

driven blower or a mechanical linkage between the engine and the turbocompressor for starting and light-load operation. In addition, it is preferable to declutch the power turbine for starting and during that part-power operation where there is insufficient exhaust energy to drive the power turbine. For these reasons, overrunning or sprague type clutches have been identified for CCE and would be installed in the compound gearing module to separately handle these power requirements. Simultaneous cranking of the diesel engine and the turbocompressor is the preferred starting method. This avoids the weight and SFC penalty of adding the roots blower often used in production 2-stroke cycle engines to generate starting and light-load air flow.

### 3.5 Other Thermodynamic Studies

The screening studies showed that engine weight and firing pressure constraints dictated a combination of high boost pressure and relatively low compression ratio, irrespective of the type of diesel engine. Compromises of diesel cylinder compression ratio and supercharging compressor pressure ratio were arrived at after a matrix of variables were evaluated affecting performance effects including maximum firing pressure, installed weight, and BSFC. Figure 23 shows the relationship of the sensitivity selection variables. High supercharging pressures reduce weight sufficiently to offset the small penalty that lowered compression ratio causes on engine SFC. The best SFC and engine weight relationship was found to exist at high compressor pressure ratios (more than 10). The diesel core effective compression ratio was limited to 7.5 in order to keep peak firing pressures below 3400 psia (234.5 bar).

The effects of variable compressor inlet geometry and/or adjustable power turbine nozzle area on part-load performance were also investigated. Variable nozzle area would be necessary

NOTES: 1000 HP (745.7 KW), SEA LEVEL, STANDARD DAY  
 TRAPPED EQUIVALENCE RATIO = 0.68  
 6-CYLINDER DESIGN  
 BORE/STROKE RATIO = 1.05  
 COMPRESSOR PRESSURE RATIO =  $P_{rc}$   
 DIESEL COMPRESSION RATIO = C/R  
 AFTERCOOLER EFFECTIVENESS = 0.40  
 $P_{rc}$ , COMPRESSOR PRESURE RATIO  
 CR, DIESEL COMPRESSION RATIO

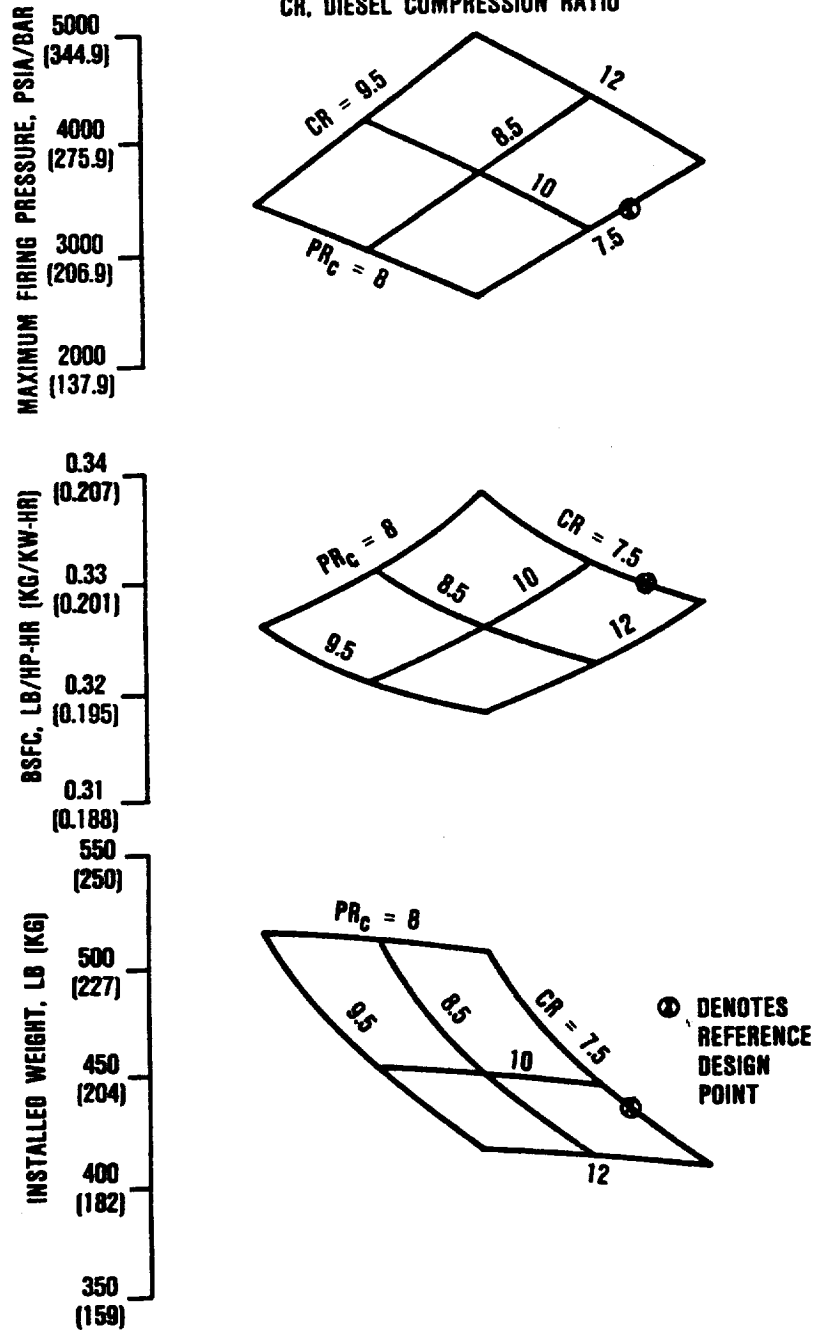


Figure 23. Engine Sensitivity Studies on the Effects of Compression Ratio and Compressor Pressure Ratio.



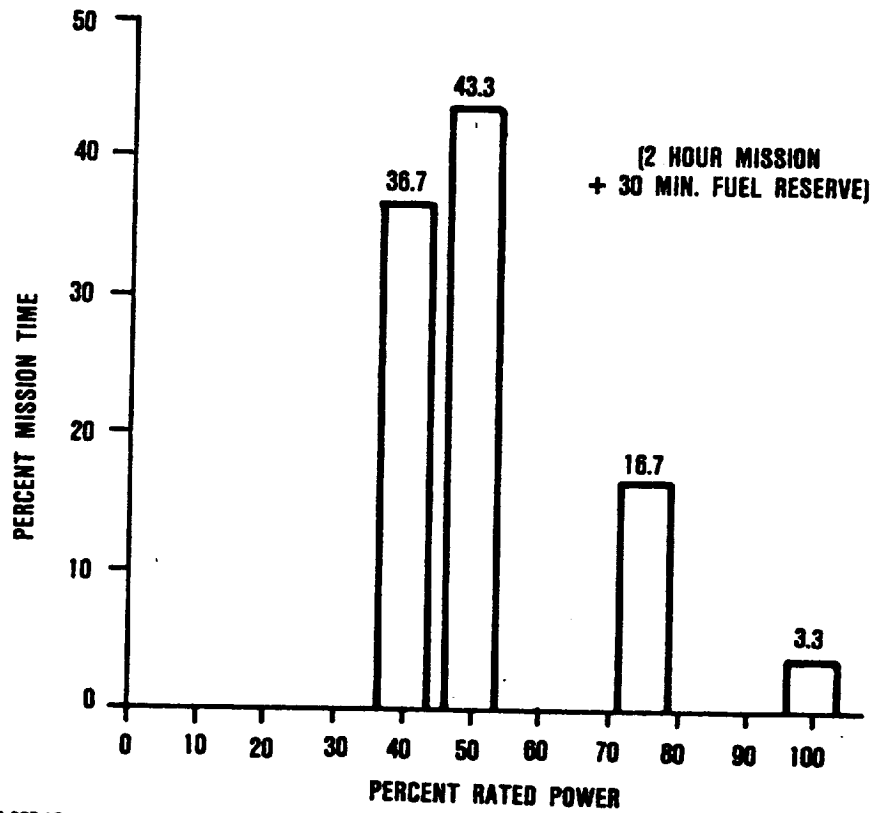
when operated with 4-stroke cycle engines because these engines are positive displacement devices and run at constant speed across a wide (2/1) load range. The combustion airflow also varies considerably, and variable geometry is necessary to improve turbomachinery part-load efficiencies and load response. In the case of 2-stroke engines that breathe as an orifice, variable geometry for either the compressor or the turbine was found to be of small benefit and the extra complexity not justified.

### 3.6 Best Candidate Engine Selection

The design point results of the engine configuration matrix study are shown in Figure 19. The 2-stroke uniflow engine with 1-1/2 spool turbocompounding was selected as the best candidate. This selection was based on engine weight and fuel consumption in the 50-percent power range, where as much as 80 percent of the time is spent as shown in the mission profile (Figure 24). This mission-power profile was used to estimate the magnitude of the CCE gains over the contemporary gas turbine, described in paragraph 5.2.

The six-cylinder configuration was chosen for the following reasons:

- o Relative freedom from torsional vibration and unbalance
- o Three cylinders per exhaust manifold give improved energy for turbocharging because of uniform intervals between pressure pulsations that are noninterfering
- o Adequate bore diameter permitted to install four exhaust valves and a unit injector
- o Reliability and simplicity associated with lesser number of cylinders



65-287-10

Figure 24. Mission Power/Time Profile.

## 4.0 FURTHER DEFINITION AND OPTIMIZATION OF THE BEST CANDIDATE

### 4.1 The 1-1/2-Spool Uniflow Engine

Having identified the 1-1/2-spool uniflow engine configuration as preferred, the study effort concentrated on ways to enhance performance and reduce system weight. The selected reference cycle was a six-cylinder CCE delivering 1000 hp (746 kW) to the rotor gearbox at sea-level, 59F (15C) ambient conditions. Computer-generated descriptive data for the reference cycle is listed in Table 5; station locations are identified in Figure 25. No installation pressure losses were calculated because they would be installation specific. However, cooling fan power was deducted and 2 percent internal duct pressure loss was included at appropriate locations in the flow path. When present, the aftercooler also imposed a 2 percent pressure loss on the engine airflow side and a 3 percent loss on the coolant side. At off-design, duct-pressure loss was computed as a function of corrected flow.

To avoid a serious degradation of power turbine efficiency at part power, the turbine match point at full power was set at a velocity factor below that associated with peak efficiency. Part-load operation at constant speed causes the operating point to shift toward higher specific flow where the turbine efficiency is higher. For the design-point parametric study, the power turbine physical speed was varied to obtain the same design point efficiency.

### 4.2 Design-Point Performance

Diesel core cylinder pressure drop exerts a marked influence on design performance, including the power split between the diesel and the gas turbine. BSFC, installed weight, diesel

TABLE 5. COMPUTER-GENERATED DESCRIPTIVE DATA FOR THE  
REFERENCE CYCLE.

|  |          |                   |           |                      |         |
|--|----------|-------------------|-----------|----------------------|---------|
| CCTDE UNIFLOW CORE, 1.5 SPOOL, ER=0.680, CR=7.5, N=66910 RPM, S.L., STD 04 |          |                   |           |                      |         |
| TAPE2 TITLE: 1-CYLINDER 2-STROKE UNIFLOW ENGINE                            |          |                   |           |                      |         |
| DATE - 85/09/27  |          |                   |           |                      |         |
| TIME - 10:26:15  |          |                   |           |                      |         |
| IDENT: 2-STROKE  |          |                   |           |                      |         |
| 1.5 SPOOL TURBO-COMPOUND   |          |                   |           |                      |         |
| UNIFLOW  |          |                   |           |                      |         |
| AFTERCOOLED  |          |                   |           |                      |         |
| NO. OF CYLS 5.99951  |          |                   |           |                      |         |
| ALT  | 0.       | NET SHP           | 999.99    | N-DIESEL             | 6122.   |
| MACH NO  | 0.00     | WF(LB/HR)         | 330.03    | N-TURB CHG           | 66910.  |
| V(KIAS)  | 0.00     | BSFC              | .3300     | N-PWR TUR            | 19000.0 |
| V(KTAS)  | 0.00     | WA(LB/SEC)        | 2.441     | DISPL(CU IN)         | 133.20  |
| V(MPH)   | 0.00     | SHP/WA            | 409.58    | SHP/CU IN            | 6.08    |
|  |          | ESTD WGHT         | 355.5     | LBS H                |         |
| BNX VOL  | 10.65    | DISPL INDEX       | .080      | FLOW INDEX           | 4.361   |
|  |          |                   |           | POWER INDEX          | 93.9    |
| EFFICIENCIES:  |          |                   | OVERALL   |                      | DIESEL  |
| SCAVENGE   | 81.10    | TRAPPING          | 74.63     | BRAKE THERMAL        | 42.60   |
|  |          |                   |           | IND THERMAL          | 37.00   |
| *****  |          |                   |           |                      |         |
| PAM  | 14.70    | DIESEL NET HP     | 758.57    | DIESEL LOSSES(HP)    | 57.65   |
| TAM(F)   | 59.00    | BRAYTON NET HP    | 241.43    | BRAYTON LOSSES(HP)   | 10.66   |
| TAM(C)   | 15.00    |                   |           | OIL COOLER FAN HP    | 51.00   |
| ETA RAM  | 1.00     |                   |           | AFTERCOOLER FAN HP   | 0.00    |
| INLET DP/P   | 0.       |                   |           | CUSTOMER HP EXTR     | 0.00    |
| EXH DP/P   | 0.       |                   |           | CUSTOMER BLEED (PPS) | 0.00    |
| COMPRESSOR:  |          | H P TURBINE:      |           | L P TURBINE:         | DIESEL: |
| P/P  | 10.611   | P/P               | 4.118     | P/P                  | 2.139   |
| COR FLOW   | 2.442    | COR FLOW          | .360      | COR FLOW             | 2.124   |
| PCT SPD  | 1.000    | PCT SPD           | 1.202     | PCT SPD              | .798    |
| AERO HP  | 523.27   | AERO HP           | 533.92    | AERO HP              | 241.43  |
| EFFICIENCY   | .7900    | EFFICIENCY        | .9453     | EFFICIENCY           | .8479   |
| BLEED PCT  | 4.00     | COOL WA(PCT)      | 4.00      | AREA RATIO           | 1.200   |
| BETA   | 3.00     |                   |           | COOL WA(PCT)         | 0.00    |
|  |          | AFTERCOOLER:      |           | MAX EFF AREAS:       |         |
|  |          | DP/P AIR          | .0200     | INTAKE               | 2.188   |
|  |          | DP/P COOL         | .0300     | EXHAUST              | 1.511   |
|  |          | EFFECT.           | .4000     |                      |         |
| *****  |          |                   |           |                      |         |
| STATION  | PRESSURE | TEMP(R)           | FLOW(PHY) | DIESEL:              |         |
| AMBIENT  | 14.696   | 518.7             |           | MANIF IN TEMP(F)     | 436.27  |
| 1  | 14.696   | 518.7             | 2.441     | MANIF IN PRESS       | 149.76  |
| 2  | 14.696   | 518.7             | 2.441     | MANIF EX TEMP(F)     | 1753.87 |
| 3  | 14.696   | 518.7             | 2.441     | MANIF EX PRESS       | 134.79  |
| 4  | 155.938  | 1137.4            | 2.344     | FUMIGANT TYPE        | NONE    |
| 5  | 152.819  | 1137.4            | 2.344     | FUMIGANT BURNED      | 0.00    |
| 6  | 149.763  | 896.0             | 2.344     | FUM IN EXH GAS       | 0.0000  |
| 7  | 134.787  | 2213.6            | 2.436     | METHANOL/H2O         | 0.00    |
| 10   | 132.091  | 2213.6            | 2.436     | MAX CYL TEMP(F)      | 3423.6  |
| 11   | 32.076   | 1687.2            | 2.436     | MAX CYL PRESS        | 3361.8  |
| 12   | 14.696   | 1428.1            | 2.533     | IMEP(PST)            | 421.144 |
| 13   | 14.696   | 1428.1            | 2.533     | BMEP(PST)            | 393.146 |
| COMPR TEMP   |          | 2407.0            |           | EQUIV. RATIO         | .680    |
|  |          |                   |           | SCAVG. RATIO         | .708    |
|  |          |                   |           | EFF COMP RATIO       | 7.50    |
|  |          |                   |           | CYL HEAT LOSS(PCT)   | 5.82    |
|  |          | BLOWBACK FRACTION | .0668     |                      |         |

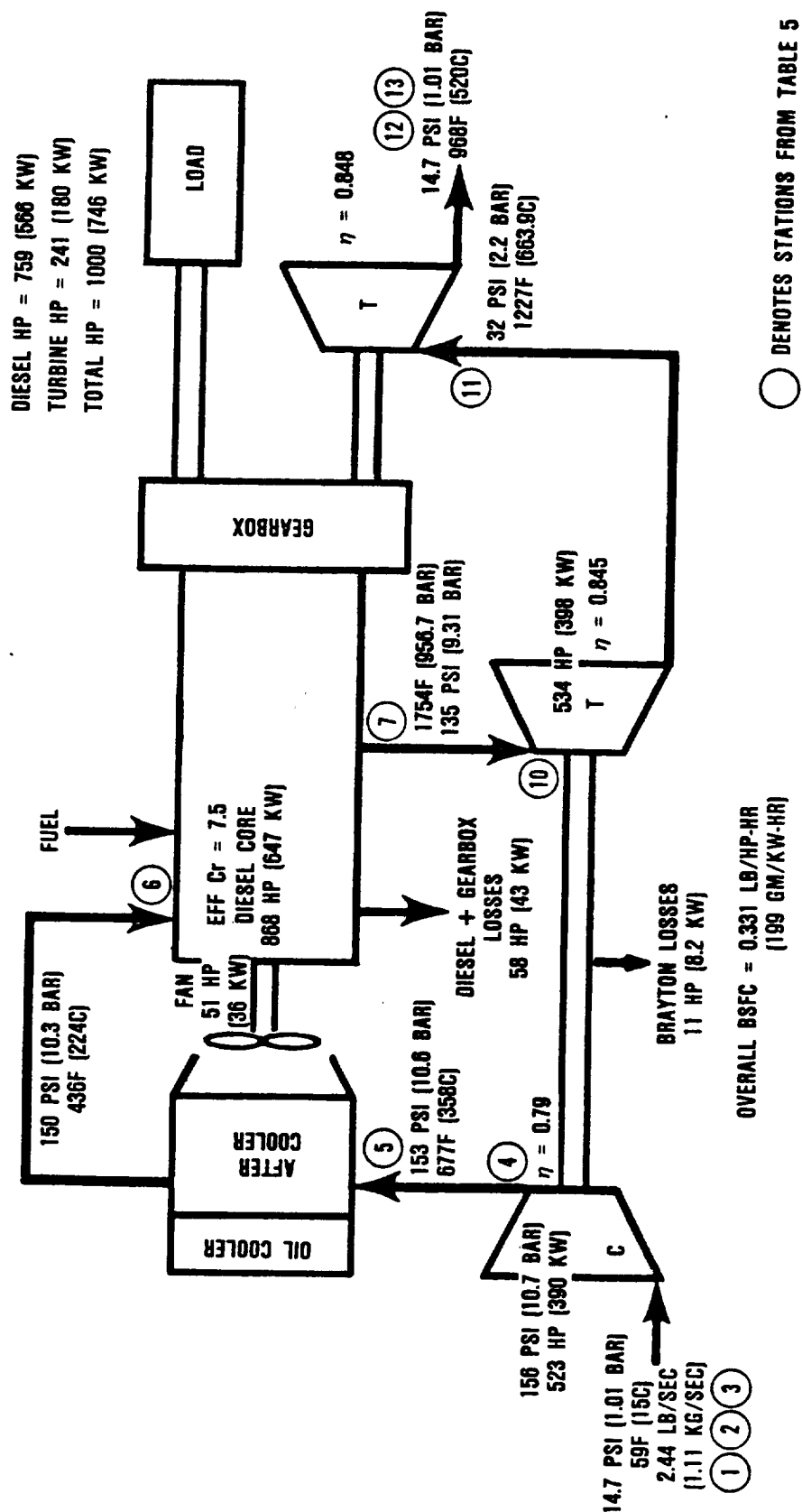


Figure 25. 1-1/2-Spool CCE Engine Flow/Cycle Schematic.

exhaust temperature, and turbine power ratio are plotted versus core fractional pressure drop in Figure 26. A diesel core pressure drop of 10 percent was chosen to achieve the best compromise between overall cycle efficiency and weight. The total fuel weight for a two-hour mission plus 30 minutes reserve fuel supply was slightly larger than the design study CCE installed weight. Therefore, BSFC and engine weight were of equal importance.

Cylinder number and bore/stroke ratio were held constant, while actual cylinder dimensions and crankshaft speed were varied. Figure 27 shows the effect of mean piston speed on BSFC, weight, and other variables. The selected mean piston speed of 3000 ft/min (15 m/sec) was nearly optimum with respect to BSFC.

The effect of trapped equivalence ratio on design-point performance is illustrated in Figure 28. The improvement in overall cycle efficiency with increased trapped equivalence ratio was attributed to the higher exhaust temperature that can be exploited for useful energy conversion in a compound cycle. However, the indicated thermal efficiency of the diesel core drops off at higher trapped fuel-to-air ratios. The reference cycle trapped equivalence ratio of 0.68 was set at the exhaust smoke limit as determined by reference data from C.F. Taylor<sup>13</sup> and in consideration of exhaust valve temperatures.

The influence of aftercooler effectiveness on firing pressure, weight, and bore size is shown on Figure 29. A minimum installed weight exists for constant 1000 shp (746 kW), due to offsetting weights of diesel core [reduced displacement (-) and increased firing pressure (+) and aftercooler (+)]. As the aftercooler effectiveness became greater, the BMEP and firing pressure increased because the displacement (bore size) was reduced to maintain constant engine power.

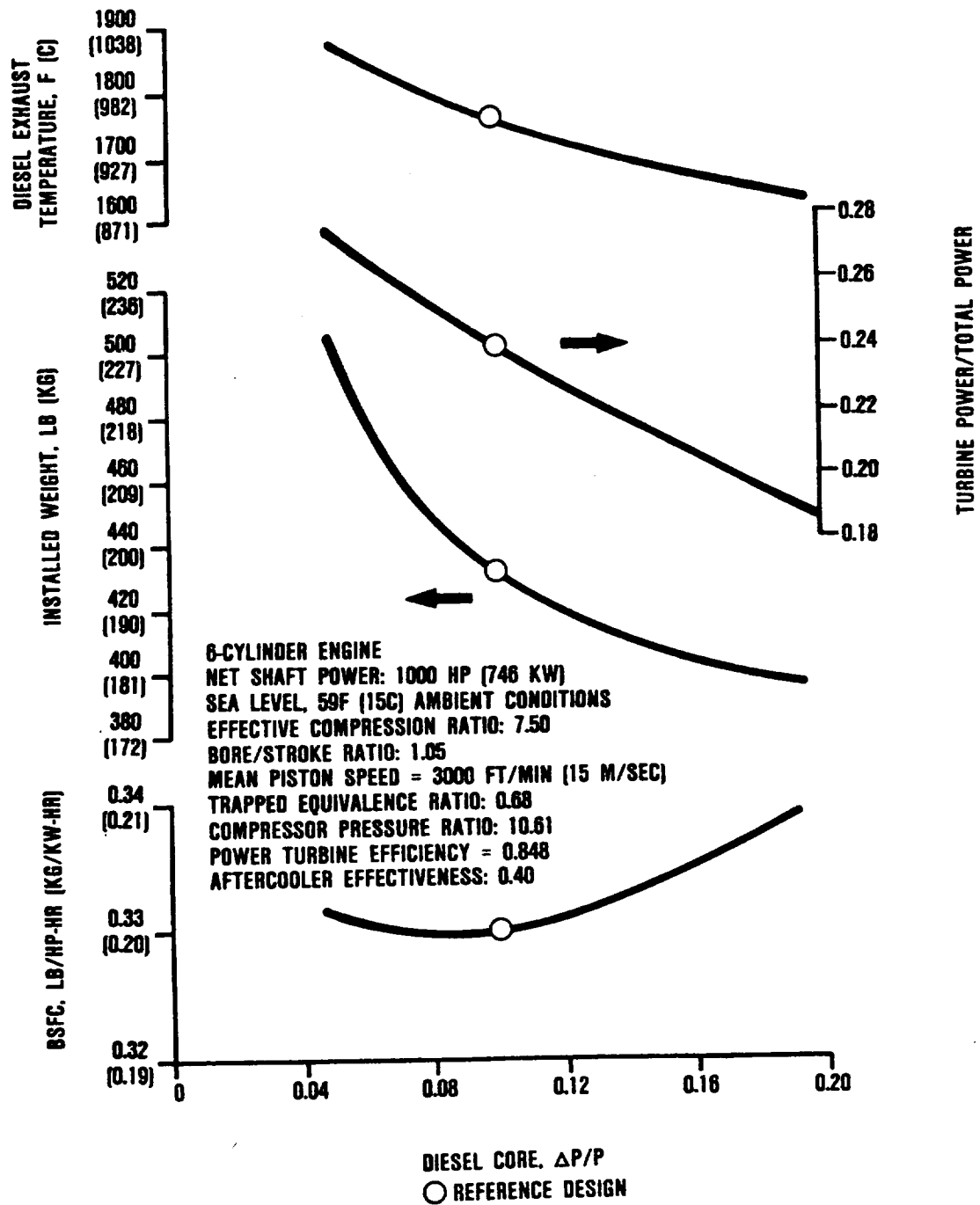


Figure 26. Effect of Diesel Core Pressure Drop on CCE Design Performance.

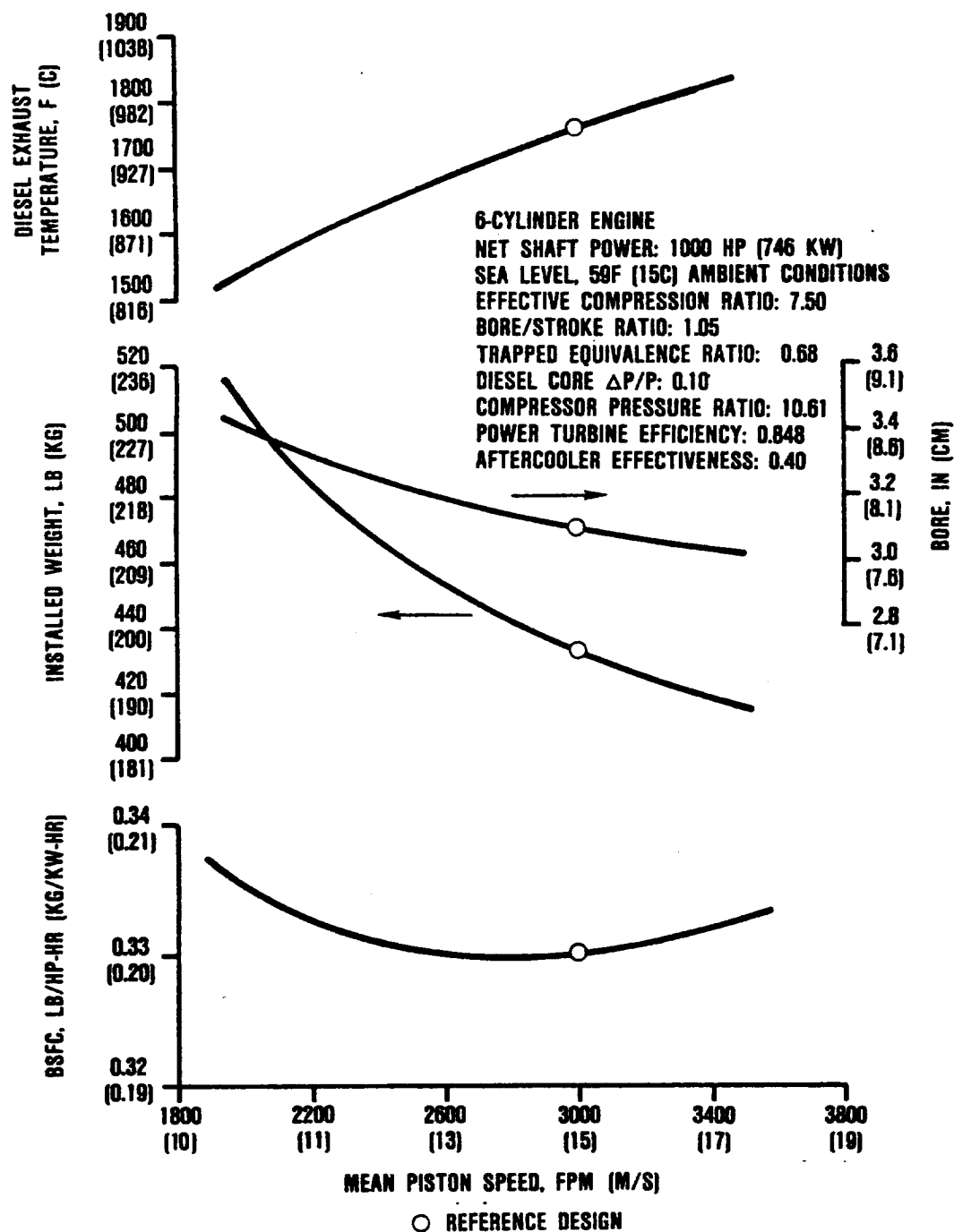


Figure 27. Effect of Mean Piston Speed on CCE Design Performance.



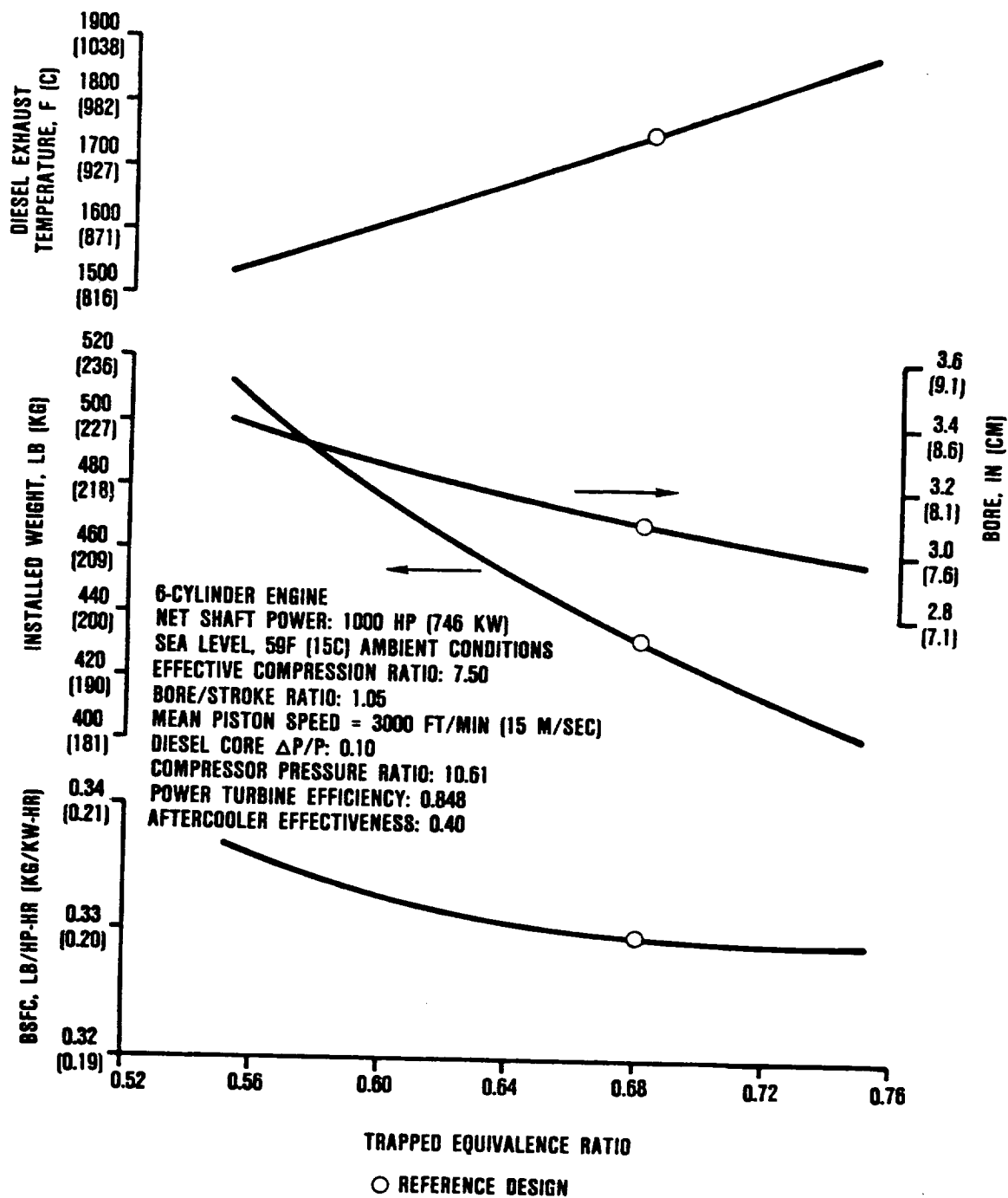


Figure 28. Effect of Trapped Equivalence Ratio on CCE Design Performance.

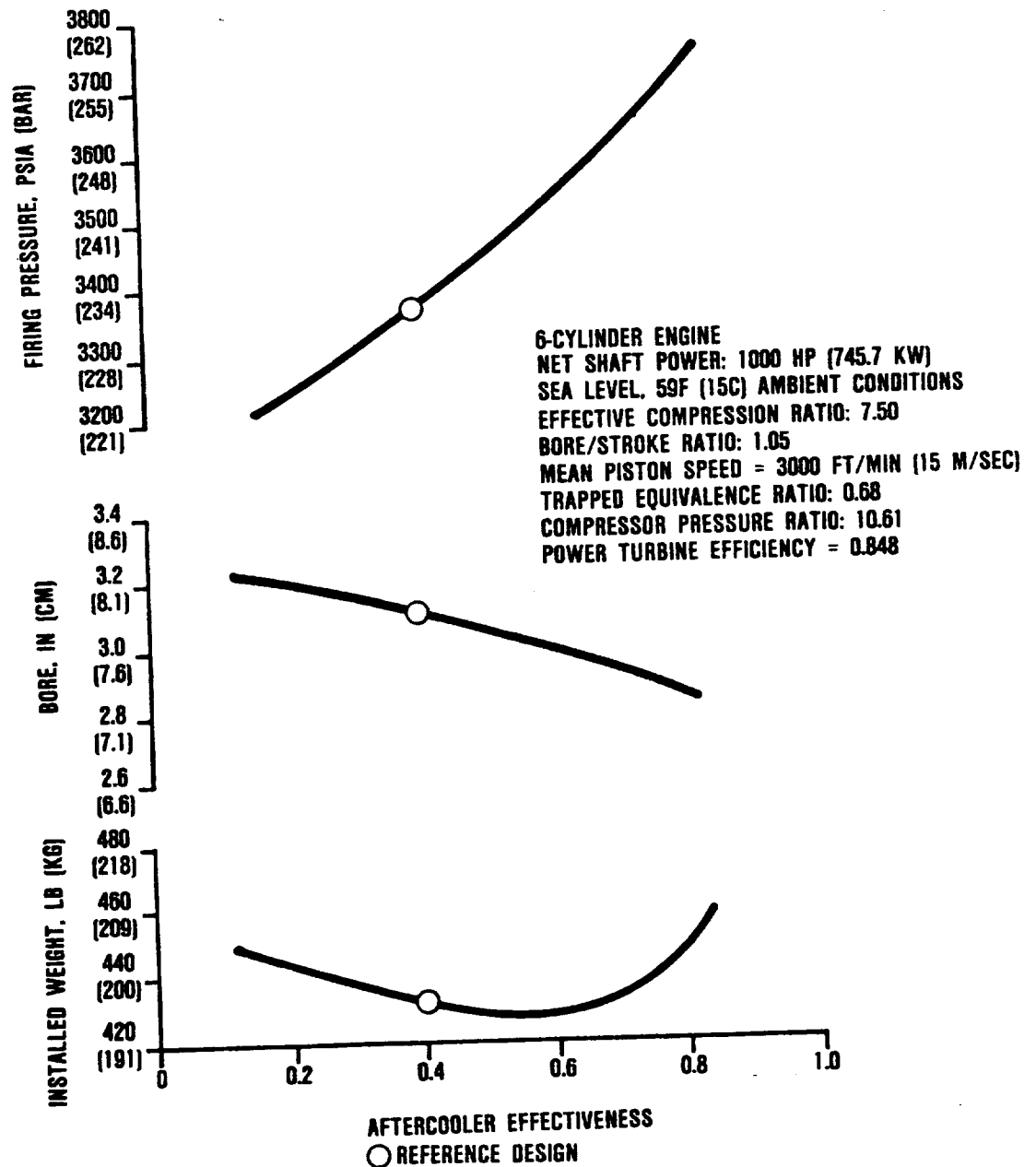


Figure 29. Effect of Aftercooler Effectiveness on CCE Design Performance.

Aftercooling reduced the cycle thermodynamic efficiency of a compound engine when firing pressure constraints (reduced compression ratio) and cooling fan power requirements were considered. It may be seen in Figure 30 that increasing the aftercooler effectiveness considerably reduces the intake manifold temperature, lowers the exhaust gas temperature about half as much, and slightly increases the BSFC. The nonaftercooled intake manifold temperature would be in excess of 700F (371C) at full load and 532F (277C) at 50 percent load. These high gas temperatures were believed to be deleterious to lubricant performance, ring/liner wear, and exhaust valve reliability. Therefore, an aftercooler effectiveness of 40 percent at rated load was chosen, which provided 436F (224.4C) air as the best compromise between installed weight, BSFC, and engine life/reliability requirements. The manifold air temperature was much lower at cruise power [300F (149C)], because the compressor pressure ratio at this load point was considerably reduced and the aftercooler effectiveness increased to 50 percent.

Installed weight and BSFC are depicted in Figure 31 as functions of compression ratio and compressor pressure ratio. Lower BSFC could be attained with a higher compression ratio, as would be expected. However, when applying the maximum firing pressure constraint, the best compromise between engine weight and thermodynamic efficiency was secured with a relatively low compression ratio. Effective compression ratio is defined in terms of trapped (volume at valve closure), rather than total, (BDC) displacement. Based on the compromise, the selected engine, therefore, has a compressor pressure ratio of 10.6 and a cylinder compression ratio of 7.5.

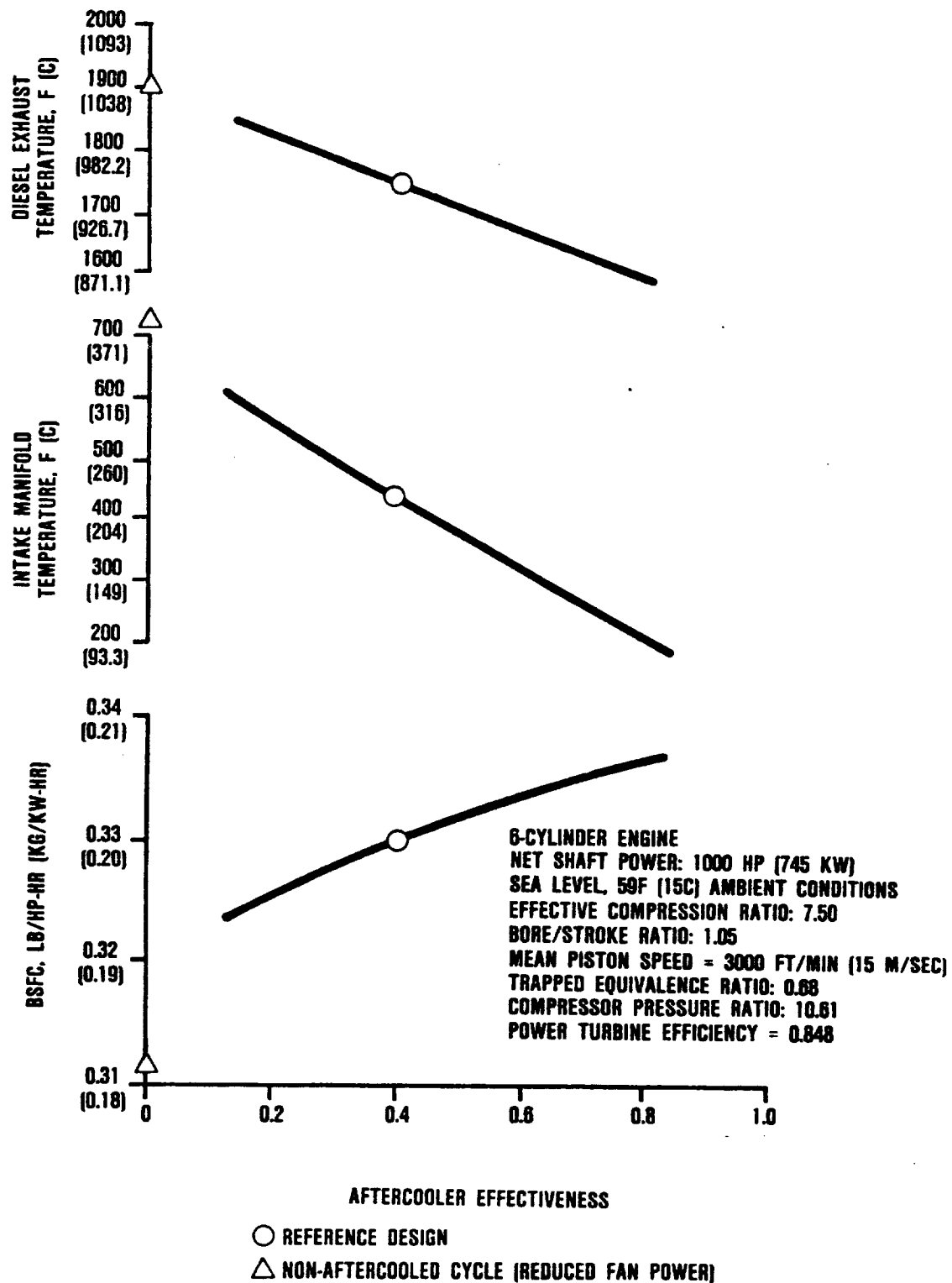


Figure 30. Effect of Aftercooler Effectiveness on CCE Design Performance.

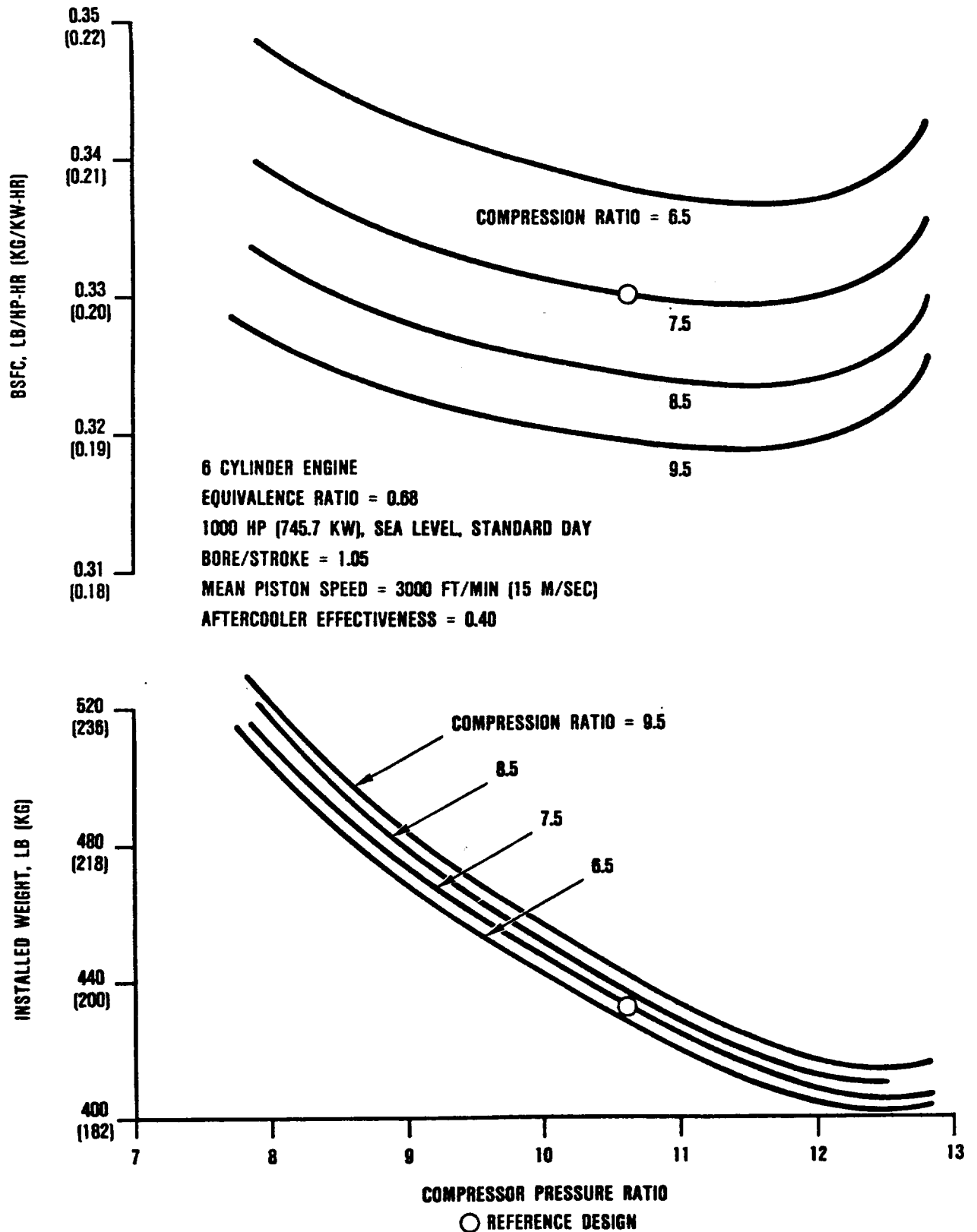


Figure 31. Effects of Compression Ratio and Compressor Pressure Ratio on CCE Design Performance.

### 4.3 Part-Power Performance

CCE part-power performance is depicted in Figure 32, wherein BSFC and trapped equivalence ratio are plotted versus net shaft power. It may be seen that a greater (richer) trapped fuel-to-air ratio (0.68 versus about 0.80) was required to produce the same sea-level power, at 4000 feet, 95F (1.22 km, 35C). Selected engine load points are itemized in Table 6 and it may be seen that the engine operating conditions at cruise power (80 percent of mission time) are very nearly at the levels of current diesel engines.

### 4.4 Engine Flat Rating

As a function of altitude for the selected CCE, Shaft horsepower and SFC are shown in Figure 33 for hot-, standard-, and cold-day conditions. Flat rating at 1000 shp (746 kW) for the various conditions was achieved by allowing the equivalence ratio to temporarily increase to a value of 0.80. This condition was reached at 4000, 7000, and 9600 feet (1.22, 2.13 and 2.93 km) for hot, standard, and cold days, respectively.

Flat rating in this study pertains to the means of restricting certain operating parameters at extreme ambient conditions, with particular reference to sea-level, 4000 feet (1.22 km), and 8000 feet (2.44 km) flight altitudes. In order to secure adequate piston ring and exhaust valve life, it was important that design-point firing pressure and mean exhaust gas temperature not be exceeded except under short-term emergency conditions on a 4000 feet, 95F (1.22 km, 35C) day.

In order to limit engine power and firing pressure to design values on a cold day between sea level and 9600 feet (2.93 km), both trapped equivalence ratio and injection timing must be

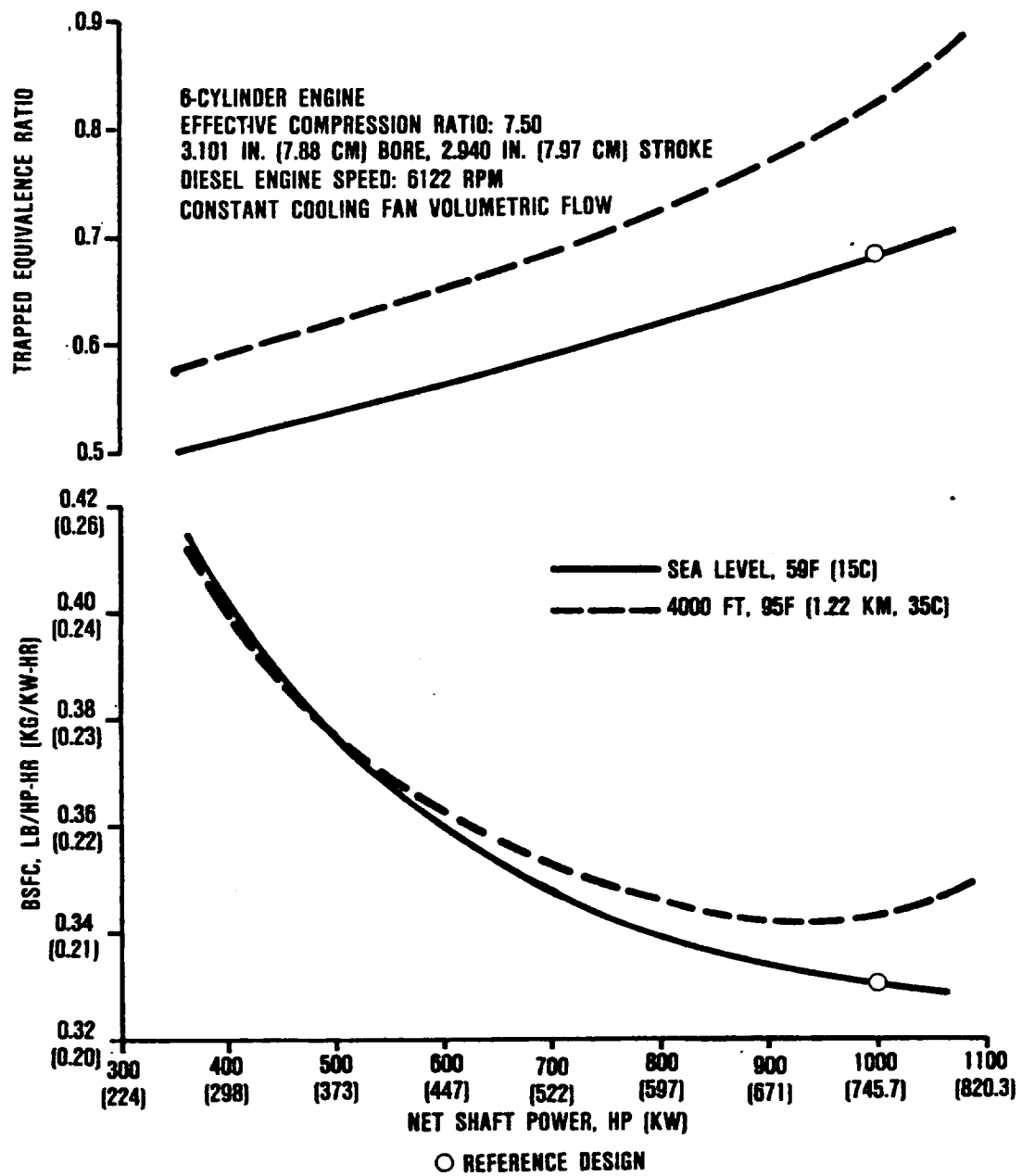


Figure 32. CCE Off-Design Performance.

Table 6. Selected Engine Conditions at 40 to 100 Percent Power.

| Percent power, sea level,<br>standard day  | 100                | 75  | 50                 | 40                 |
|--|--------------------|---|--------------------|--------------------|
| Shaft horsepower (kW)  | 1000<br>(746)      | 750<br>(559)  | 500<br>(373)       | 400<br>(298)       |
| Diesel power, hp (kW)  | 759<br>(566)       | 593<br>(442)  | 420<br>(313)       | 347<br>(259)       |
| Brayton power, hp (kW)   | 241<br>(180)       | 157<br>(117)  | 80<br>(60)         | 53<br>(40)         |
| BSFC, lb/hp-hr (kg/kW-hr)  | 0.3300<br>(0.2007) | 0.3438<br>(0.2091)  | 0.3763<br>(0.2289) | 0.4016<br>(0.2243) |
| $W_a$ , lb/sec (kg/sec)  | 2.442<br>(1.1)     | 2.072<br>(0.94)   | 1.640<br>(0.75)    | 1.441<br>(0.65)    |
| Trapping efficiency  | 74.63              | 75.36   | 76.25              | 76.71              |
| Indicated thermal efficiency   | 37.0               | 38.32   | 39.54              | 40.01              |
| Equivalence ratio  | 0.68               | 0.607   | 0.540              | 0.514              |
| Peak firing pressure, psia (bar)   | 3362<br>(231.9)    | 2859<br>(197.2)   | 2268<br>(156.4)    | 1995<br>(137.6)    |
| Compressor pressure ratio  | 10.61              | 8.65  | 6.56               | 5.66               |
| BMEP, psia (Bar)   | 393<br>(27.1)      | 313<br>(21.6)   | 229<br>(15.8)      | 194<br>(13.4)      |
| Exhaust temperature, F (C)   | 1754<br>(956.7)    | 1583<br>(861.7)   | 1416<br>(768.9)    | 1348<br>(731.1)    |
| Aftercooler effectiveness  | 0.40               | 0.45  | 0.51               | 0.54               |
| Manifold inlet temperature, F (C)  | 436<br>(224)       | 371<br>(188)  | 300<br>(149)       | 267<br>(130)       |
| Turbocompressor rpm  | 66,910             | 63,344  | 58,618             | 56,049             |
| Engine Parameters  |                    |   |                    |                    |
| $\text{rpm} = 6122$<br>$N = 6$<br>$B = 3.101 \text{ in}$<br>$(7.88 \text{ cm})$<br>$S = 2.940 \text{ in}$<br>$(7.47 \text{ cm})$ |                    | $D = 133.2 \text{ in}^3$<br>$(2.18 \text{ t})$<br>$WT = 432 \text{ lb}$<br>$(196 \text{ kg})$<br>$C/R = 7.50$ |                    |                    |



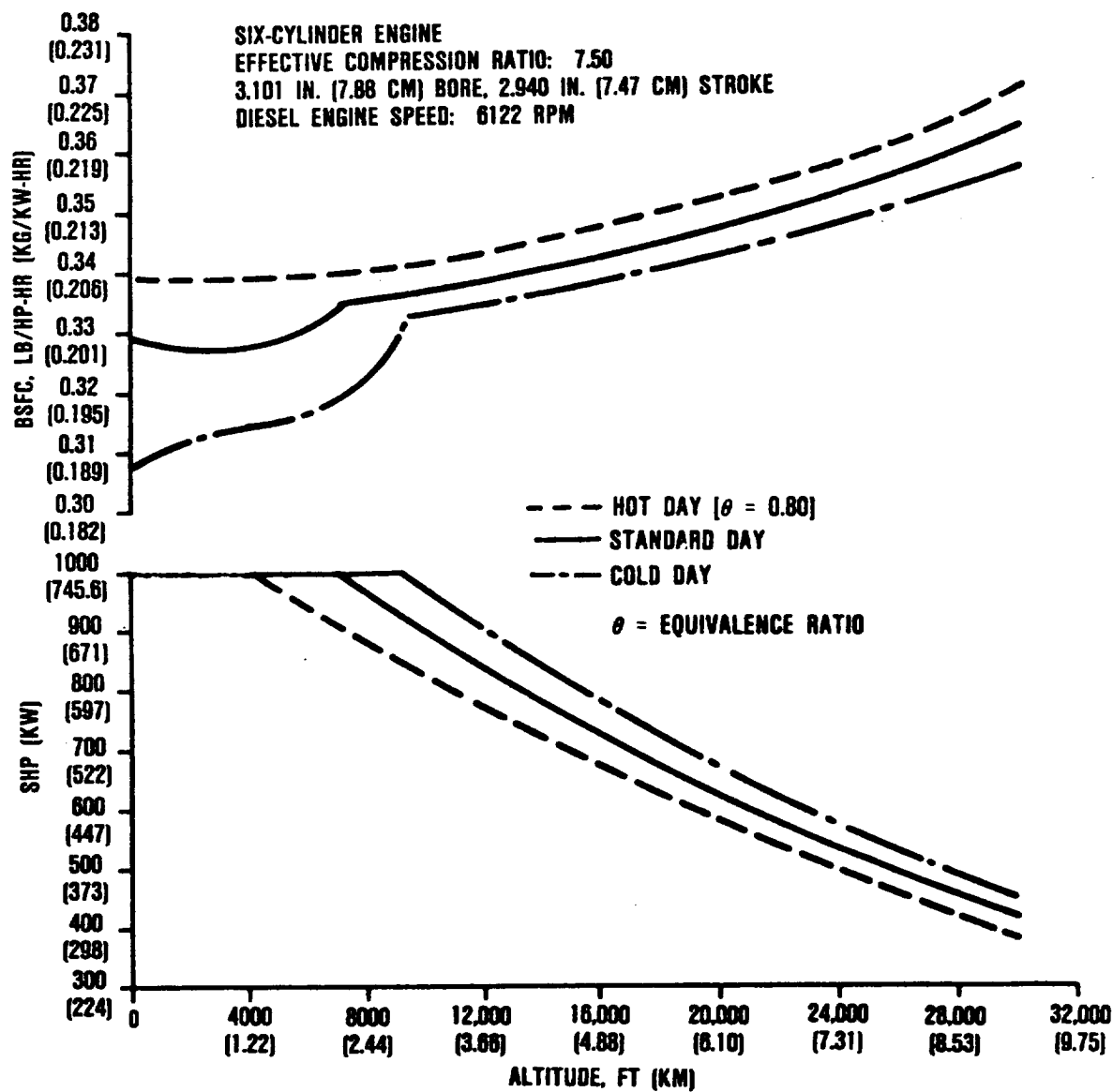


Figure 33. SHP and BSFC Performance of CCE Versus Altitude.

varied with ambient temperature. This schedule is shown in Figure 34 and would limit the maximum power to 1000 shp (746 kW) and the firing pressure to 3362 psia (231.8 bar) by the means of reducing fuel input and retarding the beginning of combustion. At temperatures above 59F (15C), the beginning of combustion remains constant at 23 degrees BTC and the equivalence ratio increases to a maximum of about 0.80.

Power lapse at altitude can be minimized by increasing trapped fuel-to-air ratio above the nominal smoke limit by fumigation. Figure 35 shows for a standard day, the degree where the power lapse can be minimized. Shaft horsepower, mean exhaust temperature, intake manifold temperature, and firing pressure are plotted versus trapped equivalence ratio with the design points identified. Trapped equivalence ratio includes both fumigant and injected fuel. Full power can be maintained up to 4000 feet (1.22 km) without exceeding the design firing pressure or the intake manifold temperature. However, the mean exhaust temperature is about 75F (41.7C) higher when the engine delivers 1000 horsepower (746 kW) at 4000 feet (1.22 km).

Similar data is depicted in Figure 36 for a hot-day atmosphere. It is necessary for the trapped equivalence ratio (fumigated plus injected fuel) to be increased to 0.76 so that rated (1000 shp) power can be obtained on a sea level, hot day. The exhaust gas temperature at this rating is 1920F (1049C), which is 170F (94C) hotter than for a standard day and is close to the limiting value. The 4000 (1.22 km) and 8000 feet, (2.44 km) hot-day power levels have been increased to the equivalence ratio of 0.80, at which point the exhaust gas temperatures approach 2000F (1093C). Extended operation at these temperatures would be detrimental to exhaust valve life unless special measures were taken on material, preferential cooling, and insulation.

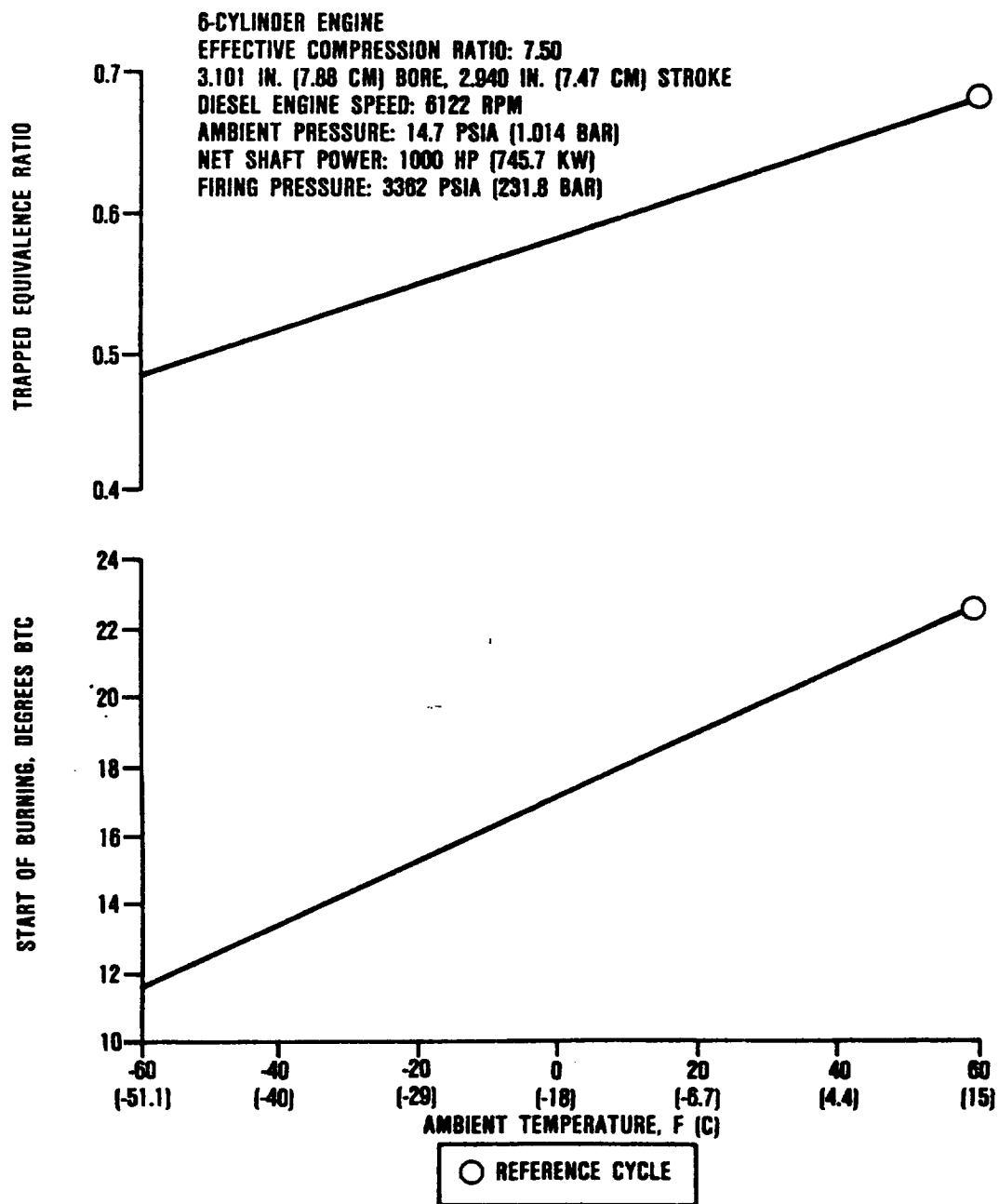


Figure 34. Injection Timing Schedule at Low Ambient Temperature.

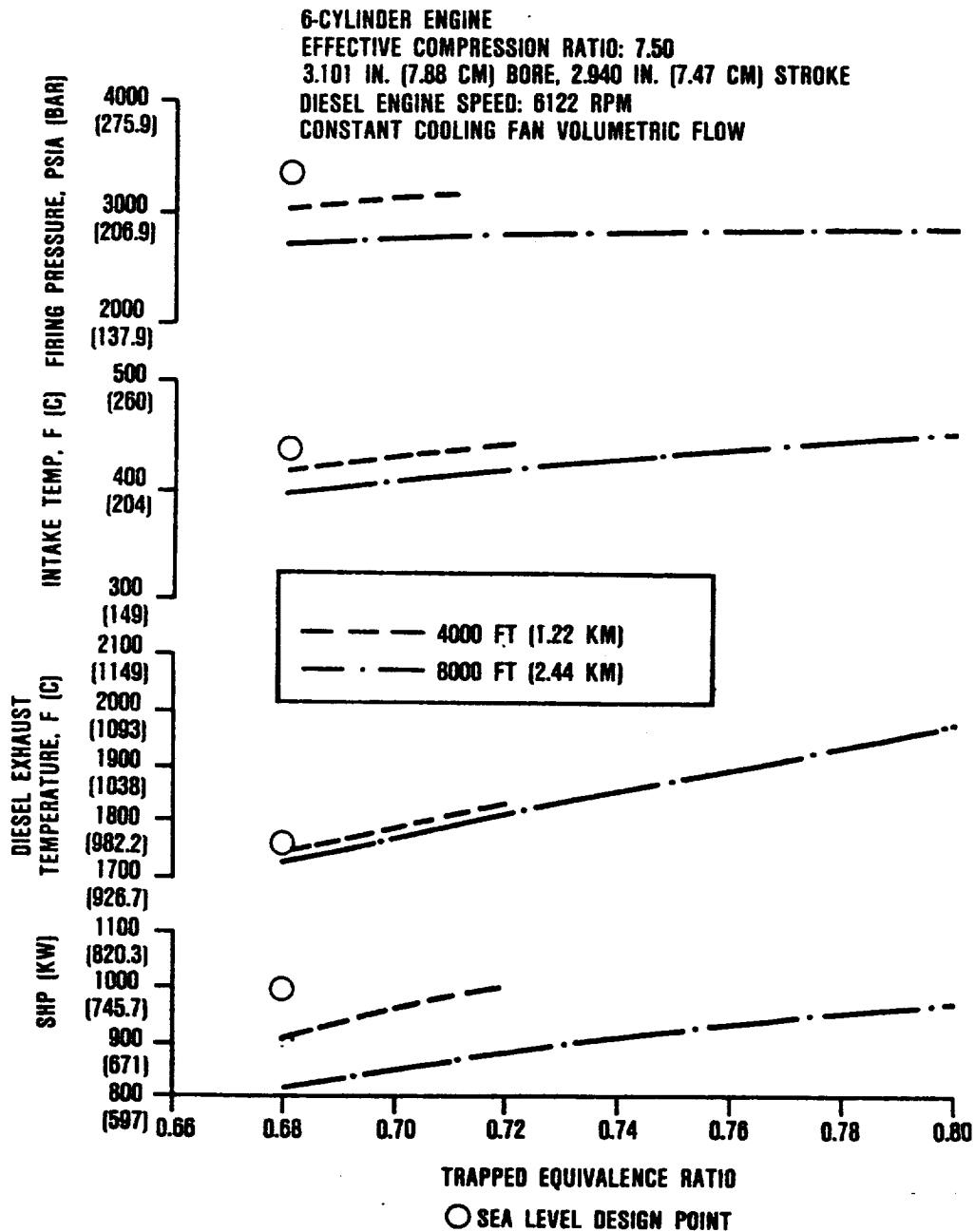


Figure 35. CCE Standard-Day Performance.

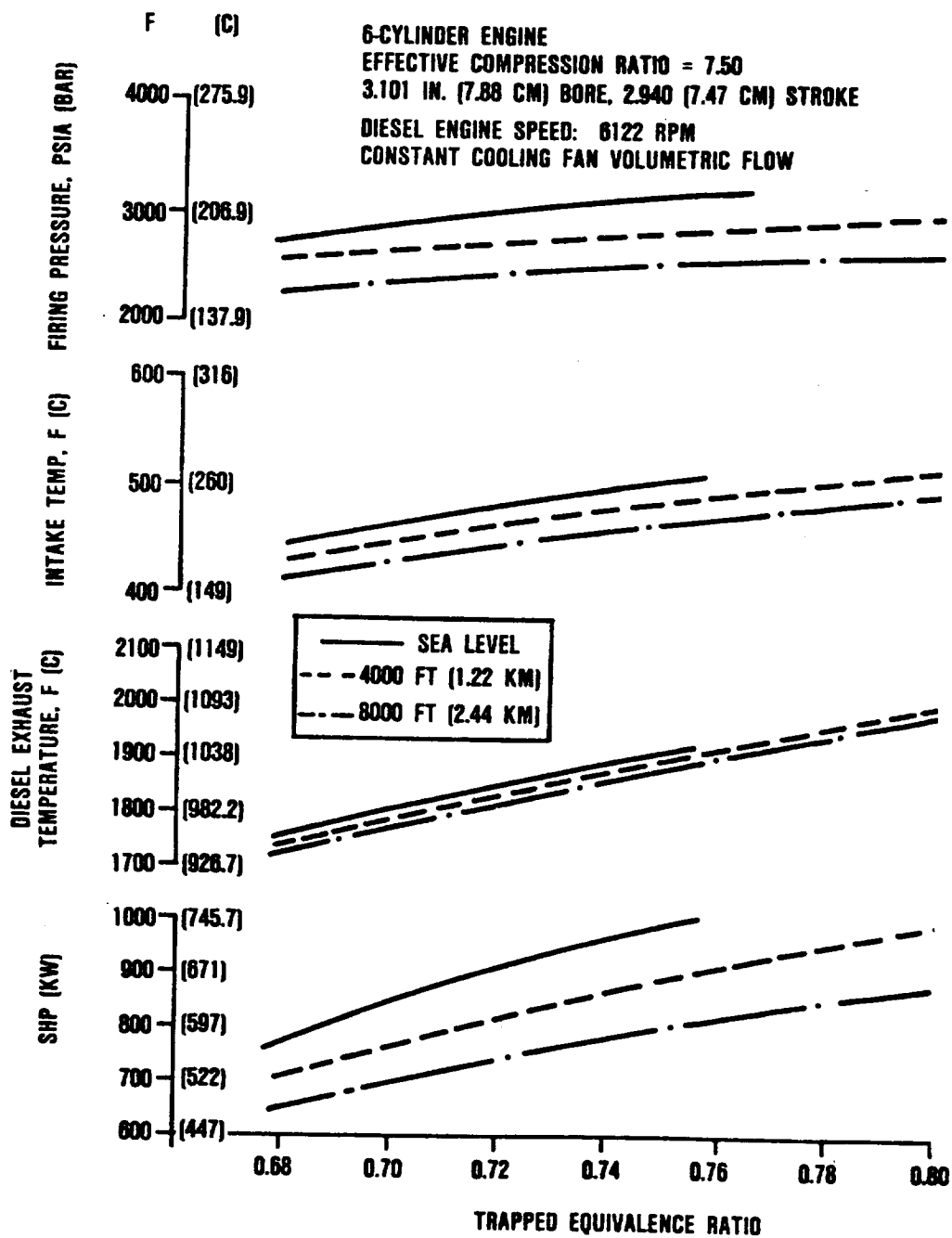


Figure 36. CCE Hot-Day Performance.

#### 4.5 Contingency and Emergency Power Requirements

Twin engine helicopters are often sized by power requirement of safe mission completion after the failure of one of the two engines.<sup>20</sup> Emergency or contingency power requirements for the helicopter are shown in Table 7, and represent a wide range of engine output and required life. The typical mission profile (Figure 24) indicates that 50 percent or less of the rated power is required for 80 percent of the time and this power profile is the basis for the 2000 hour TBO. As the emergency power level is increased, the required life is drastically reduced, until at the 120 percent rating, a normal one-time-only requirement is shown.

##### 4.5.1 Power Increase by Fumigation

Emergency, short-term power augmentation can be obtained by introducing diesel fuel or a water-alcohol mixture into the intake manifold. This technique has been called "fumigation" by Schweitzer<sup>21</sup> and makes it feasible to increase the smoke-free output of a diesel engine to a greater extent than by in-cylinder fuel injection alone. In addition, the evaporative cooling with water-methanol causes the charge air density to be greater and is comparable to increasing the aftercooler effectiveness.

It is necessary to know the cylinder-trapped air content so that the correct amount of fumigated plus injected fuel may be simulated and their heat release contributions added to the cycle.

Since the Benson model does not recognize the difference between pure air and a fumigant-air mixture, the injected trapped equivalence ratio is corrected to account for fumigant fraction entering with the air. The fumigation program was subsequently incorporated into the combined cycle model to facilitate power

**Table 7. Contingency or Emergency Power Requirements.**

| <b>Engine Power, Percent</b> | <b>Load Type</b>   | <b>Life Requirement</b> | <b>Special Notes</b>                  |
|------------------------------|--------------------|-------------------------|---------------------------------------|
| ---                          | <b>Start/Stop</b>  | <b>2000 cycles</b>      |                                       |
| <b>70</b>                    | <b>(MCP)</b>       | <b>2000 hours</b>       | <b>(Cruise)</b>                       |
| <b>100</b>                   | <b>(IRP)*</b>      | <b>30 minutes</b>       | <b>(Each time)</b>                    |
| <b>105</b>                   | <b>(OEI)</b>       | <b>10 minutes</b>       | <b>(Maneuvers)</b>                    |
| <b>110</b>                   | <b>Contingency</b> | <b>2-1/2 minutes</b>    | <b>(Inspection required)</b>          |
| <b>120</b>                   | <b>Burnout</b>     | <b>30 seconds</b>       | <b>(One time Inspection required)</b> |

**Definitions**

**MCP** Maximum Continuous Power

**IRP** Intermittant Rated Power

**OEI** One Engine Inoperative

**\*Take Off/Hover**

boosting studies. Some of the fumigant is lost due to imperfect scavenging. Fumigant fraction in the exhaust is calculated and accounted for in the energy balance.

The effect of fumigation and engine overspeed on performance was investigated for the six-cylinder reference engine at sea-level, standard-day, and hot-day ambient conditions. Based on available trapped air, injected fuel trapped equivalence ratio is held constant at 0.68. The combined (injected plus fumigant) fuel heat release schedule is assumed to be identical to that of the nonfumigated engine, due to lack of specific information to define a different method.

The 110 percent contingency power operating conditions for sea level, 95F (35C) with 10 percent overspeed are displayed in Table 8 for comparison with those of the 1000 shp (746 kW) design point. Although this is not necessarily a diesel limit, for practical purposes, it is feasible for the engine to run for the required 2-1/2 minutes at the 110 percent power operating point, which has a 10 percent higher speed and 230F (128C) hotter exhaust gas temperature.

Figure 32 shows the effects of fumigant-increased equivalence ratio on shaft horsepower, diesel exhaust temperature, intake manifold temperature, and firing pressure when diesel fuel was employed as the fumigant. The curves are shown for both rated (6122 rpm) and 10 percent engine over speed. For example, at the 1200 shp (895 kW) output, it is possible to run at a lower equivalence ratio (0.03 less) at the overspeed. However, the diesel exhaust temperature and intake temperature for both cases are about equal. The firing pressure is 150 psi (10.3 bar) lower for the 110 percent speed condition because of the reduced BMEP and manifold pressures.



**Table 8. Comparison of Selected Engine Conditions--Sea Level, Standard Day, and Contingency Power at Sea Level, 95F (35C).**

|   | <b>Rated<br/>Power<br/>Sea Level,<br/>59F (15C)</b> | <b>Contingency<br/>Power<br/>Sea Level,<br/>95F (35C)</b> |
|---|---|---|
| Shaft horsepower (kW)   | 1000<br>(746)                                       | 1100<br>(820)   |
| Diesel power, hp (kW)   | 759<br>(566)  | 810<br>(604)  |
| Brayton power, hp (kW)  | 241<br>(180)  | 290<br>(21.6)   |
| BSFC, lb/hp-hr (kg/kW-hr)   | 0.33<br>(0.20)                                      | 0.337<br>(0.205)  |
| Engine rpm  | 6122  | 6734  |
| $W_a$ (lb/sec) (kg/sec)   | 2.442<br>(1.11)                                     | 2.442<br>(1.11)   |
| Trapping efficiency   | 74.6  | 75.6  |
| Ind. thermal efficiency   | 37.0  | 35.4  |
| Equivalence ratio   | 0.68  | 0.75  |
| Peak firing pressure, psia (bar)  | 3362<br>(231.9)                                     | 3318<br>(228.8)   |
| Compressor pressure ratio   | 10.61   | 11.26   |
| BMEP, psia (bar)  | 393<br>(27.1)                                       | 386<br>(26.6)   |
| Exhaust temperature, F (C)  | 1754<br>(956.7)                                     | 1986<br>(1085.6)  |
| Aftercooler effectiveness   | 0.4   | 0.4   |
| Manifold inlet temperature, F (C)   | 436<br>(224.4)                                      | 511<br>(266.1)  |
| Turbocompressor rpm   | 66,910  | 70,529  |
| <div> <div> N = 6<br/>B = 3.101 inch<br/>(7.88 cm)<br/>S = 2.940 inch<br/>(7.47 cm) </div> <div> D = 133.2 in<sup>3</sup> (2.182)<br/>WT = 432 lb (196 kg)<br/>C/R = 7.50 </div> </div> |   |   |

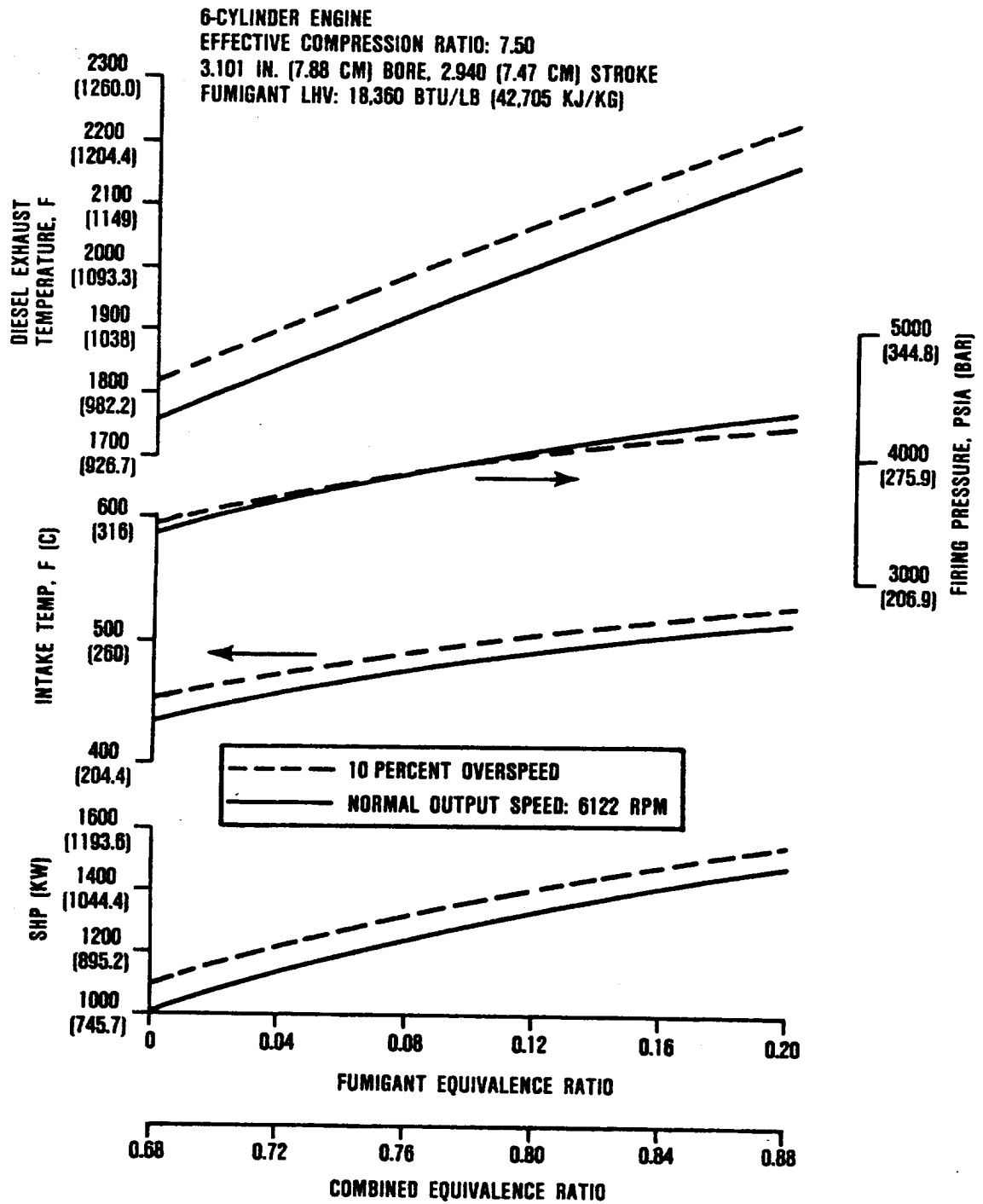
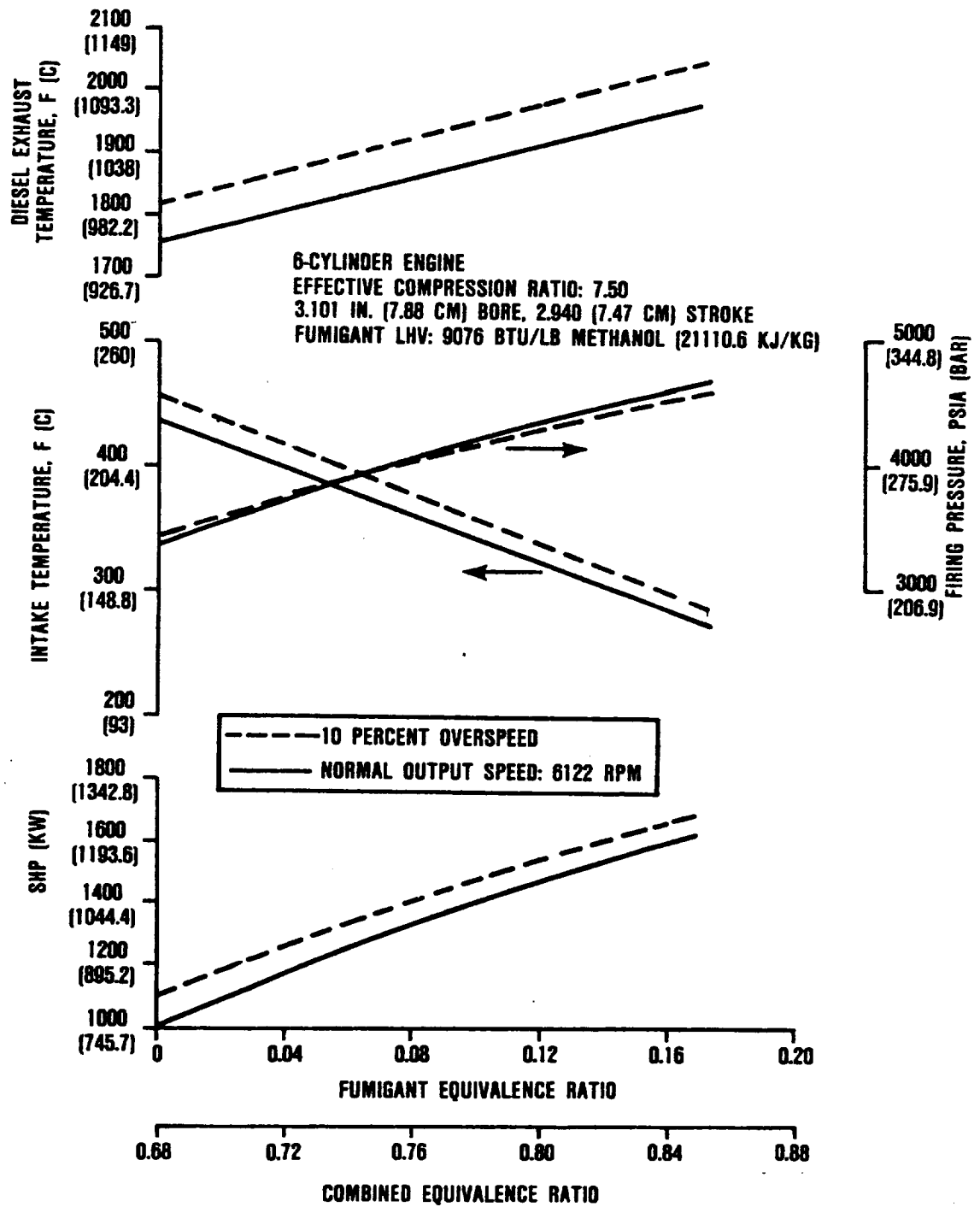


Figure 37. Fumigation Power Boosting with Diesel Fuel.

The 140 percent power boost point is about 0.08 higher equivalence ratio than at 120 percent output for the same engine speed comparison. The diesel exhaust temperature is 150F (83C) above the 120 percent value and almost 300F (167C) higher than at 1000 shp or 100 percent rated power. The peak firing pressure at 140 percent power is 4200 psi (289.7 bar), which is 840 psi (57.9 bar) greater than at rated power and speed. At the overspeed condition, the firing pressure is 4000 psi (275.9 bar), which is 640 psi (44.1 bar) higher than at rated condition.

Similar data is plotted in Figure 38 for methanol-water fumigation and it may be seen that both the intake and exhaust manifold temperatures are lower at the same power output than when diesel fuel is the fumigant. In fact, the exhaust temperatures at 120 and 140 percent power are about 150F (83C) lower with methanol-water fumigation than when diesel fuel was employed. Conversely, the cylinder firing pressure is somewhat greater with the methanol-water fumigant. However, the potential benefits must be weighed against the disadvantages of supplying an additional subsystem plus the weight of fumigant, tank, and control system on board the helicopter.

Emergency power requirements are just that. The alternative to these temporary higher power outputs is that the helicopter will no longer be airborne or controllable in flight. In view of this, the increases in engine output on a short-time basis is justified even though the resultant engine life may be drastically shortened. The actual benefits and penalties of power boosting by fumigation will be determined by engine tests, but a requirement for increased output on a short-time basis can be met.



**Figure 38. Fumigation Power Boosting with 40-Percent Methanol-Water.**

## 5.0 MISSION COMPARISON BETWEEN A COMPOUND CYCLE ENGINE AND A GAS TURBINE

The major objective of the helicopter application feasibility study was to identify a CCE design that has the potential of 30 percent savings in mission fuel consumption, when compared with a contemporary simple-cycle gas turbine. The CCE used in the comparison was a 2-stroke cycle uniflow engine equipped with 1-1/2 spool turbomachinery and aftercooling. Another objective was to minimize overall engine plus fuel weight in order to maximize range plus payload product.

### 5.1 Gas Turbine Description

The contemporary simple-cycle gas turbine used for the comparison study is considered an advanced design that employs demonstrated state-of-the-art component technology improvements and is scheduled for production in the early 1990s. Although specific power is expected to increase, no significant SFC reduction is envisioned for this gas turbine engine by the year 2000.

### 5.2 Results of Comparison

A comparison of some of the key engine parameters for both engines at rated power, sea level, standard day is shown in Table 9.

It is evident that the CCE T<sub>4</sub> exhaust temperature is some 480F (267C) cooler than for the gas turbine inlet and that the core airflow of the CCE is about 30 percent of that of the turbine. The comparison of maximum cycle pressure ratios shows why the CCE thermodynamic efficiency is much higher than that of gas

**Table 9. Comparison of Key Engine Parameters.**

| <b>Parameter</b>                                | <b>CCE</b>             | <b>Gas Turbine</b>      |
|---|------------------------|-------------------------|
| <b>T<sub>4</sub> Maximum Temperature, F (C)</b> | <b>1,754<br/>(956)</b> | <b>2,234<br/>(1223)</b> |
| <b>Core Air Flow, lb/sec (kg/sec)</b>           | <b>2.44<br/>(1.11)</b> | <b>8.34<br/>(3.79)</b>  |
| <b>Maximum Cycle Pressure Ratio</b>             | <b>109:1</b>           | <b>14.1:1</b>           |
| <b>Diesel (constant), rpm</b>                   | <b>6,122</b>           | <b>--</b>               |
| <b>Gas Generator, rpm</b>                       | <b>66,910</b>          | <b>43,797</b>           |
| <b>Power Turbine, rpm</b>                       | <b>19,000</b>          | <b>23,000</b>           |

turbines--there being almost an 8:1 difference between their expansion ratios.

The part-load performance characteristics of the CCE and the gas turbine are compared in Figure 39. This shows a considerable margin of fuel consumption savings for the CCE over the full helicopter flight-load range. For example, at 50 power rating, the CCE uses 88.7 pounds (40.3 kg) less fuel per hour, or 32 percent less fuel than the gas turbine.

Both engines were designed to be flat-rated at 1000 shp (746 kW) to 4000 feet (1.22 km), 95F (35C) day, for the mission weight (engine plus fuel) comparison. Flat-rating of the CCE was accomplished by burning more fuel, thereby raising the trapped equivalence ratio from 0.68 (sea level, standard day) to 0.80 (4000 feet, 95F) (1.22 km, 35C). The trapped equivalence ratio includes both fumigated and injected fuel. Gas generator or turbocompressor speed was increased about 7 percent to 71,775 rpm, peak firing pressure was held at 3362 psi (231.9 bar), and the diesel cylinder exhaust gas temperature peaked at 2042F (1116C). The core airflow decreased slightly to 2.20 lb/sec (1.0 kg/sec). The gas turbine was designed for 1400 shp (1044 kW) at sea-level, standard-day conditions so that it would produce 1000 shp (746 kW) at 4000 feet, 95F (1.22 km, 35C), while limiting the  $T_4$  (turbine inlet) maximum temperature to 2234F (1223C). Gas generator speed decreased to 42,176 rpm, and core air flow decreased to 7.65 lb/sec (3.47 kg/sec) at 4000 feet (1.22 km) altitude.

The results of the comparison study are shown in Table 10 for the specified 2.5-hour composite mission/load profile. Total fuel, tank, and engine weight have been calculated based on engine power versus time operating conditions. A review shows that the CCE uses 31.4 percent less mission fuel. Also, even though the CCE is heavier, the overall engine plus fuel weight

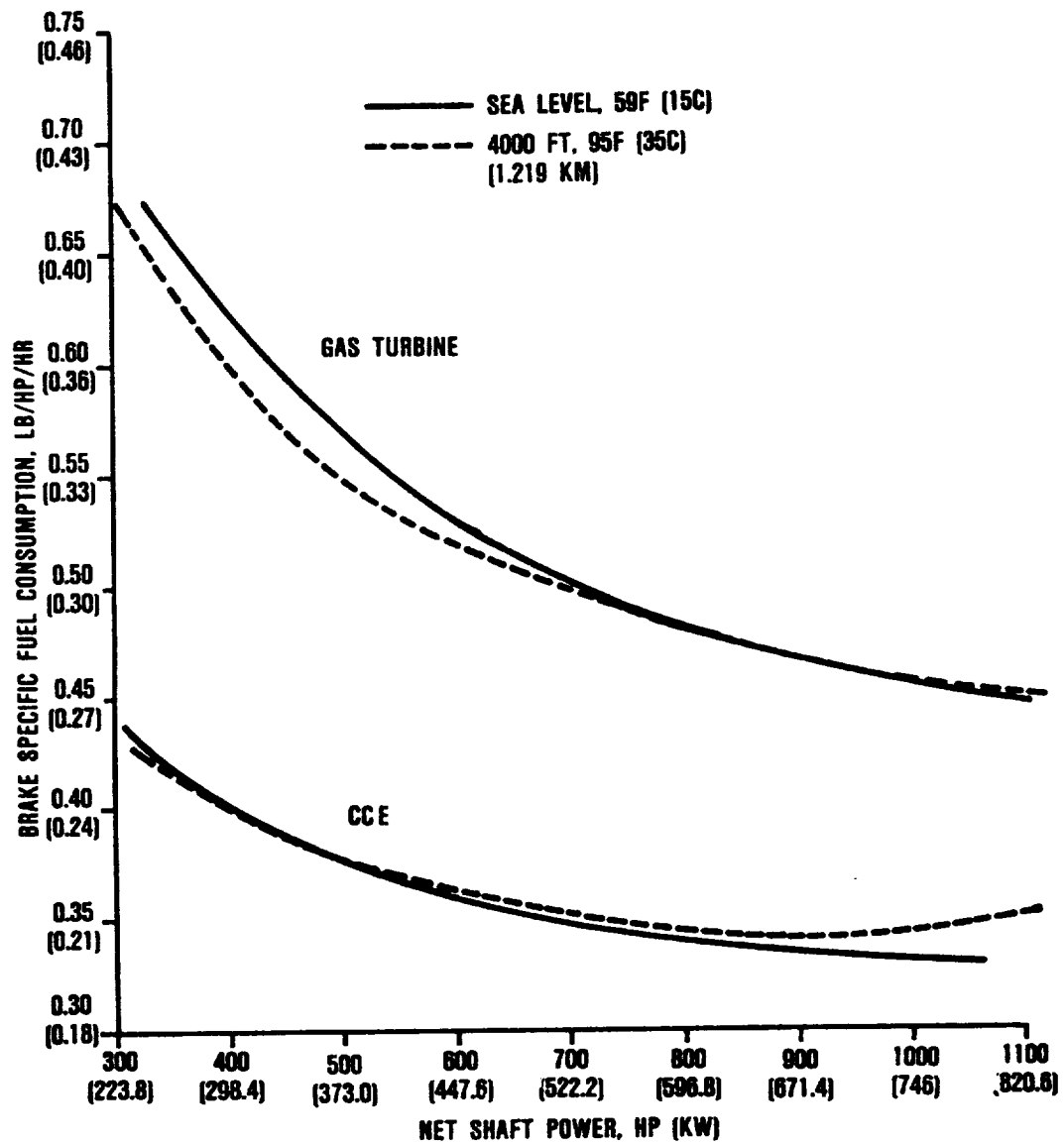


Figure 39. Brake Specific Fuel Consumption Comparison, CCE Versus Simple-Cycle Gas Turbine.



Table 10. CCE/GAS Turbine Weight Comparison at 4000 Feet, 95F, Static Conditions\*\*\*.

| CCE                             |             |                           | Gas Turbine          |                           |                      |
|---------------------------------|-------------|---------------------------|----------------------|---------------------------|----------------------|
| Percent Power                   | Time, hours | BSFC, lb/hp-hr (kg/kW-hr) | Weight Fuel, lb (kg) | BSFC, lb/hp-hr (kg/kW-hr) | Weight Fuel, lb (kg) |
| 100                             | 0.08        | 0.342 (0.208)             | 28.6 (13.0)          | 0.457 (0.278)             | 38.1 (17.3)          |
| 75                              | 0.42        | 0.349 (0.212)             | 109.2 (49.6)         | 0.490 (0.298)             | 153.3 (69.6)         |
| 50                              | 0.58        | 0.377 (0.229)             | 110.0 (49.9)         | 0.553 (0.336)             | 161.5 (73.3)         |
| 40                              | 0.92        | 0.400 (0.243)             | 146.1 (66.3)         | 0.603 (0.367)             | 221.4 (100.5)        |
| 50 (reserve)                    | <u>0.50</u> | 0.377 (0.229)             | <u>94.3</u> (42.8)   | 0.553 (0.336)             | <u>138.5</u> (62.9)  |
| Totals                          | 2.50        |                           | **488.7 (221.6)      |                           | 712.8 (323.6)        |
| Fuel =                          |             |                           | 488.7 (221.6)        | **712.8 (323.6)           |                      |
| Fuel Tank Weight =              |             |                           | 83.0 (37.7)          | 121.1 (55.0)              |                      |
| Installed Engine Weight =       |             |                           | 432.4 (196.3)        | 358.0 (162.5)             |                      |
| Total: Fuel, Tank, and Engine = |             |                           | * 1004.1 (455.6)     | *1191.9 (541.1)           |                      |
| For Two Engines =               |             |                           | 2008.3 (911.8)       | 2383.9 (1082.3)           |                      |

$$\text{*Percent Weight Savings: } 1.0 - \frac{\text{CCE Total Weight}}{\text{Gas Turbine Weight}} = 158$$

$$\text{**Percent Fuel Savings: } 1.0 - \frac{\text{CCE Total Fuel Weight}}{\text{Gas Turbine Fuel Weight}} = 31.4$$

\*\*\*Reference Figure 3 Mission Power/Time Profile

for the CCE is 15.8 percent less. These numbers may also be translated into more range or more payload for the same gross weight vehicles:

- o 36.5 percent increase in payload, or
- o 40.7 percent increase in range

The potential exists for one-third more missions for a given quantity of fuel.

The engine box volumes for the CCE and the gas turbine are 14 ft<sup>3</sup> (0.39 m<sup>3</sup>) and 11.5 ft<sup>3</sup> (0.32 m<sup>3</sup>), respectively. However, the helicopter will have 5.03 ft<sup>3</sup> (0.14 m<sup>3</sup>) less of fuel tankage (including a 15 percent expansion space) when the more fuel-efficient CCE is installed. Thus, when both the engine box and fuel tank volumes are taken into account, the CCE could have a net of 8.5 percent savings in total volume over the gas turbine engine.

### 5.3 Infrared Signature

Having a greater thermal efficiency than a comparable gas turbine, the CCE engine will discharge at full power, exhaust gases at a lower temperature (970F versus 1130F [521C versus 610C]). In addition, the oil cooler and aftercooler discharge airflow is 4.2 times the full-load combustion airflow. This cooling air stream is designed to be mixed with the power turbine exhaust flow, further reducing its mean gas temperature. Figure 40 shows that the CCE discharge gas temperature does not exceed 350F (177C). In fact, it is some 800F (444C) cooler than the exhaust gas of a contemporary gas turbine engine at 4000 feet (1.22 km), 95F (35C) conditions.

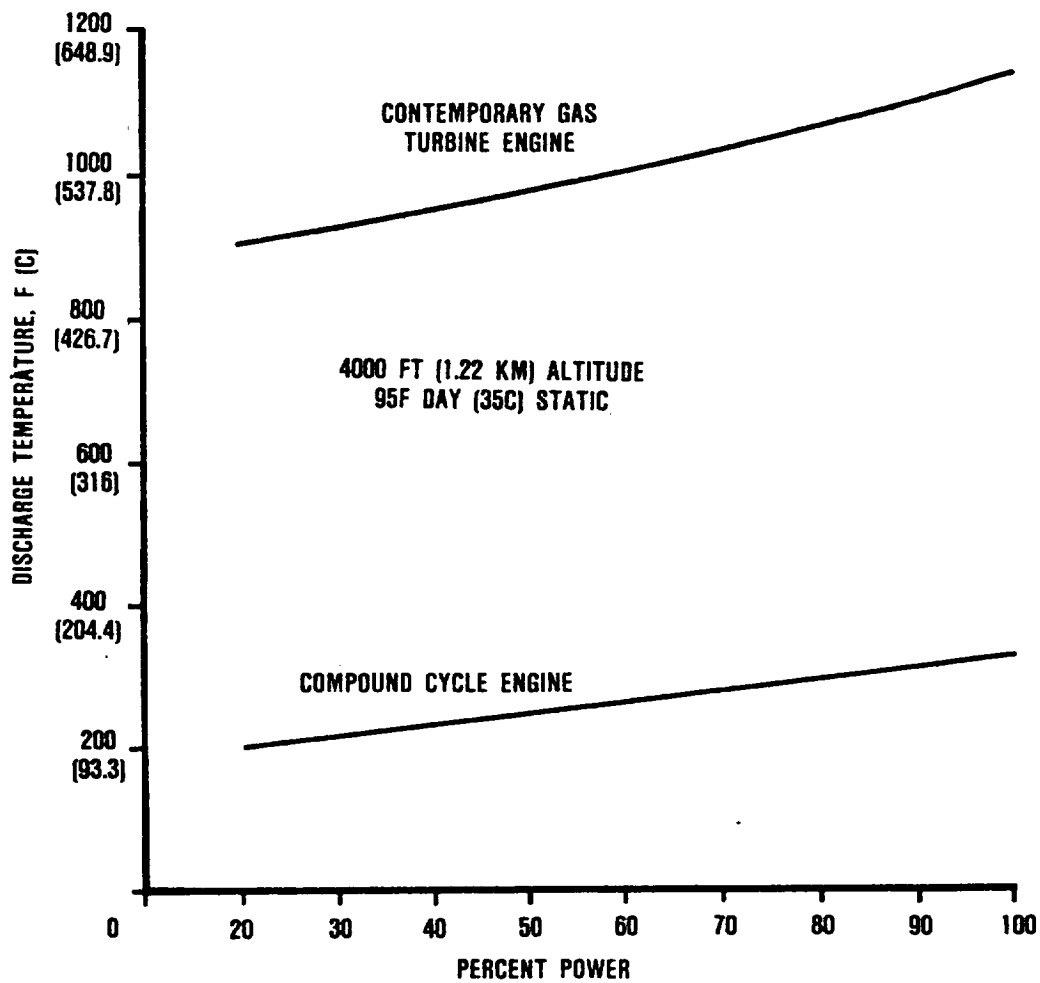


Figure 40. Comparison of Exhaust Discharge Temperatures for Gas Turbine and CCE.

## 6.0 CONCEPTUAL ENGINE DESIGN

### 6.1 CCE Configuration

The engine conceptual design layout is shown in Figure 41. However, the design layout is flexible and can be configured to specific aircraft requirements. The engine consists of the diesel core and turbomachinery major modules. The turbomachinery module consists of a turbocharging spool with a two-stage, backward-curved, broad-range, high-pressure-ratio centrifugal compressor driven by a single-stage radial inflow turbine and a single-stage axial power turbine that is geared into the compounding gearbox. The turbomachinery is mounted into the V-form of the diesel core. This minimizes the overall box volume to less than 14 ft<sup>3</sup> (0.39 m<sup>3</sup>), which includes the oil cooler and aftercooler. The 2-stroke cycle diesel module consists of six cylinders that are uniflow scavenged. The engine is oil cooled and fully self-contained, with all engine required-to-run controls and accessories. Total installed weight, including oil cooler with oil, oil cooler fan, and inlet air particle separator, is 432 pounds (196 kg).

The overall cycle pressures, temperatures, efficiencies, losses, and shaft powers for the selected cycle are shown in Figure 42.

### 6.2 Conceptual Details and Materials

#### 6.2.1 Diesel Core

The 2-stroke-cycle diesel core design incorporates the six cylinders in a 135-degree V angle. Bore and stroke are 3.1 and 2.94 inches (7.9 and 7.5 cm) respectively, for a total displacement of 133 in<sup>3</sup> (2.17ℓ). The engine is uniflow scavenged, with a

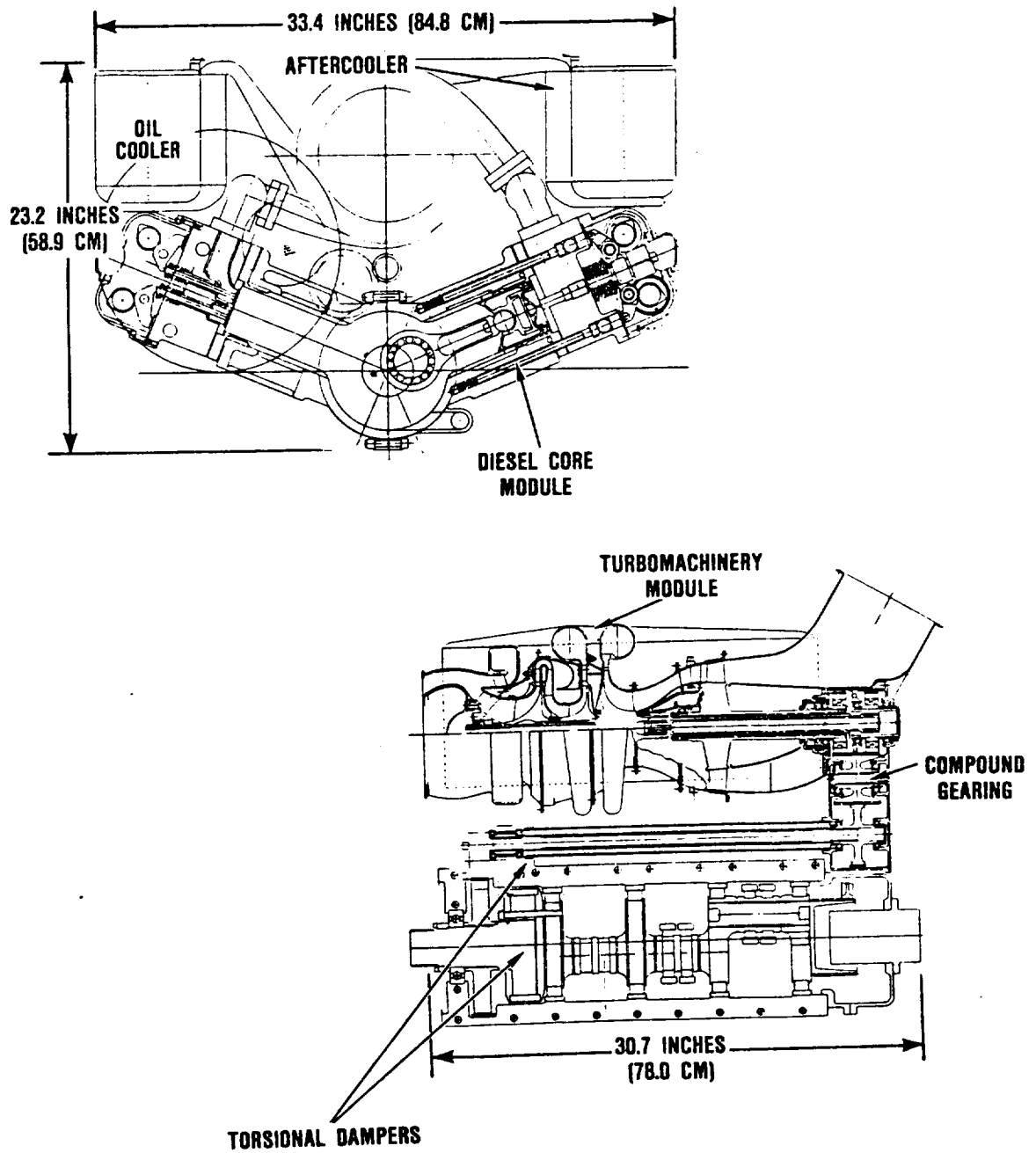
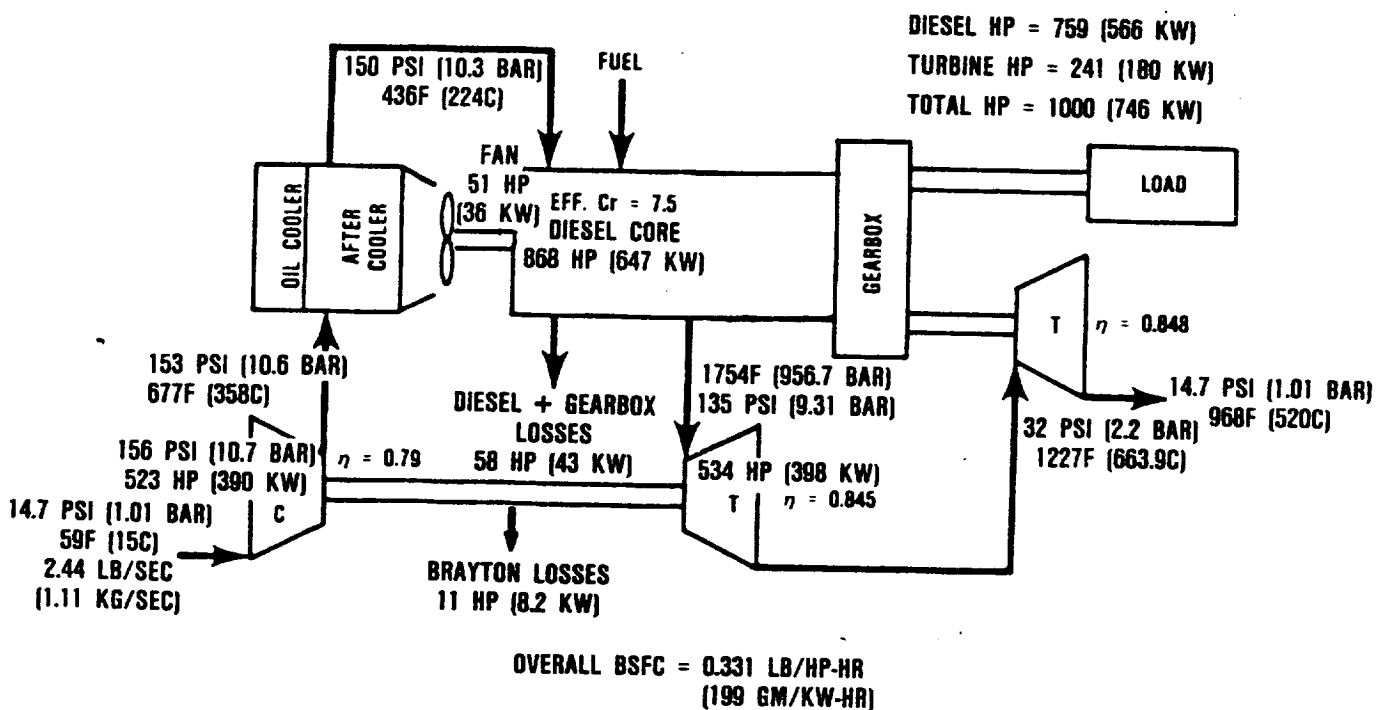


Figure 41. Conceptual Design of 1-1/2 Spool, CCE.



**Figure 42. Sea-Level, Standard-Day, Design Point Operating Conditions of Selected 1-1/2 Spool CCE.**

series of intake ports in the cylinder liner that are uncovered near BDC. Four poppet-type exhaust valves for each cylinder, located in the head are operated by dual overhead cam shafts.

The crankcase, tunnel-type is constructed of aluminum alloy and is split on the main bearing bore centerline so that the power assemblies can be installed. The crankshaft is of "built-up" construction with integral rolling element bearings made of VIMVAR M-50 steel at the main and crank pin journals. These bearings were selected to provide low drag for cold starting, minimum oil flow requirements, low friction and oil interruption capability.

Curvic couplings are used on the crankpin ends to provide for assembly of the one-piece connecting rods. A tie-bolt through each crankpin will provide the required clamp load to restrain torque, stress, and bending moments at the curvic positions. The curvic couplings will provide an accurate and repeatable positioning of the crankshaft components during assembly.

The pistons are also of "built-up" construction. The dome portion is made of heat-resistant materials that are isolated and insulated from the rest of the piston. The skirt is made of silver-plated steel and has a "ripple" finish to reduce scuffing tendencies and support an oil film. In this manner, heat loss through the piston dome is minimized. The heat that is conducted is then removed by "cocktail shaker" oil cooling. The piston rings are plasma-sprayed chrome carbide and nickel chromide in a molybdenum matrix. The M-50 steel wrist pin is designed for a squeeze film or "rocking pad" bearing, which is silver plated.

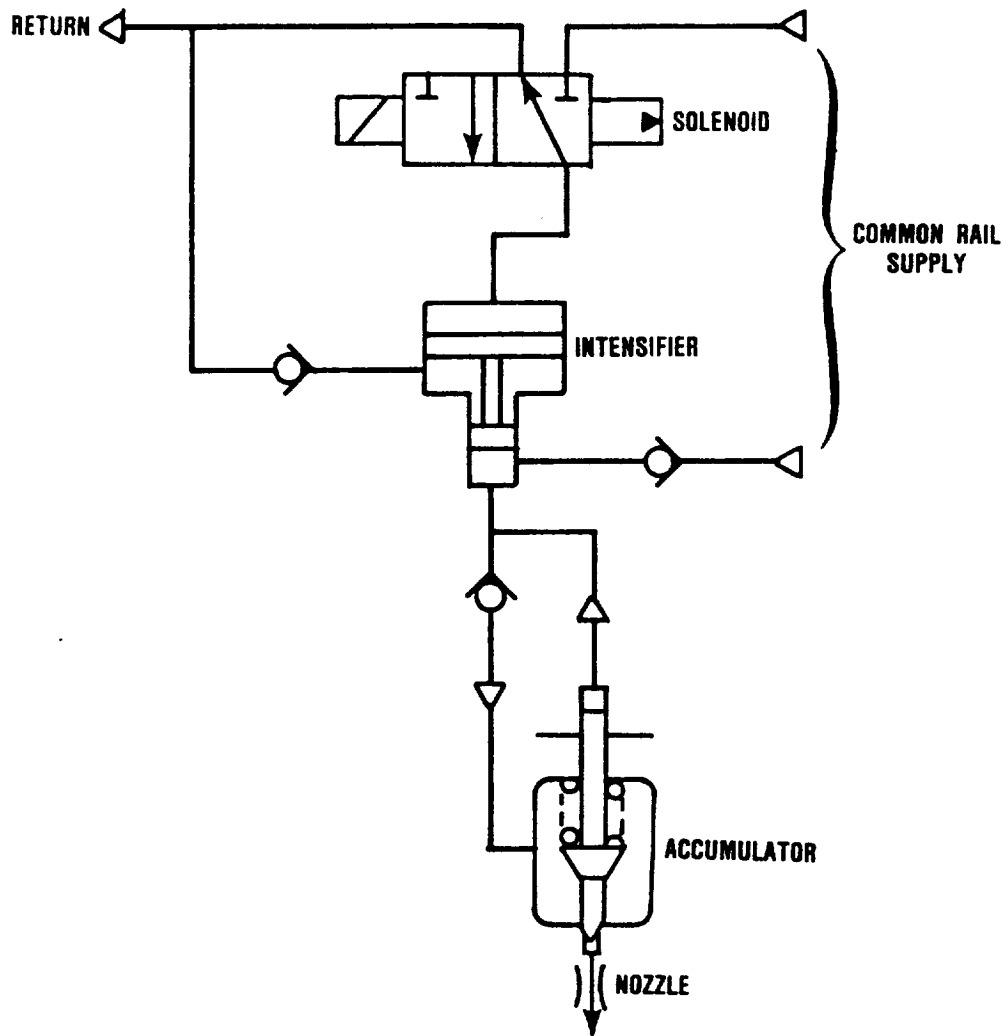
The cylinder liners are made of nitrided Nitralloy and are oil-cooled, with impingement jets located in the ring reversal region to enhance localized cooling. The cylinder head proper is

made of aluminum alloy and is designed for low heat transfer through the heat-resistant fire deck plate. In addition, the exhaust passages are insulated to reduce exhaust gas heat transfer losses and to maximize the energy going to the turbocharger and bottoming turbines. The exhaust valves are designed to be sodium cooled, if necessary, with insulating coatings and made of the high temperature materials, which are discussed in the following paragraphs.

High-speed, high-output diesel engines require injection pressures of over 20,000 psi in order to obtain good fuel efficiency at the equivalence ratios necessary for CCE performance.

The preliminary injector<sup>22</sup> selected for both the pilot (fumigation) and main injectors of CCE, capitalizes on new developments in electronics and microprocessors to offer a system with high performance and great operational flexibility. The injector concept is based on the accumulator nozzle principle coupled to a common-rail fuel supply and intensifier actuated by a digital electronic control unit as shown in Figure 43. The special significance of this injection system is that injection can be initiated at a high pressure because the energy is already stored in the nozzle at the time of needle opening. A conventional injector system requires that the fuel pressure be increased as the actual injection is taking place, resulting in a less favorable rate of injection characteristic. Therefore, the selected fuel injection system combines the desirable features of high injection pressures with timing and quantity controlled by microprocessor in a relatively simple system.





REFERENCE 22

Figure 43. CRIDEC Electronic Fuel Injector Schematic.

### 6.2.2 Candidate High-Temperature Materials

The high performance and lightweight special attributes of this compound cycle engine can be attained through use of materials that have been proven in various high temperature hydraulic and turbomachinery applications.

#### 6.2.2.1 Single-Crystal (SC) Alloys

The mechanical and thermal requirements of the valves used in the CCE suggest the use of single-crystal, cast nickel-base alloys, which will permit a significant increase in creep strength and component durability. Aligning the principal axis of the valves with the crystallographic orientation of the casting will provide greatly increased thermal fatigue life, due to the relatively low modulus in this direction. In addition, SC, cast nickel-base superalloys are compatible with the newer thermal barrier coating systems, which are planned for use in this application. However, sodium cooling is not compatible with SC construction.

#### 6.2.2.2 Thermal Barrier Coatings

Thermal barrier coating (TBC) technology offers high payoff potential in the CCE, because it allows operation of hardware at lower metal temperatures with greatly diminished thermal transients and thereby improves component durability. Programs are underway in the turbine industry to develop and characterize reliable TBC systems to enhance turbine component performance. These systems consist of oxidation-resistant metallic bonded coating with an insulating protective ceramic overlay coating. TBCs are presently used on components such as combustors, transition liners, and fuel nozzle shrouds in both production and advanced engines. They also are being tested in diesel engines

on valves, pistons, and cylinder walls. TBCs effectively reduce metal temperature and thus increase component durability.

#### 6.2.2.3 Oxide-Dispersion Strengthened Alloys

The high melting points, high-temperature creep, and fracture properties of the mechanically alloyed oxide-dispersion strengthened (ODS) alloys make them candidates for the cylinder head fire deck plate. The major attribute of ODS alloys is that they can retain useful strengths up to a relatively high fraction of their melting points. Moreover, at the high operating temperature of the fire deck, these alloys display long-term strengths beyond the capabilities of conventional superalloys.

#### 6.2.3 Turbomachinery

##### 6.2.3.1 Compressor Aerodynamic Design

The selected CCE compressor is a two-stage centrifugal unit having the following design-point characteristics:

|                  |   |                           |
|------------------|---|---------------------------|
| Pressure ratio   | - | 10.61                     |
| Corrected flow   | - | 2.45 lb/sec (1.11 kg/sec) |
| Efficiency (T-T) | - | 0.79                      |
| Corrected speed  | - | 73,210 rpm                |

The titanium alloy compressor wheels are a 0.57 geometric scale of the successful GTEC TPE331 turboprop compressor. The flowpath is shown in Figure 44. The performance level is based on the current technology F109 (TPE331 derivative) turbofan engine compressor adjusted for the smaller CCE size. This configuration was selected for its good efficiency retention into the important part-speed region and for its broad, efficient, flow range that eliminates the need for any variable geometry.

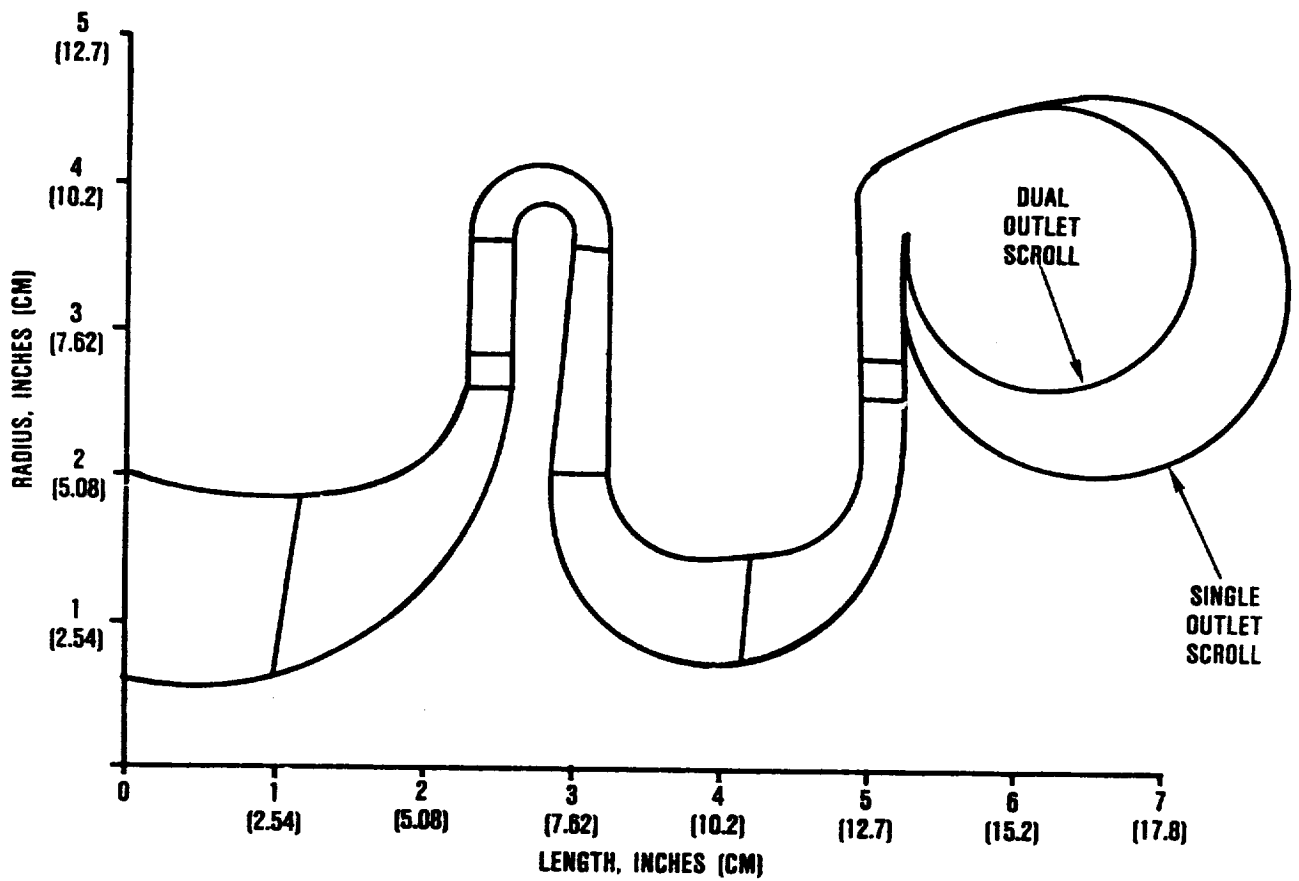


Figure 44. Compressor Gas Flow Path.

### 6.2.3.2 Turbine Aerodynamic Design

#### 6.2.3.2.1 Turbine Aerodynamic Design Points

The design points for both the high pressure and power turbines resulted from an extensive cycle study that balanced the supercharging compressor power requirements against the bottoming turbine power input to the crankshaft at both cruise and full power engine ratings. The turbine flow path is depicted in Figure 45.

Turbine design parameters for the chosen cycle are presented in Tables 11 and 12.

#### 6.2.3.2.2 High Pressure (HP) Turbine Aerodynamic Preliminary Design

The HP turbine is a radial inflow, uncooled unit having the design-point characteristics shown in Table 11.

Table 11. Turbine Design Cycle Parameter for HP Turbine.

| <u>Parameter</u>                       | <u>CCE<br/>HP Turbine</u> |
|--|---------------------------|
| Inlet corrected flow, lb/sec (kg/sec)  | 0.562 (0.255)             |
| Inlet corrected speed, rpm             | 32,321                    |
| Inlet corrected work, Btu/lb (kcal/kg) | 37.21 (20.67)             |
| Pressure ratio (Total-to-Total)        | 4.089                     |
| Efficiency, Total-to-Total (percent)   | 87.2                      |
| Inlet total pressure, psia (bar)       | 132.1 (9.1)               |
| Inlet total temperature, F (C)         | 1763 (962)                |

Due to the high turbine inlet temperatures that occur at altitude and under emergency-power conditions, [over 1800F (982C)] the rotor is constructed of IN713 blades and a low-carbon Astroloy powder disk, which is current industry practice.

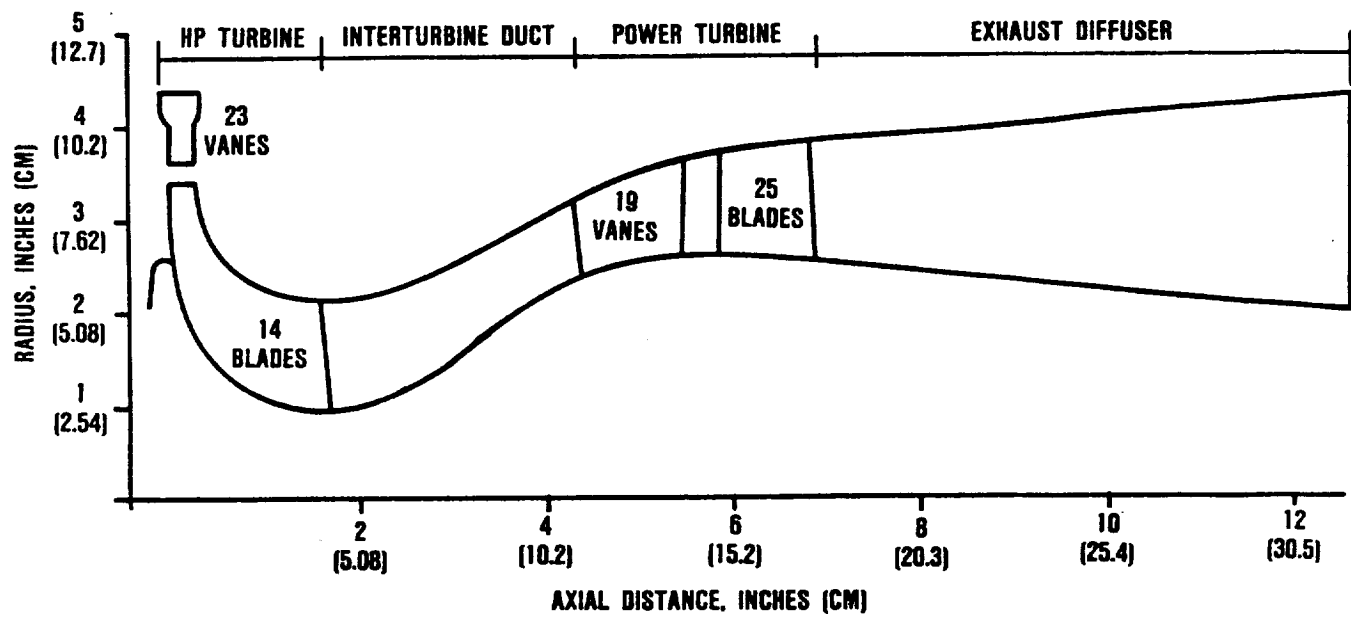


Figure 45. CCE Turbine Flow Path.

### 6.2.3.2.3 Power Turbine Aerodynamic Preliminary Design

The power turbine is an axial-flow, uncooled unit having the design point characteristics shown in Table 12.

Table 12. Turbine Design Cycle Parameter for Power Turbine.

|   |               |
|---|---------------|
| Inlet corrected flow, lb/sec (kg/sec)                 | 2.119 (0.962) |
| Inlet corrected speed, rpm                            | 25,027        |
| Inlet corrected work, Btu/lb (kcal/kg)                | 21.06 (11.7)  |
| Exit static pressure ratio<br>(Total-to-diffuser)     | 2.113         |
| Exit static efficiency,<br>Total-to-diffuser, percent | 86.6          |
| Inlet total pressure, psia (bar)                      | 31.66 (2.18)  |
| Inlet total temperature, F (C)                        | 1217 (658)    |

The power turbine preliminary design followed the logic similar to that of the HP, using a computer code that allows monitoring of performance effects due to changes in blade-row turning, trailing-edge blockage, aspect ratio, hub reaction, and rotor-tip clearances.

The axial-flow, power-turbine shaft speed was chosen from a range that provided minimum gearing to the diesel crankshaft. For the work requirement, the shaft speed, exit mean radius, exit area, and exit swirl were varied over appropriate ranges. Configurations exhibiting excessively high Mach number levels, rotor turning, flow angle, or stress parameters were eliminated. Viable configurations were then examined for performance trends and the vane/blade geometries were adjusted to obtain optimum

values of Zweifel coefficients, aspect ratio, and solidities. Low exit swirl eliminated the need for an exit guide vane.

The mission profile, which includes the exhaust diffuser, emphasizes the importance of the off-design performance that has been calculated for the power turbine configuration.

The turbine wheel is made of IN713 LC and has a shrouded blade to minimize tip clearance losses.

#### 6.2.3.2.4 Interturbine Duct Design

The interturbine duct was configured to minimize pressure losses. With the duct inlet and exit radii determined from the optimal designs for the HP and power turbines, the duct length was chosen from Sovran and Klomp<sup>23</sup> data for minimum duct length, where flow separation will not occur. The walls were then contoured to allow smooth transition.

#### 6.2.4 Gearbox

##### 6.2.4.1 Gearing

The main functions for the gearing in the CCE engine are to provide a load path from the power turbine to the crankshaft, engine accessory drive, and timing and drive for the overhead camshafts. External involute spur gears are employed throughout the design and are typical of industry power transmission hardware. Preliminary assessment of stresses, loads, and shaft speeds indicates that they are within acceptable limits. Gear pitch diameters were sized in the detail design phase to provide pitchline velocities of 28,000 ft/min (141 m/sec) or less. The gear material will be a high-temperature carburizing steel such as CBS 600 or Pyrowear alloy 53, because the bulk lubricating oil



temperature can exceed 350F (177C) at full load on a 4000-feet, 95F (1.22 km, 35C) day, which would soften the AISI 9310 material normally employed.

#### 6.2.4.2 Bearings and Curvic Couplings

For the reasons mentioned earlier in paragraph 6.2.1, all bearings in the CCE except for the piston wrist pin will be the rolling element type and made from VIMVAR M-50 steel. All of the bearing parameters are within industry experience for speed index (DN) (bore diameter in millimeters times rpm), which is the primary indicator for bearing operating speed. The design of all bearing parameters would be optimized to obtain the required life and reliability using proven computer programs.

#### 6.2.4.3 Lubrication System

The CCE dry sump lubrication system (Figure 46) supplies lubrication and cooling for all engine gears, bearings, seals, and working splines. It is a totally engine-contained system.

To improve accessibility, the major oil system components (i.e., pump, filter, oil monitor, oil cooler, pressure regulating valve, and associated lines and valves) are integrated into the accessory gearbox housing design.

A multiple-element positive displacement gerotor pump has been selected to supply oil to the lubrication system and scavenge the several sump oil pickup points. Such a pump is capable of satisfactory operation from sea level to 29,500 feet (9 km) at speeds up to 10,000 rpm.

The lubricating oil filtering system consists of a dual ultrafine (3-micron,  $\beta_3 \geq 100$ ) barrier filter, plus a centrifugal

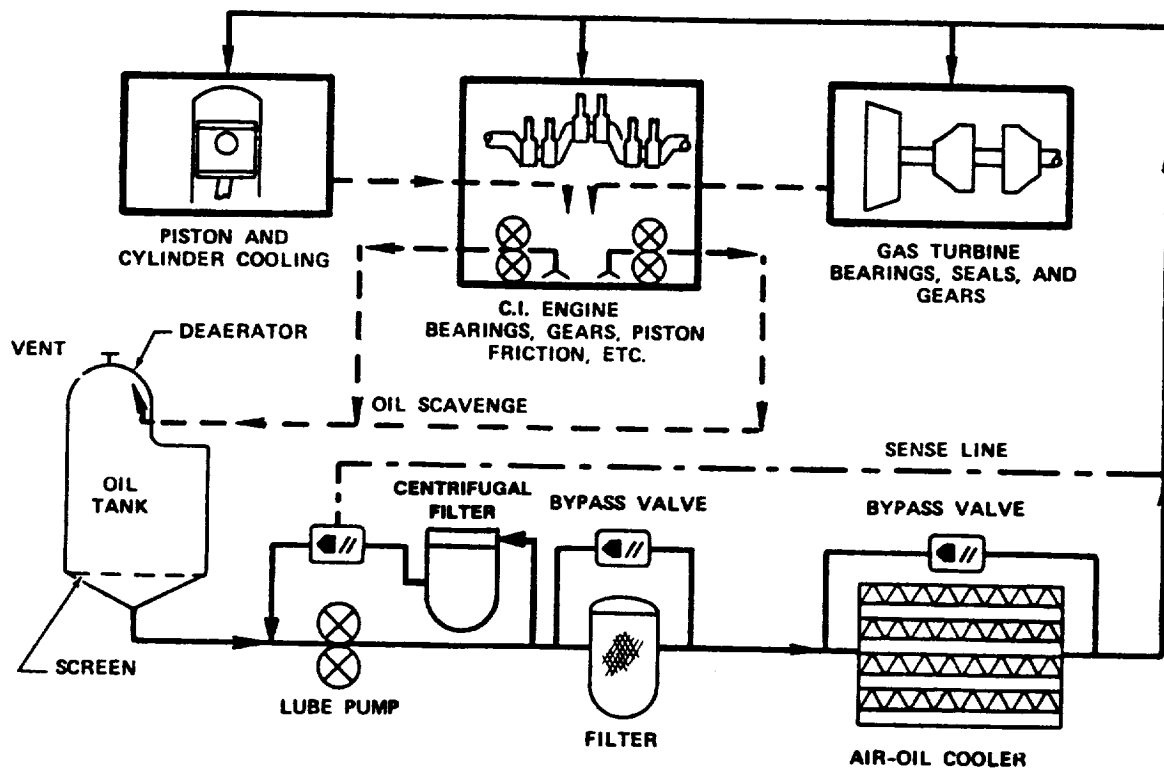


**Figure 46. Preliminary Lubrication System.**

filter in the bypass that remove dirt and soot particles as small as 0.5 micron. Radioactive tracer studies made on a truck engine have shown as much as a 50 percent reduction in ring, liner, and bearing wear with a similar filter combination.<sup>24</sup> A debris monitoring system (chip detector) is an important factor in obtaining the high degree of reliability and long life required in this application.

The oil tank is a sheet-metal aluminum weldment, Banadized for fireproofing that has been used in commerical applications.

The oil cooler was designed as a plate-fin sandwich type, because it had the greatest heat transfer rate per unit volume of the various constructions that were compared. Several fin combinations were evaluated to optimize fin effectiveness and core shape. Aluminum was selected as the material due to its light weight. The cooler was designed as a two-pass, cross-counterflow configuration with an oil cooling load estimated from the engine model, shown in Table 13.

Table 13. Estimated Oil Cooling Load.

|   | Standard Day |          | Hot Day |         |
|---|--------------|----------|---------|---------|
| Ambient temperature, F (C)                  | 59           | (15)     | 95      | (35)    |
| Altitude, ft (km)                           | 0            | (0)      | 4000    | (1.22)  |
| Net shaft power, hp (kW)                    | 500          | (373)    | 1000    | (746)   |
| Diesel mechanical loss, Btu/min (kcal/min)  | 2448         | (614.6)  | 2448    | (614.6) |
| Cylinder heat loss, Btu/min (kcal/min)      | 3329         | (836)    | 6787    | (1704)  |
| Brayton mechanical loss, Btu/min (kcal/min) | 347          | (87.1)   | 525     | (131.8) |
| Total cooling load, Btu/min (kcal/min)      | 6124         | (1537.7) | 9760    | (2450)  |

The oil cooler has been sized as a function of oil exit temperature at the engine heat rejection level associated with 500 hp (373 kW) cruise operation on a standard day. This minimizes the oil cooler size because 80 percent of the mission is flown at 40 to 50 percent power. Sizing the cooler for a cruise oil exit temperature of 200F (93C), led to core dimensions that match favorably with the aftercooler while assuring an acceptable 352F (178C) short-term oil temperature level at high ambient temperature and full power. Development of a higher temperature lubricant capability would permit a further reduction in oil cooler size.

The aftercooler was sized for 0.4 effectiveness based on the optimization studies described in paragraph 4.2 and was used throughout the comparison studies. The aftercooler was designed as a single-pass, cross-flow configuration made of stainless steel plate-fins, because of the high compressor discharge temperatures [(400 to 700F) (204 to 371C)] encountered. The design was based on the following sea-level, standard-day requirements:

- o Effectiveness, 0.4
- o Compressed air-side fractional pressure drop, 0.02
- o Cooling air-side fractional pressure drop, 0.03
- o Heat transfer rate, 8457 Btu/min (2131 kcal/min)
- o Weight: 24 pounds (10.9 kg)

In order to minimize cooling fan power and airflow requirements, the aftercooler and oil cooler were placed in series with respect to the cooling airflow path (Figure 47). The aftercooler was placed ahead of the oil cooler to obtain the lowest possible intake manifold temperatures for longer engine life at cruise. It was determined that the cooling air flow rate was 4.3 times the engine air flow in order to secure an adequate heat exchange temperature difference with the series flow arrangement. Fan

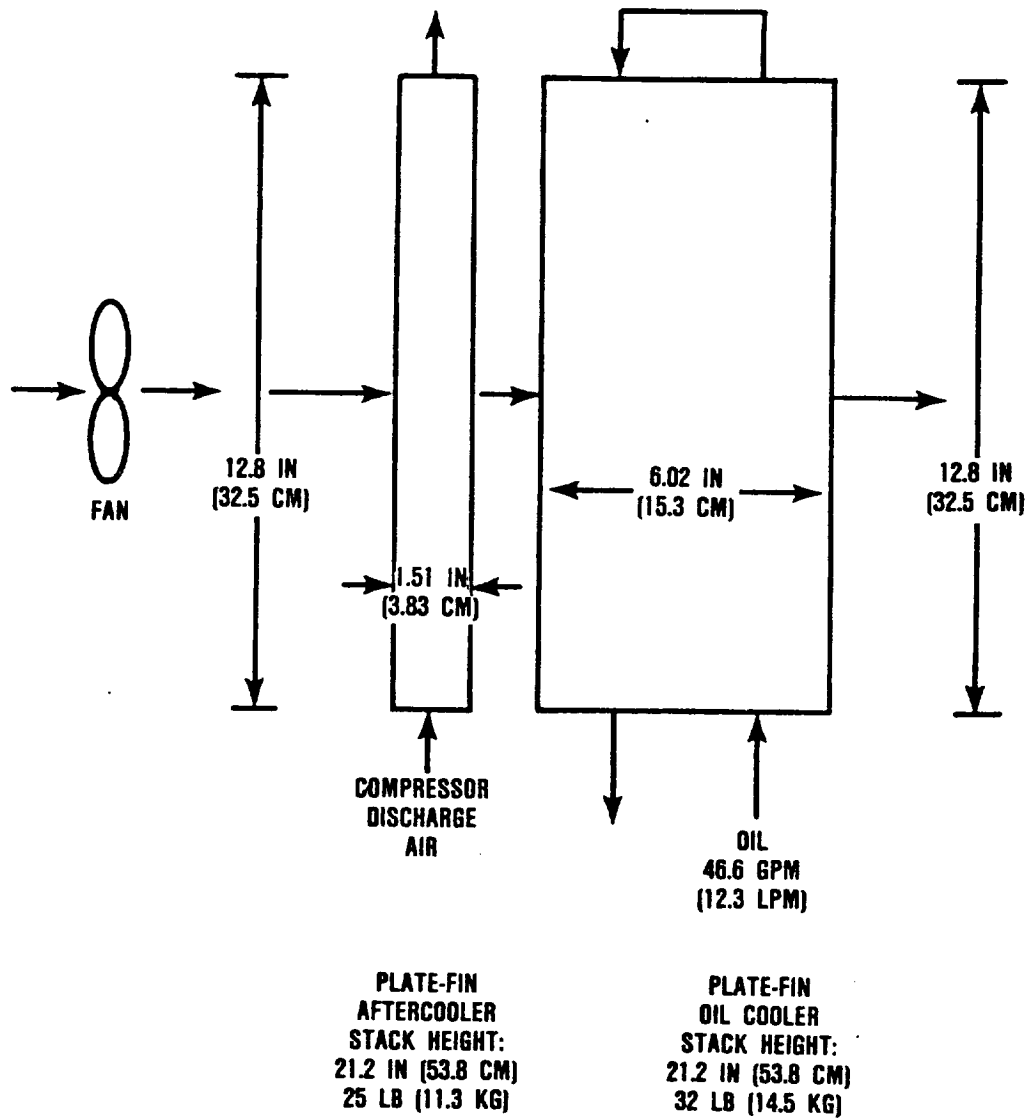


Figure 47. CCE Heat Exchanger Core Size.

power was established to be 51 hp at rated power for the after-cooled cycles, thereby allowing for about 7 percent cooling circuit pressure drop with a 60 percent fan efficiency. (The current design places the fan upstream of the heat exchangers to minimize fan shaft power).

The cooler aspect ratio (stack height/oil flow length) was set equal to that of the aftercooler in order to facilitate integration of the two heat exchangers.

#### 6.2.5 Engine Controls and Accessories

The CCE control system is a dual-channel, fully-redundant, microprocessor-based type and will meet or exceed the requirements shown in Table 14.

##### 6.2.5.1 Control System Description

The selected control system is shown in Figure 48. The dual-channel engine control unit (ECU) accepts both airframe and engine signals and includes adaptive control logic in computing command outputs to the fuel injectors. The gearbox-mounted permanent magnet alternator (PMA) provides full electrical power above approximately 50 percent speed, which is rectified and regulated to a nominal 28 vdc for the ECU. The dc airframe source used for ground starts will serve as backup for the engine-supplied power. In the event of externally supplied electrical power loss, the engine will be able to operate safely throughout the complete power range and will air-start at all engine speeds above 50 percent.

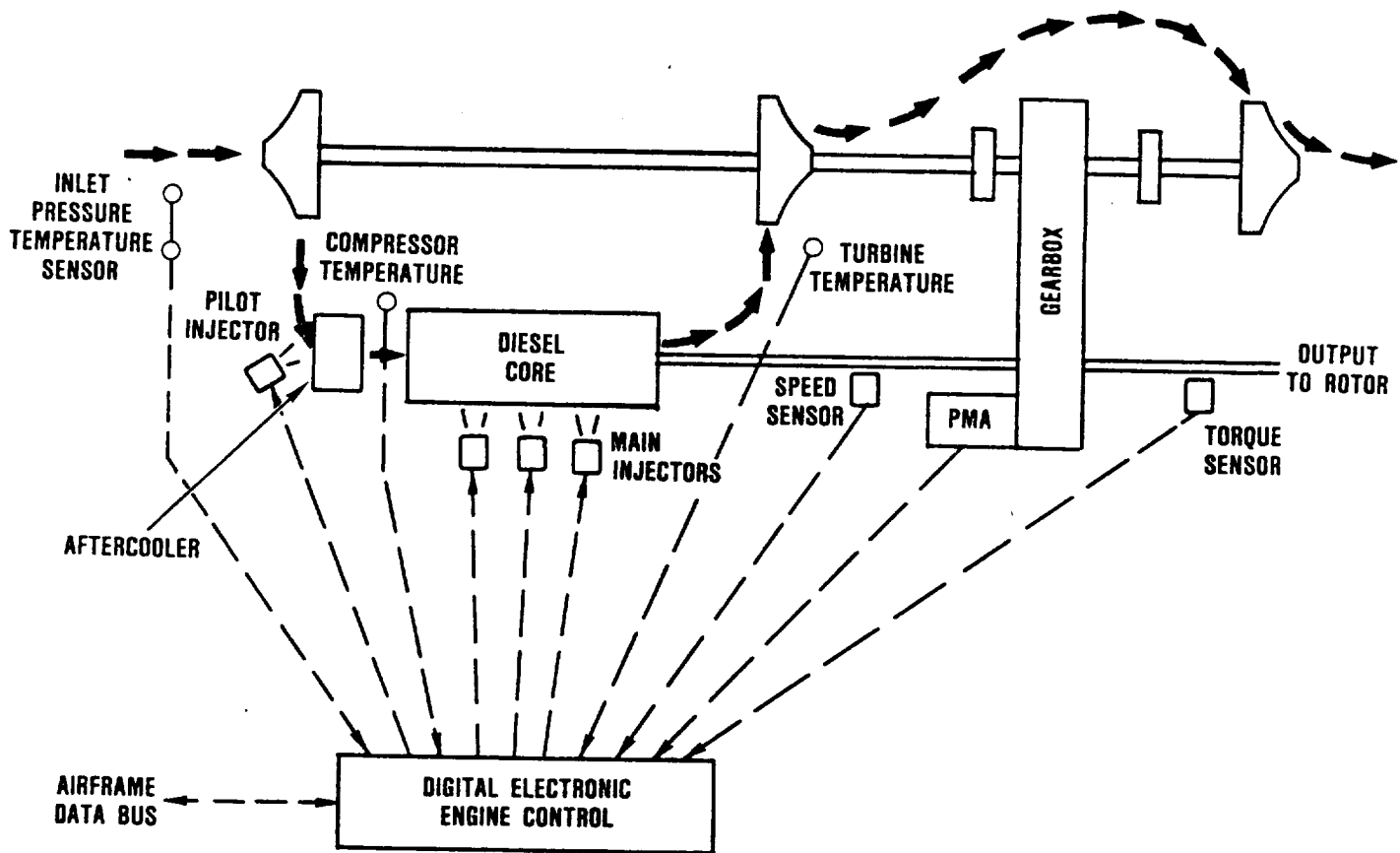


Figure 48. CCE Preliminary Control System.

**Table 14. Helicopter System Requirements.**

| <b>Requirements</b>  | <b>System Features</b>   |
|--|--|
| Compatible with modern fly-by-wire/light aircraft applications                                     | Full authority digital electronic control<br><br>MIL-STD-1553B data bus for aircraft interface<br><br>No mechanical connections<br><br>Adaptable to MIL-STD-1773 data bus<br><br>Dual-channel electronic control<br><br>Redundant fuel injector interfaces<br><br>Redundant power supply and sensors<br><br>Adaptive control logic<br><br>Engine and airframe control inputs |
| Fail-operational system with no performance degradation after any single failure                   |  |
| Limit engine speed droop to no more than 3 percent for full-load changes not faster than 2 seconds |  |

#### **6.2.5.2 Electronic Control**

The dual digital electronic channels are engine mounted and are designed to process control sensor inputs, provide signals for engine health monitoring, and forward data to an airframe computer. The primary sensed variable will be engine (and therefore rotor) speed. Redundant speed pickups are used to determine crankshaft angle for injection timing in order to control cylinder firing pressure at off-design conditions. Torque sensing and limiting is provided, as well as load sharing for twin engine applications. Engine inlet air temperature and pressure are sensed in order to establish the engine power settings over the expected ambient range. Turbine temperature must also be sensed



to provide engine protection and as an input to the health monitoring module of the ECU.

Fuel flow for starting and governing is computed by the ECU and converted to discrete signals for firing of main and pilot fuel injectors as described in the previous paragraph.

#### 6.2.5.3 CCE Starting System

The primary starting system configured for the CCE is a conventional electric system consisting of a 40 amp-hour nickel-cadmium battery connected to a commercial direct current starting motor now used on an auxiliary power unit (APU). The system is sized for low ambient temperatures where the cranking load is greatest, due to the thick viscosity of the cold oil and the low battery energy available at cold temperatures.

Figure 49 shows the estimated torque characteristics of the CCE at sea level, -40F (-40C) ambient, and the starter torques resulting from two battery conditions, [0F (-18C) and -20F (-29C)]. It can be seen that the -20F (-29C) temperature battery has an energy level for a starter torque that requires engine firing to occur at a very low speed to avoid the possibility of steady-state motoring of the engine. The energy for starter torque provided by a battery at 0F (-18C) is significantly greater (about 40 percent more) than that provided by a battery at -20F (-29C) and would result in a faster engine start time. The estimated engine torques are for a bare engine. If the helicopter installation of the CCE requires that the driven rotor load also be cranked by the starter, and that load has substantial drag torque to overcome, the starting system performance may not be sufficient to provide satisfactory starts. Obtaining satisfactory starts with these higher drag starter loads may require larger starters and batteries.

ALTITUDE: SEA LEVEL  
AMBIENT TEMPERATURE: -40F (-40C)  
BATTERY TEMPERATURE AS NOTED

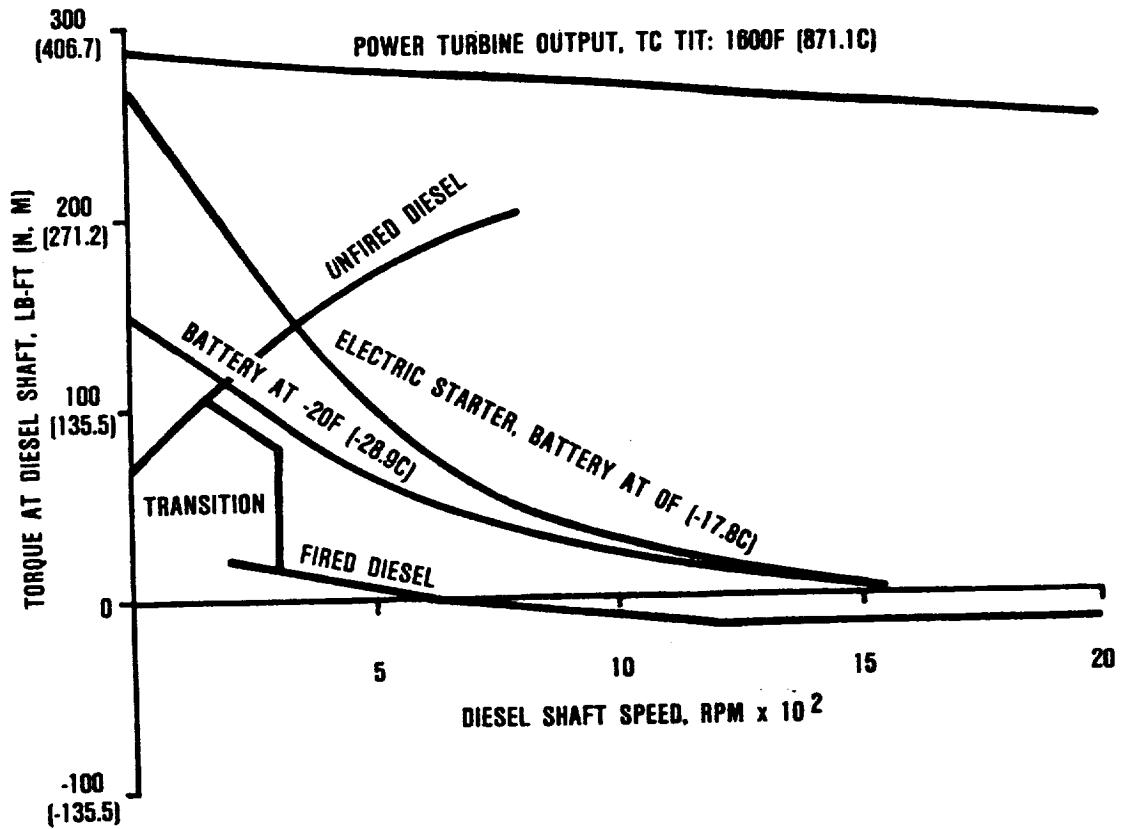
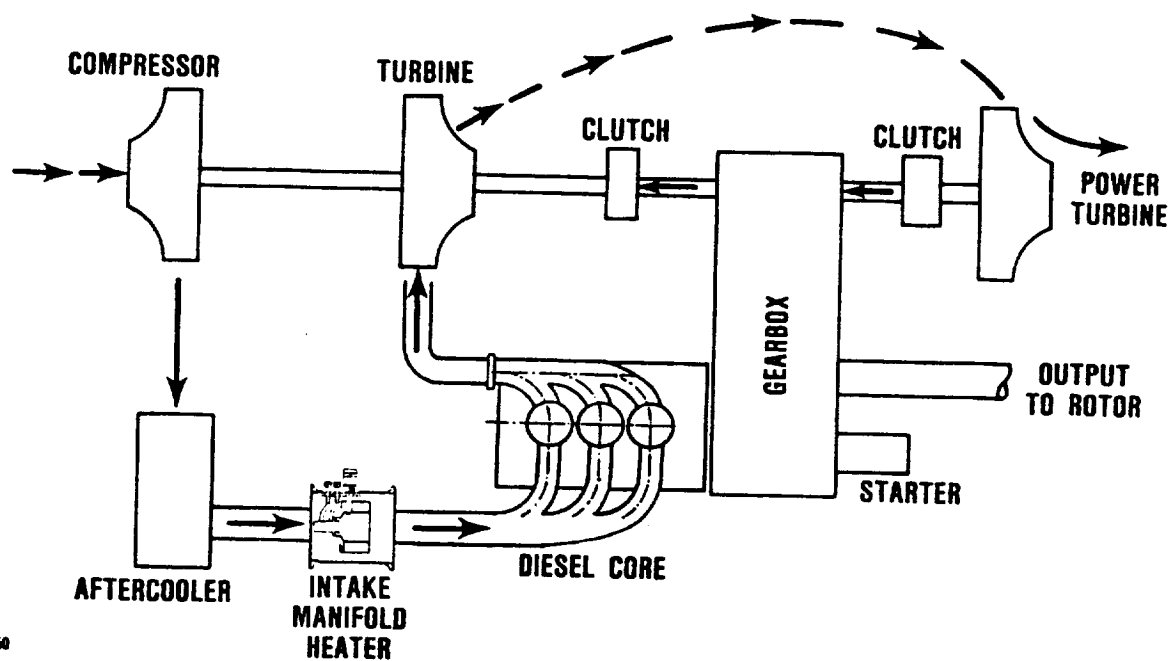


Figure 49. CCE Estimated Starting Performance.

The CCE engine is designed with an effective compression ratio of 7.50 in order to control the peak firing pressure of 3362 psia (231.9 bar) at full load. This low compression ratio (conventional direct injection diesel engines have 14 to 18:1) makes additional starting aids mandatory for operation at -40F (-40C) ambient temperature. A surface discharge ignition system and spark plugs in each cylinder have been specified for starting the CCE engine. In addition, an intake manifold heating system could be designed (Figure 50) consisting of a fuel pump and a low pressure air blower, both driven by 28 vdc electric motors. These will provide a fuel-to-air mixture to the manifold heat combustor chamber, which then fires into the intake manifold providing hot [300F (148.9C)] air to enhance the starting process. This latter system is already in use on many high output foreign tank engines that also have low (7 to 12:1) compression ratios.<sup>25</sup>

An alternative starting system has also been studied as a means of obtaining higher cold weather starter torques. This system is based on using the turbocharger with the combustor as a hot gas generator to provide hot, pressurized gas to the power turbine for cranking the diesel. This system (Figure 51) requires the insertion of valving and a combustor in the flow path between the turbocharger and the diesel core to bypass most of the turbocharger air around the diesel and add the fuel-derived energy required to drive the system. The turbocharger is started by an on-shaft starter/alternator, which brings it up to a minimum starting speed, at which point the combustor is ignited and the hot gases flow to the power turbine. The diesel cranking torque, obtained from the power turbine is substantial, as shown in Figure 49 and would reduce the starting problems associated with connected helicopter rotor loads. In this starting mode, fuel from the vehicle tank is burned in the combustor and provides the energy to crank the diesel core and the helicopter rotor load.



67-004-50

**Figure 50. CCE Starting System.**

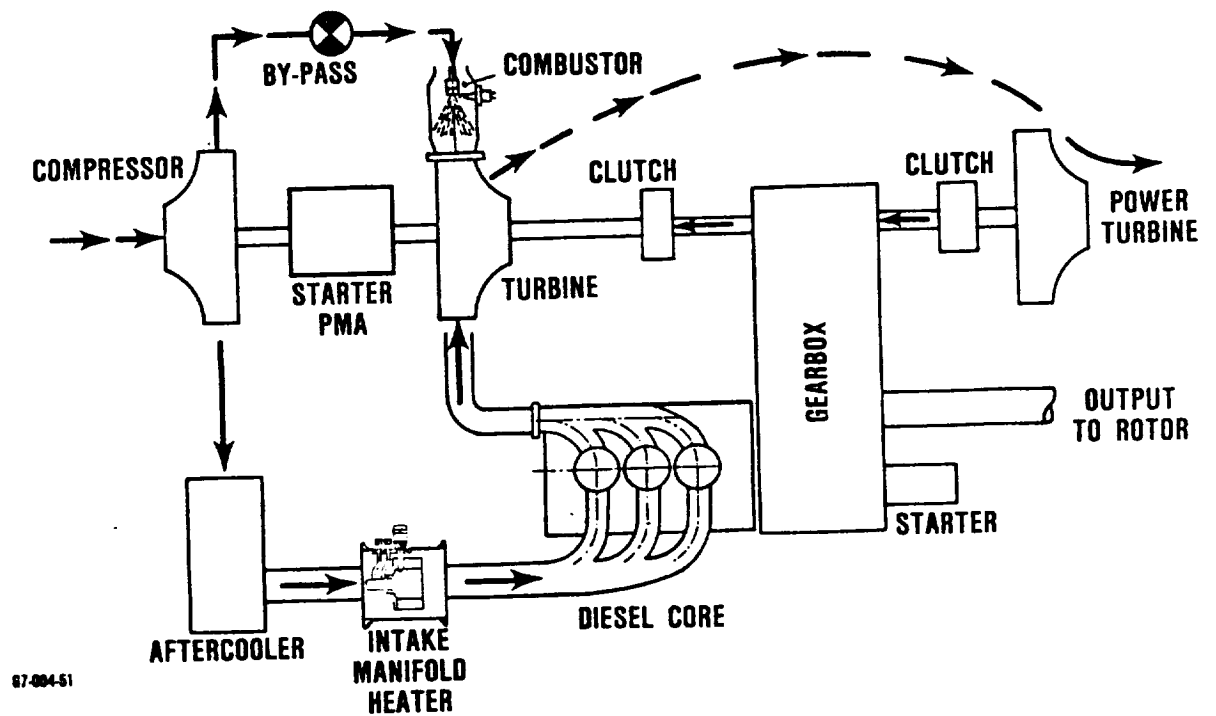


Figure 51. CCE Alternative Starting System.

### 6.3 Operation With Failed Turbomachinery

If the turbomachinery on one engine (whether it be 2- or 4-stroke) were to become inoperative during a mission, that engine would be unable to develop any substantial power. Although the 4-stroke engine is self-breathing, it would deliver only a miniscule amount of 12 hp (9 kW) to the helicopter rotor. In the 2-stroke engine, a positive pressure differential must exist across the cylinders for the scavenging and charging processes to occur. Therefore, no power would be produced. A highly compounded 2-stroke cycle engine of this configuration will not operate and deliver useful power with a failed turbo-charger.

## 7.0 CCE ENGINE SCALING

The diesel engine is unique among many heat engines because its power output is directly proportional to the number of geometrically similar cylinders connected to the crank shaft. For example, a large manufacturer of 2-stroke cycle diesel engines has a product series of in-line 2, 3, 4, 6, V-6, V-8, V-12, and V-16 cylinder engines, each of whose power output can be obtained by multiplying its displacement by the specific output of that engine series.

Similarly, a family of CCE engines may be characterized to cover the range of 500 to 2000 shp. For this study, these CCE engines are geometrically identical with respect to bore and stroke and their turbomachinery has been scaled to provide the maximum efficiencies in each flow range. Their particulars are shown in Table 15.

It may be seen that the largest engine (2000 shp) (1491 kW) has the lowest BSFC, in fact, 7 percent better than the 500 shp (373 kW) engine. This is mainly the result of the more efficient, larger turbomachinery and the scaling effect. Several thermodynamic parameters for comparison purposes are shown below:

| Number of Cylinders                       | 3             | 6             | 12            |
|---|---------------|---------------|---------------|
| Turbocharger Combined Efficiency, percent | 0.63          | 0.67          | 0.69          |
| Exhaust Temperature, F (C)                | 1827<br>(997) | 1760<br>(960) | 1723<br>(939) |
| Turbine Power/Total Power                 | 0.22          | 0.24          | 0.26          |

**Table 15. CCE Engine Family.**

|                                   | Number of Cylinders       |                  |                  |
|-----------------------------------|---------------------------|------------------|------------------|
|                                   | 3                         | 6                | 12               |
| Shaft Horsepower (kW)             | 500<br>(373)              | 1000<br>(746)    | 2000<br>(1491)   |
| BMEP, psi (bar)                   | 404<br>(27.9)             | 393<br>(27.1)    | 387<br>(26.7)    |
| Displacement, in <sup>3</sup> (l) | 66.7<br>(1.09)            | 133.4<br>(2.17)  | 266.5<br>(4.37)  |
| Diesel Power, HP                  | 390                       | 758              | 1491             |
| Brayton Power, HP                 | 110                       | 242              | 509              |
| BSFC, lb/hp-hr (Kg/kW-hr)         | 0.340<br>(0.207)          | 0.330<br>(0.201) | 0.319<br>(0.194) |
| Exhaust Temperature, F (C)        | 1827<br>(997)             | 1760<br>(960)    | 1723<br>(939)    |
| Weight, lb (kg)                   | 230<br>(104)              | 432<br>(196)     | 812<br>(368)     |
| Compressor                        |                           |                  |                  |
| Efficiency                        | 0.759                     | 0.790            | 0.811            |
| Flow                              | 1.221                     | 2.430            | 4.848            |
| P/P                               | 10.8                      | 10.7             | 10.6             |
| Turbine                           |                           |                  |                  |
| Efficiency                        | 0.830                     | 0.845            | 0.855            |
| Flow                              | 0.279                     | 0.555            | 1.106            |
| P/P                               | 4.5                       | 4.1              | 3.9              |
| Power Turbine                     |                           |                  |                  |
| Efficiency                        | 0.830                     | 0.848            | 0.858            |
| Flow                              | 1.16                      | 2.11             | 3.99             |
| P/P                               | 2.0                       | 2.2              | 2.3              |
| <b>Engine Parameters</b>          |                           |                  |                  |
| Speed = 6122 rpm                  | C/R = 7.50                |                  |                  |
| Bore = 3.101 in.<br>(7.88 cm)     | PFP = 3363 psia (232 bar) |                  |                  |
| Stroke = 2.940 in.<br>(7.47 cm)   | Fan hp $\propto W_a$      |                  |                  |



In each case, the engine with the largest number of cylinders has the most combined efficiency ( $\eta_C \cdot \eta_T$ ), lowest exhaust gas temperature, and greatest turbine power/total power ratio.

This family of engines has cylinders in groups of three, which has been the most efficient with respect to exhaust energy recovery for turbocharging. The three-cylinder engine has a 41.4 percent brake thermal efficiency, which is a comparable to that of larger displacement, slower speed engines.

## 8.0 ENGINE LIFE AND MAJOR PERFORMANCE TECHNOLOGY DEVELOPMENTS

The design life for this compound cycle helicopter engine is 2000 hours mean time between overhaul (MTBO), based on the mission profile shown in Figure 4. The diesel core has been determined to be the life-limiting module and three major technology areas have been identified for life and performance. They are, in order of priority.

- o Piston ring/liner interface wear life
- o Exhaust valve life
- o Fuel injection with high-heat-release-rate combustion.

### 8.1 Piston Ring/Liner Interface Wear Life

The primary development challenge, or life-limiting factor, of most concern is the wear rate of the piston ring/liner interface materials. Wear is a dynamic process that is dependent on the environmental conditions existing at the rubbing couple. The major factors influencing wear rate are addressed in succeeding paragraphs.

#### 8.1.1 Piston Ring/Liner Geometries

The running-in process between the piston rings and cylinder liner of a high output diesel engine, is a most critical element in obtaining long life. The final ring profile is usually a flattened parabola. The closer that the ring's initial shape can approximate the final one determines its resistance to scuffing and wear. Properly "run-in" rings have been known to have one-third the early-wear rate of incorrect geometries. Another critical factor in forming the ring face profile is the relationship of the piston ring grooves to the liner surface. If the piston ring grooves are out of plane with the liner surface because of thermal distortion, it is necessary to contour the ring's bottom surface angle to compensate for the piston groove misorientation.

### 8.1.2 Surface Topography

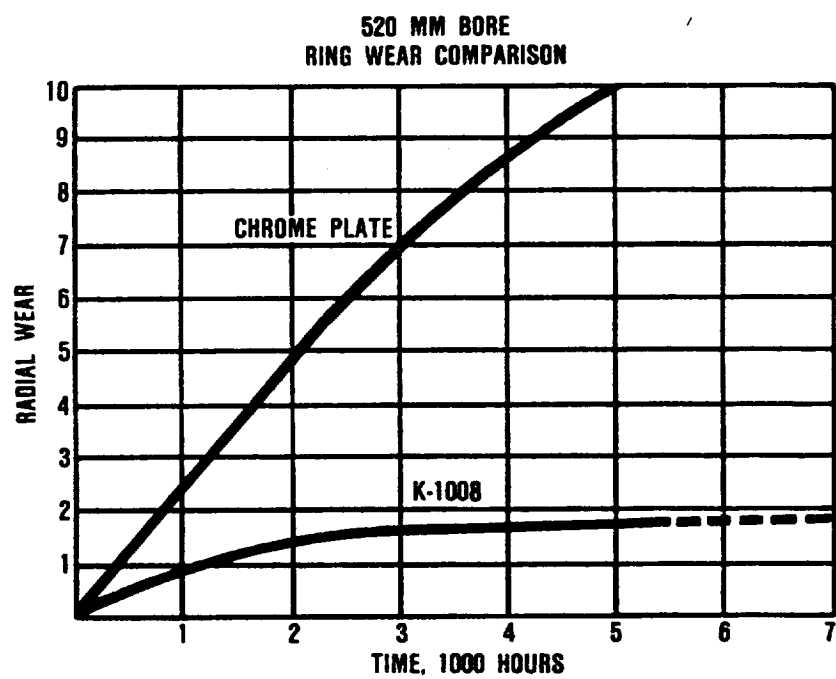
Piston ring and cylinder liner surfaces are used to retain minute quantities of lubricating oil, which act to prevent metal-to-metal contact. In the critical top dead center (TDC) ring reversal region, the oil film thickness is on the order of one micron (40 millionth of an inch) or less. Plasma-sprayed ring coatings are designed with 10 to 20 percent porosity for oil retention. Also, the cylinder liner surface topography may be modified through honing, laser imprints, and controlled electro-etching or plating to provide a textured surface, which will serve as an oil reservoir and also provide a collection place for worn metal and abrasive particles.

### 8.1.3 Material Chemistry and Properties

The use of plasma-sprayed coatings on rings has enabled diesel engines to simultaneously increase their specific output and their life (TBO) by at least a factor of two over the past 20 years. It has recently been possible, using a chrome carbide-molybdenum ring facing, to obtain a five-fold increase in piston ring life as compared to a conventional chrome-plated surface<sup>26</sup> (Figure 52). Similar improvements have been made on cylinder liner metallurgy such as hardened cast iron, nitrided Nitralloy, laser hardened surfaces, and plasma-sprayed Cermet<sup>R</sup> coatings.

### 8.1.4 Piston Velocity and Physical Speed

Engine physical size and speed have a major influence on service life. Figure 53 shows the effect of engine speed on wear-out life for several diesel engines. The Caterpillar engine life data was obtained at 1200 and 1800 rpm<sup>27</sup> and the DDA 53 engine data at 2500 rpm<sup>28</sup>. The ADEPT Super "53" data is based on a wear prediction formula that will be verified with a surface layer activation (SLA) technique. A 6000-rpm "loop-scavenged" CCTE data point of 200 hours of life shown in Figure 53 is based



REFERENCE 26

**Figure 52. Ring Wear Comparison of Chrome Plate and K-1008 Material Coatings.**

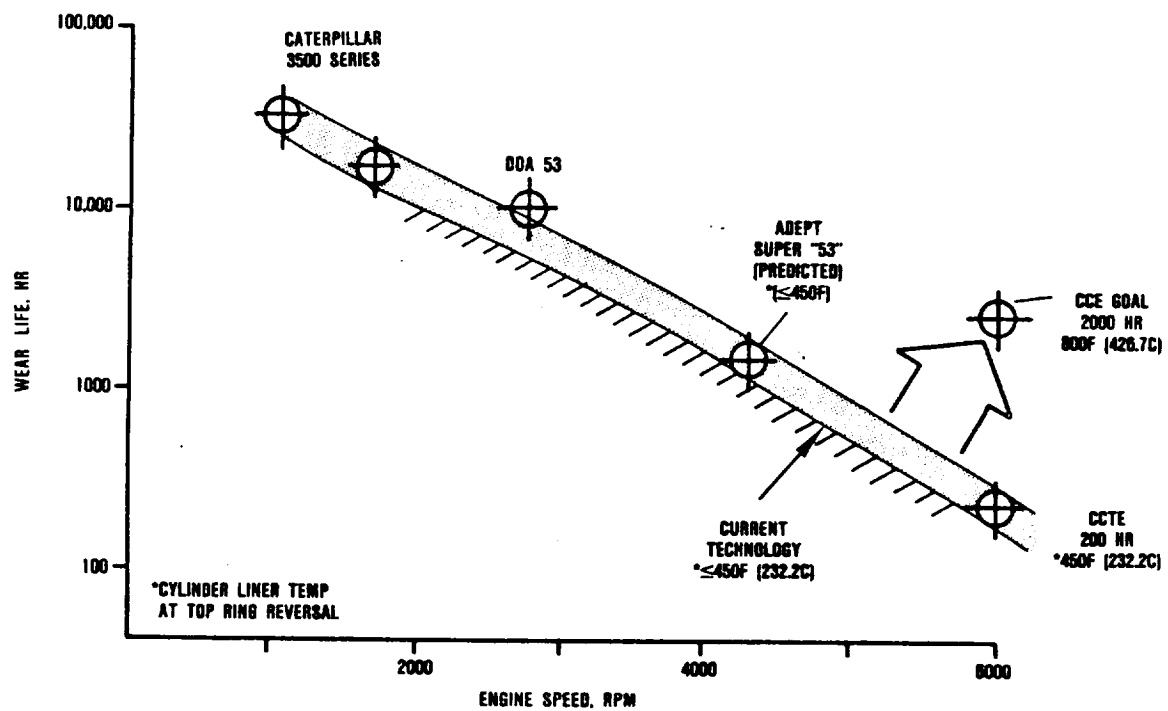


Figure 53. Engine Life as a Function of Speed.

on actual measured piston ring wear rates when applied to the mission profile and as obtained with the SLA instrumentation. A tenfold increase in engine life over CCTE is required to meet the CCE goal of 2000 hours TBO. At the same time, the ring-reversal temperature has been projected from the current technology level of 450F to 800F (232 to 427C) in order to minimize heat rejection to the cooling media and therefore provide more thermal energy to the power turbine.

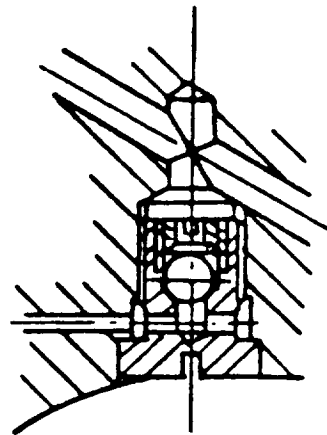
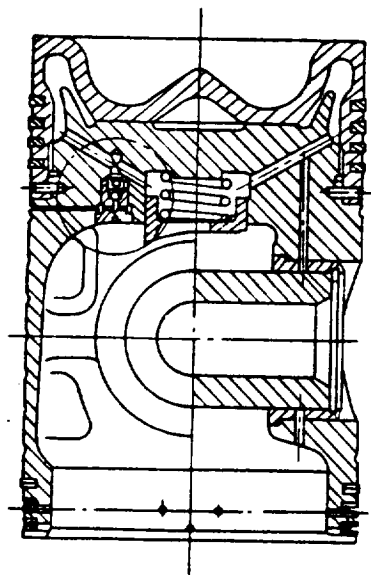
#### **8.1.5 Oil Type and Film Thickness**

The oil film thickness is determined by the oil viscosity, oil-film temperature, piston-ring profile, and piston velocity. At both TDC and BDC, where the piston velocity is zero, the oil-film thickness approaches zero, whereas at midstroke when the piston velocity is a maximum, the oil film may be as great as 10 microns (400 millionths) thick. Some high output diesel engines<sup>29</sup> use an inertia pump lubricant delivery system within the piston that forces lubricating oil to the critical interfaces in the vicinity of TDC as shown in Figure 54. Large marine engines have "quills" or openings in the cylinder liner surface to place lubricating oil on that surface where required. This technique was also used on the CCTE engine. Some form of preferential lubrication will be used for the selected CCE type engine.

Sleeve valve engines have been reported to have a 50 percent longer MTBO than conventional poppet valve engines.<sup>30</sup> This is due to the fact that when the piston speed is low or zero, the cylinder liner is moving, thereby maintaining an oil film to keep the piston ring and liner from rubbing dry.

#### **8.1.6 Operating Pressure and Temperatures**

Metal-to-metal (wear) contact occurs when the lower limit of film lubrication (LLFL) thickness is violated. The region of LLFL may vary based on engine operating conditions; but



DETAIL DRAWING  
OF LUBRICATOR

REFERENCE 29

Figure 54. Sectional View of Piston Lubricator.

generally, the most severe violation of film lubrication occurs at TDC at the beginning of the power stroke. Gas pressure behind the top ring is usually at a maximum. Therefore, the radial force exerted on the oil film on the liner wall is also a maximum. The piston velocity is very slow, thus the hydrodynamic film thickness on the liner wall is at a minimum. The oil viscosity also is at a minimum due to the high liner surface temperature. For these reasons, the oil film thickness is at a minimum.

#### 8.1.7 Contamination

Foreign and Self-Generated - Recent radioactive piston ring studies<sup>31,32</sup> have shown that engine life can be increased by a factor of two to three times by removing those foreign and self-generated particles as small as 5 microns in size in the lubricating oil. The lubricating oil system that has been specified for the CCE consists of 10 micron full-flow filtration and a centrifugal bypass filter capable of removing contaminants as small as 1 micron.

Adequate intake air and diesel fuel filtration also are mandatory for longer engine life in the dust-laden environment of military field operations. The critical particle size for these contaminants is also 5 microns<sup>33</sup> absolute rating.

Lubricant Type and Additives - Being a marriage of a diesel engine with a gas turbine, the CCE engine requires a new type of lubricant, one that is compatible with the critical environments and requirements of both engine types. Historically, lubricants have limited the rate at which pressures and temperatures (therefore output) could be raised in piston engines. These high pressures and temperatures and the sliding velocities attendant with a high power density CCE, necessitate low-friction and low-wear material combinations.

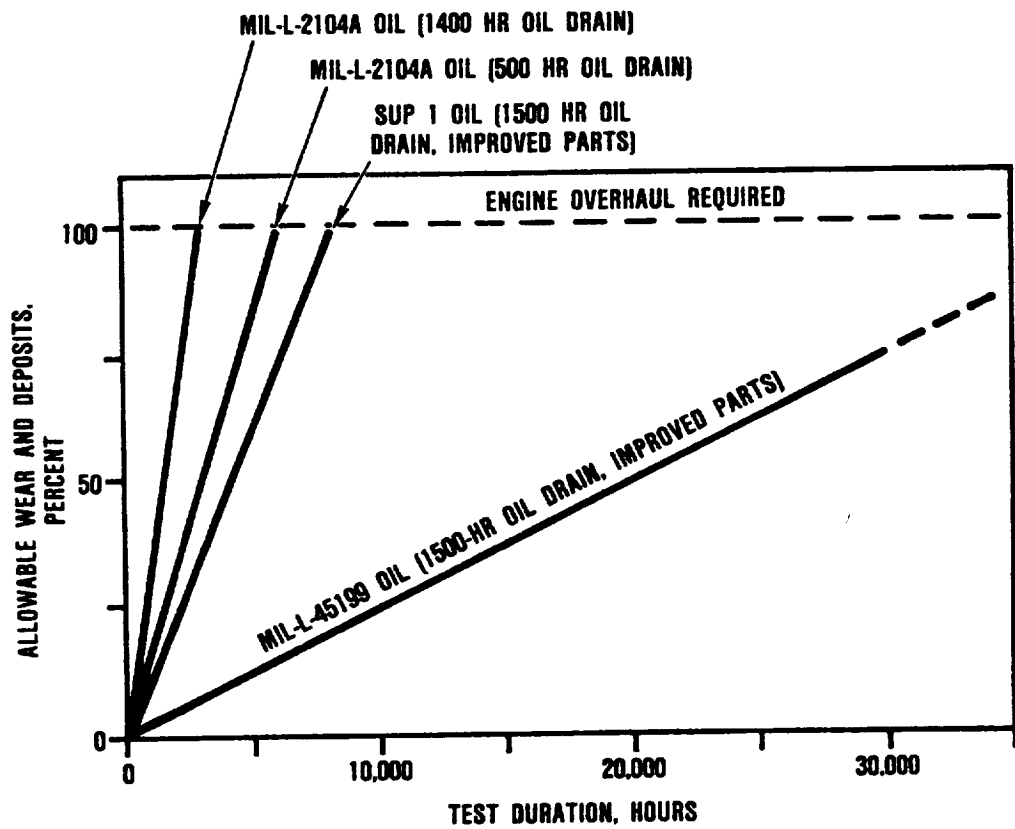


Therefore, the CCE lubricant must be essentially a gas turbine lube oil of the MIL-L-23699 type, combined with those additives required to counteract the highly oxygenated and burning conditions that occur in the diesel combustion chamber. The gas turbine lubricants under consideration are of the polyolester type base stocks, which have high viscosity index values and possess excellent oxidation stability.

Lubricating oil additives are used to impart new and improved properties to the base fluid, thereby lessening the harmful effects of the environment. Types of additives that are used include:

- |               |                        |
|---------------|------------------------|
| o Antifoam    | o Dispersants          |
| o Antioxidant | o Extreme pressure     |
| o Antiwear    | o Corrosion inhibitors |
| o Detergents  |                        |

Although it is presently impossible to quantitatively predict the piston ring/liner wear life for the pressure, velocity, and temperature (PVT) conditions estimated for the selected CCE, there is some encouraging reciprocating engine history that shows what might be possible with further development of lubricants and improved mechanical design. The history of a D-17000 diesel-powered 100 kW genset running at 80 percent load factor is shown in Figure 55.<sup>34</sup> The use of higher detergent oil and improved component design were major reasons for a tenfold increase in engine life. Advanced technology designs and new lubricants being pursued under various Army contracts are addressing this critical issue. However, activities need to be expanded in order to expedite development of a lubricant for CCE in the 1990 to 2000 time frame.



REFERENCE 34

**Figure 55. Engine-Life Improvements Are Significantly Pared by Lubricant Development.**

#### 8.1.8 Time Between Oil Changes

Changing the lubricating oil of a diesel engine serves several purposes:

- o Removal of contaminants, i.e., coolant, airborne, and self-generated debris
- o Replenishment of lubricating oil additives
- o Restoration of new oil viscosity due to oxidation, dilution, and shearing

However, compromise must be reached between the advantages of frequent oil changes and the logistic burden of a large supply of lubricating oil.

Complex interactions between the different elements of the system make it difficult to quantify their overall effect on engine life. However, the qualitative effects of the wear factors are well understood. A great deal of experience exists for low power density engines and has been exercised through well-established "rule-of-thumb" methods. This technique is limited in its extension into the unknown design regions of the CCEs discussed here. Total system (single-cylinder) testing under controlled and repeatable PVT condition, lubrication, contamination levels, etc., and under conditions using the best lubricant formulations and tribological couples, are vital for establishing a baseline of technology for CCE wear-life predictions. It also is imperative to use an in-situ wear measuring system, such as Surface Layer Activation (SLA) so that wear-life determination conditions are not disturbed by engine teardown for physical wear measurements. Such a system is being developed at GTEC under the AVSCOM/NASA ADEPT program.

## 8.2 Exhaust Valve Life

Two-stroke cycle diesel engine exhaust valves operate in a severe environment. Their frequency of operation is twice that of comparable four-stroke engine valves and the metal temperature may be up to 300 to 400F (166 to 222C) hotter than the measured exhaust gas temperature at the port. Four-stroke cycle engine valves operate somewhat cooler than the exhaust gas temperature. Current two-stroke exhaust valves operate at 2000 to 2500 cycles per minute with 1100F (593C) exhaust gas temperature. They are relatively trouble free for up to 400,000 (644,000 km) miles in trucks or 10,000 hours of operation in off-highway applications.

Table 16 shows the exhaust port gas temperatures for various operating conditions of the CCE. Under some conditions [4000 ft, 95F day (1.23 km, 35C)], the gas temperature could be 400 to 900F (222 to 500C) hotter than in current production designs. Special materials, thermal insulation/isolation schemes, or preferential cooling methods will be required for peak operating conditions.

**Table 16. CCE Diesel Average Exhaust Gas Temperatures at Various Operating Conditions.**

|                       | Percent Mission Time |               |               |               |
|-----------------------|----------------------|---------------|---------------|---------------|
|                       | 3.3                  | 16.7          | 43.3          | 36.7          |
| Operation             | Percent Power        |               |               |               |
|                       | 100                  | 75            | 50            | 40            |
| o Cold Day, Sea Level | Degrees F (C)        |               |               |               |
|                       | 1331<br>(722)        | 1168<br>(631) | 1036<br>(558) | 983<br>(528)  |
|                       | 1754<br>(957)        | 1583<br>(862) | 1416<br>(769) | 1348<br>(731) |
|                       | 1924<br>(1051)       | 1738<br>(948) | 1558<br>(848) | 1485<br>(807) |
|                       | 2042<br>(1117)       | 1802<br>(983) | 1597<br>(869) | 1517<br>(825) |

A listing of potential exhaust valve materials is shown in Table 17. Nimonic 80A is the material used in current production engines at the 1100F (593C) exhaust gas temperature. Astroloy would probably be selected for use at 1400F (760C). Other aerospace materials either have corrosion/oxidation problems or are limited by coatings, architecture, or brittleness. Therefore, it becomes necessary to reduce the metal temperature by other means. The use of sodium cooling, which was developed to a very high state in World War II reciprocating aero-engines, can reduce metal temperatures by 300 to 400F (166 to 222C).<sup>35</sup> It is expected that the combination of sodium cooling and thermal shielding of the valves plus preferential cooling of the valve seat inserts will reduce the valve metal temperatures to acceptable levels for those brief periods at rated power and high, hot ambient conditions. Sleeve valves were mentioned in paragraph 8.1 as a means to increase the piston ring/liner interface life. These devices would also replace poppet valves and possibly could solve the exhaust valve problem because of the much cooler top edge of the sleeve.

### 8.3 Fuel Injection and Combustion Requirements

Fuel injection with high heat release combustion is considered to be the third most critical area for development. The primary requirement of the fuel injection equipment for a direct-injected diesel core is to distribute a uniform and finely atomized charge of fuel throughout the combustion chamber. The charge must be delivered at the proper time, duration of delivery must be controlled to a reasonable number of crankshaft degrees (20-30CA), and the quantity injected must be accurately controlled. Timing, duration, and quantity also must be repeatable from one injection to the next. If not, excessive peak cylinder pressure will occur, exhaust smoke will increase, and engine life will be shortened. The difficulty associated with providing these injection characteristics becomes more complex as the engine speed is increased and the quantity of fuel ( $m^3/\text{cycle}$ )

Table 17. Potential Exhaust Valve Materials.

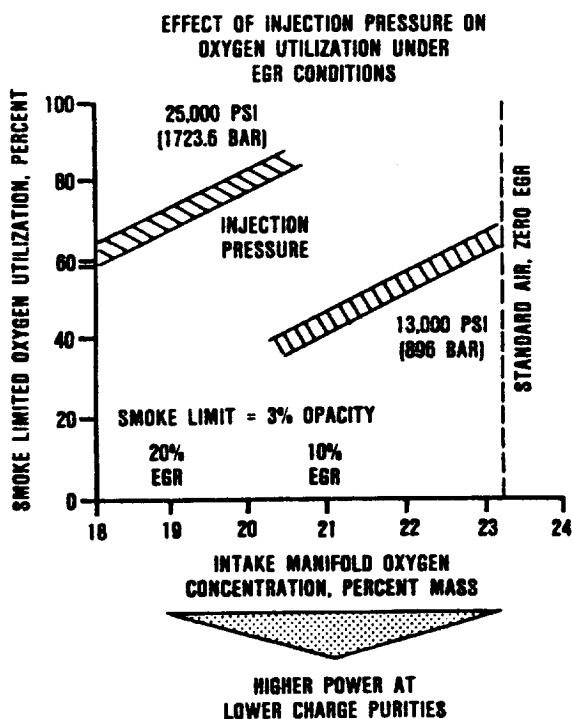
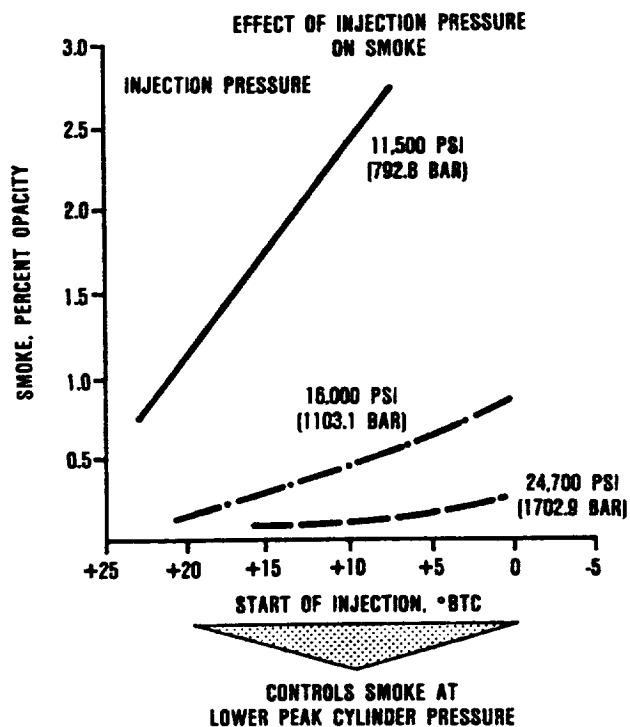
| Mean Gas Temperature, F (C)<br>Metal Temperature, F (C)<br>(uncooled)                              | 1100<br>(593)<br>1450<br>(788)     | 1400<br>(760)<br>1750<br>(954)   | 1650<br>(899)<br>2000<br>(1093)  | 2050<br>(1121)<br>2400<br>(11316) | Remarks  |
|--|------------------------------------|----------------------------------|----------------------------------|-----------------------------------|--|
| Nimonic 80A<br>0.2% Yield, ksi (kbar)<br>UTS, * ksi (kbar)<br>0.2% Creep/100 Hours,<br>ksi (kbar)  | 65(4.48)<br>75(5.17)<br>40(2.78)   | 11(0.76)<br>18(1.24)<br>6(0.41)  | --<br>--<br>0.3(0.02)            | --<br>--<br>0                     | Current Production   |
| Astrolloy<br>0.2% Yield, ksi (kbar)<br>UTS, ksi (kbar)<br>0.2% Creep/100 Hours,<br>ksi (kbar)      | 125(8.62)<br>160(11.0)<br>68(4.67) | 48(3.31)<br>75(5.17)<br>20(1.38) | 12(0.83)<br>15(1.03)<br>5(0.34)  | --<br>--<br>0                     | Special Applications<br>Current Production                               |
| MAR-M 247<br>Yield, ksi<br>UTS, ksi<br>0.2% Creep/100 Hours,<br>ksi (kbar)                         | 115(7.93)<br>140(9.66)<br>30(2.07) | 60(4.14)<br>85(5.86)<br>35(2.41) | 35(2.41)<br>45(3.10)<br>12(0.83) | --<br>--<br>1(0.07)               | Corrosion/Oxidation  |
| WC 3015 (Columbium)<br>Yield, ksi (kbar)<br>UTS, ksi (kbar)<br>0.2% Creep/100 Hours,<br>ksi (kbar) | 110(7.59)<br>70(4.82)<br>NA        | 90(4.14)<br>65(4.48)<br>NA       | 60(4.13)<br>35(2.41)<br>18(1.24) | 40(2.76)<br>30(2.07)<br>9(0.62)   | Aerospace Material<br>Corrosion/Oxidation Coating<br>Limited             |
| Carbon/Carbon (Coated)<br>0.2% Yield, ksi (kbar)<br>UTS, ksi (kbar)<br>Creep, ksi (kbar)           | 50(3.45)<br>50(3.45)<br>50(3.45)   | 50(3.45)<br>50(3.45)<br>50(3.45) | 50(3.45)<br>50(3.45)<br>50(3.45) | 50(3.45)<br>50(3.45)<br>50(3.45)  | Advanced Aerospace Material<br>Limited by Coating and<br>Architecture    |
| Ceramics<br>Yield, ksi (kbar)<br>UTS, ksi (kbar)<br>Creep, ksi (kbar)                              | 70(4.82)<br>70<br>Low              | 70(4.82)<br>70<br>Low            | 70(4.82)<br>70<br>Low            | 70(4.82)<br>70<br>Low             | Advanced Aerospace Material<br>Brittle, Notch and Strain<br>Rate Limited |

\*Ultimate Tensile Strength

burned in each cylinder per stroke is increased. High speed mandates high heat release rate combustion because the physical time for combustion is decreased.

The benefits of higher injection pressures on exhaust smoke and oxygen use (smoke limited equivalence ratio) may be seen in Figure 56.<sup>36</sup> These high pressures are instrumental in improving the fuel-to-air mixing process through momentum exchange of the small fuel droplets moving at high velocity along the plume.

Detailed analysis of existing combustion and injection technologies indicate that a direct-injected, high-pressure (>20,000 psi) (1400 bar) electronically controlled hydromechanical-type injector is the prime candidate for CCE development. High cylinder temperature dictates the use of nozzle tip cooling. The high cylinder pressure and operating speed means that special emphasis also must be taken to minimize nozzle seat Hertz stresses and impact loads. Also, special attention must be given to operating spring stresses or to designs that eliminate springs.



REFERENCE 36

Figure 56. The Effect of Injection Pressure On Exhaust Smoke and Oxygen Use.



## 9.0 MISSION PAYOFF SENSITIVITIES

The major technological development areas have been identified:

- o Piston ring/liner wear - Influenced by engine speed
- o Exhaust valve life - Determined by exhaust gas temperature
- o Combustion/heat release rate - Controlled by trapped equivalence ratio

It is not presently possible to quantify or predict component wear, life, or heat release rate at the operating conditions of the CCE. Therefore, mission sensitivity payoff studies have been made on three key engine parameters that affect engine life--engine speed, exhaust gas temperature, and trapped equivalence ratio. Their effects on mission fuel, weight, payload, and range payoffs, as compared with the contemporary gas turbine, have been evaluated. A family of six-cylinder CCEs was specified with a fixed bore/stroke ratio of 1.055, fixed effective compression ratio of 7.50, and peak firing pressures of approximately 3400 psi (234.5 bar). Boost pressure ratios range from 9.5 to 10.5, and piston velocities from 2700 to 3000 ft/min (13.5 m/sec and 15 m/sec). The narrow range in parameter values was required to maintain the six-cylinder configuration.

This family of CCE engines was operated over the two-hour composite mission/load profile at 4000 ft, 95 F day (1.23 km, 35C), and the mission performance parameters were calculated.

### 9.1 Diesel Engine Speed

Figure 57 shows the percent improvements with the CCE over a contemporary gas turbine in engine SFC (mission fuel weight), and

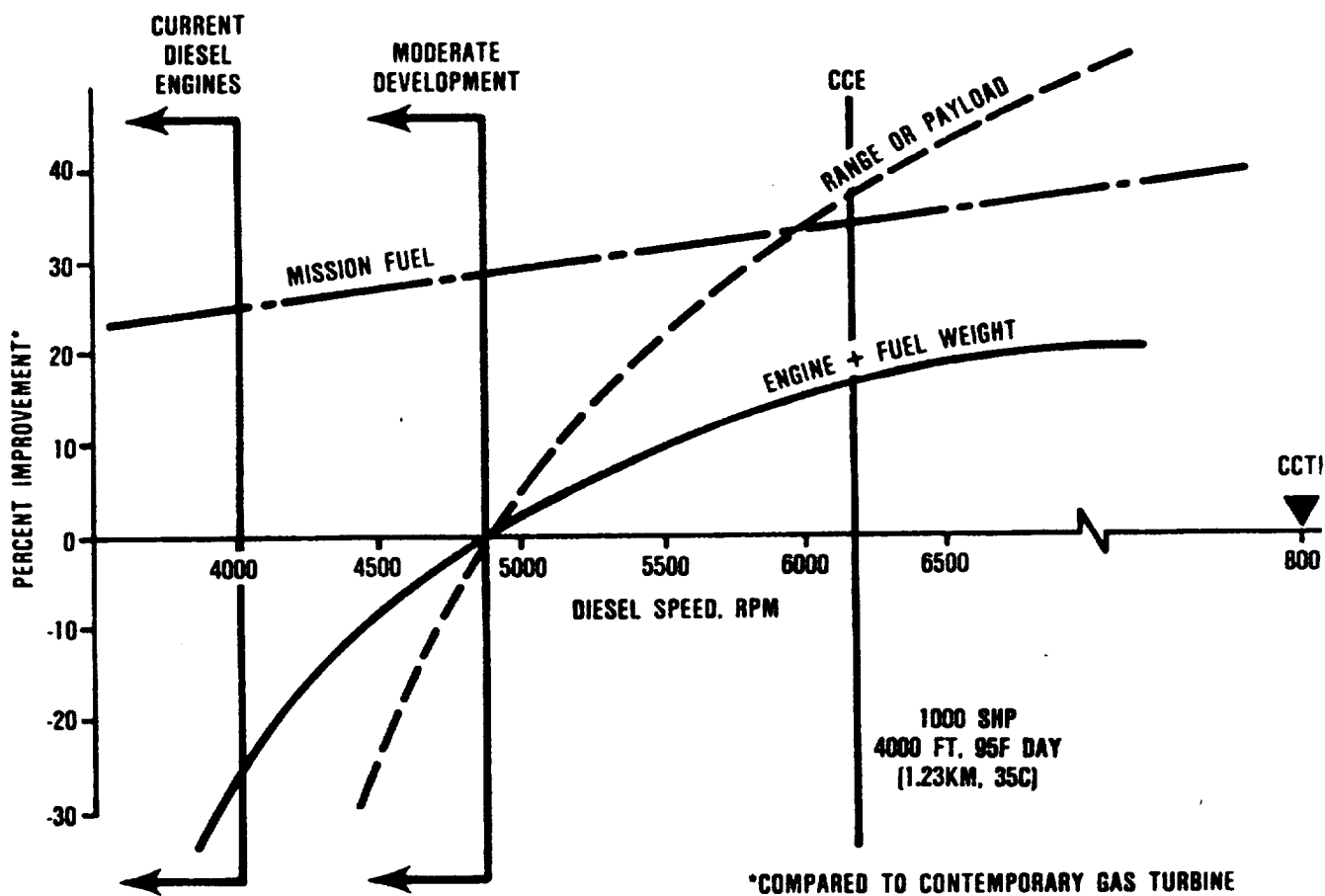


Figure 57. Compound Cycle Engine Design Point Payoff As a Function of Diesel Core Speed.

range or payload as a function of diesel core speed. As diesel core rpm is increased, the required technology levels in the three major development areas are also increased for the improved performance.

A CCE with a diesel core based on application of current technologies could provide a 20 percent savings in mission fuel; however, its weight would be unacceptable. Near-term (moderate) technology development could produce 25 percent fuel savings at an acceptable engine weight, but with no gain in range or payload. The aggressive technologies proposed for the CCE study result in a 31.4 percent savings in fuel and about a 40 percent improvement in range or payload over a contemporary gas turbine engine for the same vehicle gross weight. Again, it should be noted that the CCTE engine was run at 8000 rpm under the AF/DARPA program and that the targeted speed for the CCE is well under that value.

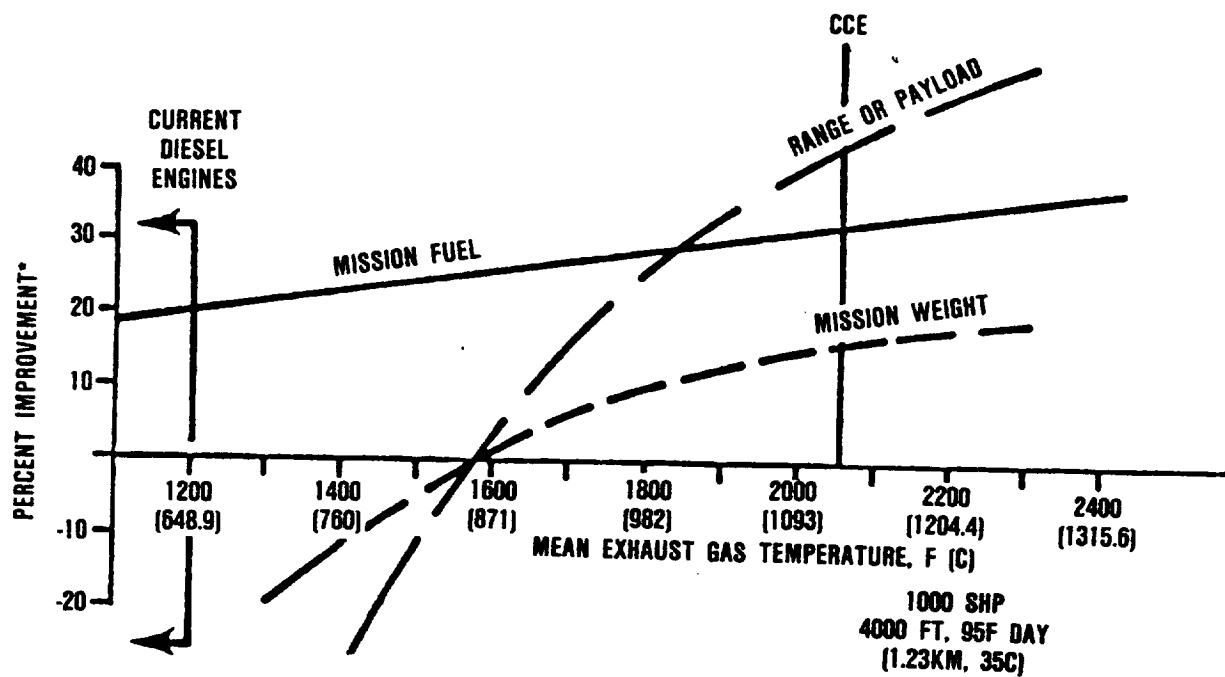
## 9.2 Exhaust Gas Temperature

Similar sensitivity computations were made as a function of exhaust gas temperature, which was varied by engine displacement and equivalence ratio changes for a 4000 ft, 95F (1.23 km, 35C) day. These data are shown in Figure 58. At a 1550F(843C) exhaust gas temperature, the mission fuel savings is 25 percent. As the exhaust gas temperature is increased to the 2042F (1117C) rated point, the payoffs increase to their maximum values of, as follows:

- o 15.4 percent on mission weight
- o 31.8 percent on mission fuel
- o 42.5 percent on range or payload

## 9.3 Trapped Equivalence Ratio

The trapped equivalence ratio, has a strong influence on in-cylinder gas and metal temperatures, exhaust gas temperatures,



\*COMPARED TO CONTEMPORARY GAS TURBINE

Figure 58. Compound Cycle Engine Design Point Payoff As a Function of Diesel Average Exhaust Gas Temperature.

and BSFC. This parameter was varied in the range of 0.50 to 0.82 units. This was accomplished by changing the engine displacement and BMEP to maintain a constant 1000 shp for a 4000 ft, 95F (1.23 km, 35C) day. As seen in Figure 59, the "break-even" point was determined to be 0.62 equivalence ratio, where the mission fuel savings was 25 percent. When the trapped equivalence ratio was increased to 0.80, the payoffs on mission fuel, weight, and range or payload increase to 31.0, 15.2, and 36.5 percent, respectively.

#### 9.4 Mission Payoff Recapitulation

The mission payoff studies have shown that an engine based on application of current technologies could provide a 20 percent saving in mission fuel; however, its weight would be unacceptable. Near-term, (moderate) development could produce 25 percent fuel savings at an acceptable engine weight, but with no gain in range or payload. However, with the aggressive technologies proposed in this study, the selected CCE offers a 31.4 percent savings in fuel and about a 40 percent improvement in range or payload for the same vehicle gross weight.

These payoffs can be achieved only with advanced tribology, low friction and wear material couples, and near-ashless, high-temperature lubricants, which can be applied preferentially at the ring-reversal areas. An alternative solution that may have a high potential for success is an engine design with sleeve-valve porting. With the sleeve valve, there is always relative motion between the piston ring and cylinder liner so that some oil film exists at TDC and BDC.

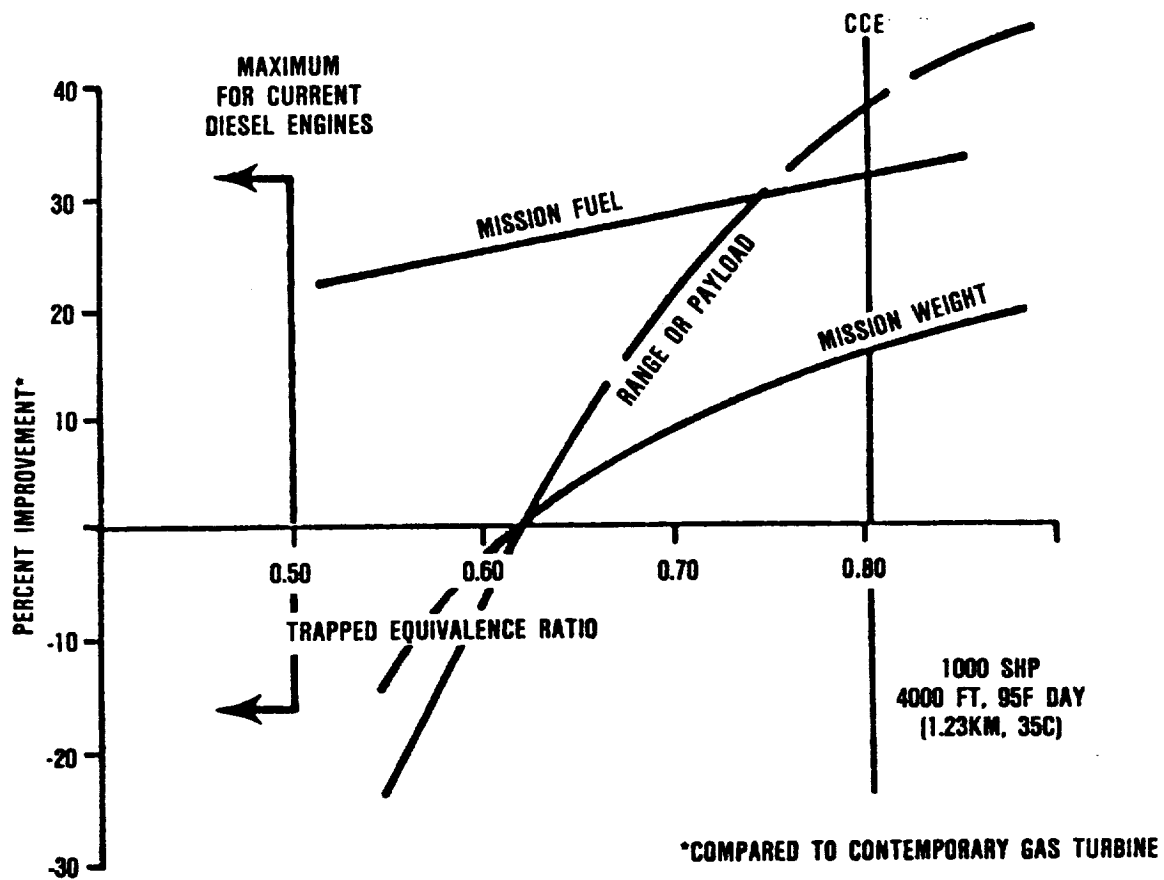


Figure 59. Compound Cycle Engine Design Point Payoff As a Function of Trapped Equivalence Ratio.

## 10.0 CCE POTENTIALS BEYOND THE YEAR 2000

The performance and weight predictions specified in this study are based on materials and component technologies that are currently in commercial use. An exception is the lubricating oil and some are presently under development. Therefore, the performance and weight of the first generation of CCE can be projected for production in the 1990s with confidence. However, as discussed in Section 7, engine life cannot be confidently predicted.

### 10.1 Assumptions Used in the Year-2000 Study

Performance predictions for the year-2000 CCE engine have been made using projections for advances in material strength, friction, durability, and the operating environment (i.e., maximum temperature and pressure) beyond those used for the study engine.

The friction mean effective pressure has been decreased from 28 to 14 psi (1.93 to 0.97 bar) (50 percent) based on reduced number of piston rings, roller bearings and improved lubricants. This level of improvement has been projected by other industry investigators. This assumption will increase the engine mechanical efficiency from 93 to 96 percent and reduce the BSFC by 3 percent.

It was assumed that cylinder heat loss could be reduced by an additional 50 percent due to improvements in ceramics, insulating materials, and lubricants. This reduction in cylinder heat loss would increase the energy in the exhaust gases, thereby adding to the power from the bottoming turbines and also decrease BSFC by 3 percent.

Advanced materials such as carbon-carbon, composites, and polyimides were projected to reduce the installed

engine weight by 25 percent compared to the 1995 CCE, which would increase the mission payoff a considerable amount.

It is assumed that lubricants, exhaust valves, and piston rings/liners will also be improved and that an aftercooler for the engine inlet air may be omitted. This reduces the installed weight and fan power requirement and increases the exhaust energy available for the compounding turbine.

Peak firing pressure was projected to be increased from 3000 to 4000 (207 to 276 bar) psi because of improved lubricants and materials. This increases the brake thermal efficiency of the cycle, thereby reducing the BSFC by another 3 percent.

It is projected that for the year 2000, the competitive gas turbine will still have the same component efficiencies and BSFC as the current model. However, improved materials will reduce the installed weight from 358 to 256 (162 kg to 116 kg) pounds.

## 10.2 Year-2000 Mission Predictions

It is recognized that reaching the projected advanced goals requires much more component technology development than that required for the selected CCE study engine. Figure 60 shows a fuel consumption comparison between gas turbine and CCE engines. The benefits based on 4000 ft, 95F (1.22 km, 35C) are substantial:

- o 41.4 percent savings in mission fuel
- o 26.7 percent savings in fuel and engine weight
- o 56.6 percent increase in payload for the same range
- o 73.7 percent increase in range with the same payload

These impressive payoffs would justify the development efforts necessary to achieve them.



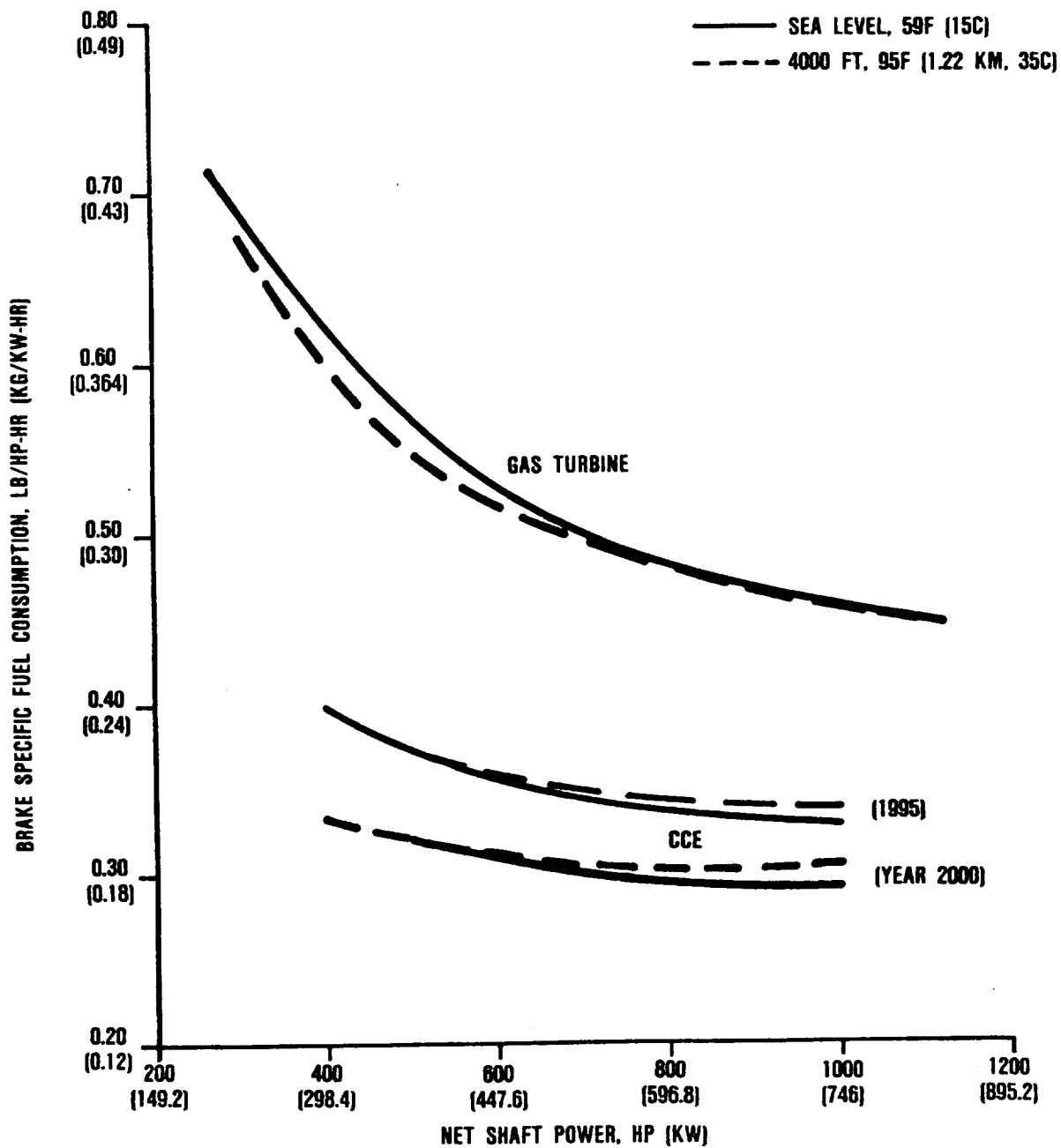


Figure 60. Fuel Consumption Comparison for Gas Turbine and CCTDE.

## 11.0 CONCLUSIONS AND RECOMMENDATIONS

### 11.1 Conclusions

CCE has been compared with a contemporary gas turbine engine for a two-hour composite mission. The engine rating of 1000 shp (745.7 kW) is based on 4000 feet (1.22 km) altitude and 95F (35C) day and is flat rated from sea level. The results of this comparison are:

- o 31.4 percent reduction in mission fuel consumption
- o 15.8 percent lower fuel plus installed engine weight
- o 36.5 percent increase in payload for the same range, or, 40.7 percent increase in range for the same payload
- o 8.5 percent reduction in volume over a contemporary gas turbine

The 1.5-spool, turbocompounded, 2-stroke cycle diesel engine of this study is a viable alternative to a contemporary simple-cycle gas turbine engine for a light helicopter application. The engine described in this study offers significant payoffs in terms of mission fuel, weight, range, and payload. The technology to achieve these goals can be attained with suitable developmental programs. The following key component technology development areas have been identified:

- Piston ring/cylinder liner wear interface
- High temperature lubricants
- Exhaust valve metal temperature
- Fuel injection/combustion

## 11.2 Recommendations

Based on the results of this analytical study, the merits of a turbocompounded diesel helicopter engine have been established. The enabling technologies have been defined and the following technology program recommendations are proposed:

- o Continue expanded high-temperature (800F TRRT [427C]) lubricant formulation and advanced tribology activities
- o Design, fabricate, and test a high-power density, high-speed uniflow-scavenged, single-cylinder engine to demonstrate performance and life characteristics
- o Continue piston ring/liner interface wear rate studies using the radionuclide technique
- o Initiate a development program for poppet exhaust valves to operate at high gas temperatures
- o Evaluate alternate valving schemes
- o Conduct a high-speed fuel injection system development program using an electronically controlled hydromechanical-type fuel injector
- o Develop diesel engine combustion at the CCE high speed, equivalence ratio, and heat release rates
- o Initiate the design of a multicylinder diesel core engine
- o Fabricate and test the multicylinder diesel core engine to demonstrate integration of single-cylinder technologies for performance and engine weight prediction validation

## APPENDIX A

### THE NAPIER NOMAD AIRCRAFT DIESEL ENGINE

During the early 1950s, D. Napier & Son, a British aviation engine firm, designed and developed the "Nomad,"<sup>14</sup> an aircraft diesel engine with a 35 percent lower fuel consumption than contemporary turboprop engines. The engine is horizontally opposed, 12 cylinders, and of 2-stroke loop scavenged design. The power plant consists of the reciprocating engine and a gas turbine combined to form a "compound" engine, whose operating cycle is devised for each component to make its maximum contribution to the overall results.

In the compound engine, the cycle of operations is shared between a 2-stroke diesel engine and a turbine that is powered by the exhaust gases expelled from the engine. The back pressure imposed by the turbine on the engine cylinders establishes the lower pressure level of the operating cycle in the cylinders. This also determines the degree of supercharge necessary to pass the required quantity of air through the engine.

#### Engine Design and Construction

The mechanical layout of the Napier Nomad is shown in Figure 61. An "infinitely variable gear" has been interposed in the gear system between the turbocompressor set and the engine. This permits a range of gear ratios to be selected for any crankshaft speed and is responsible for the higher power output and fuel efficiency at an altitude, which the Nomad exhibits compared with a fixed-gear-ratio engine.

The diesel engine has 12 cylinders in banks of six, horizontally opposed on a six-throw crankshaft, and the cylinder design is a simple 2-stroke type, using piston-controlled intake

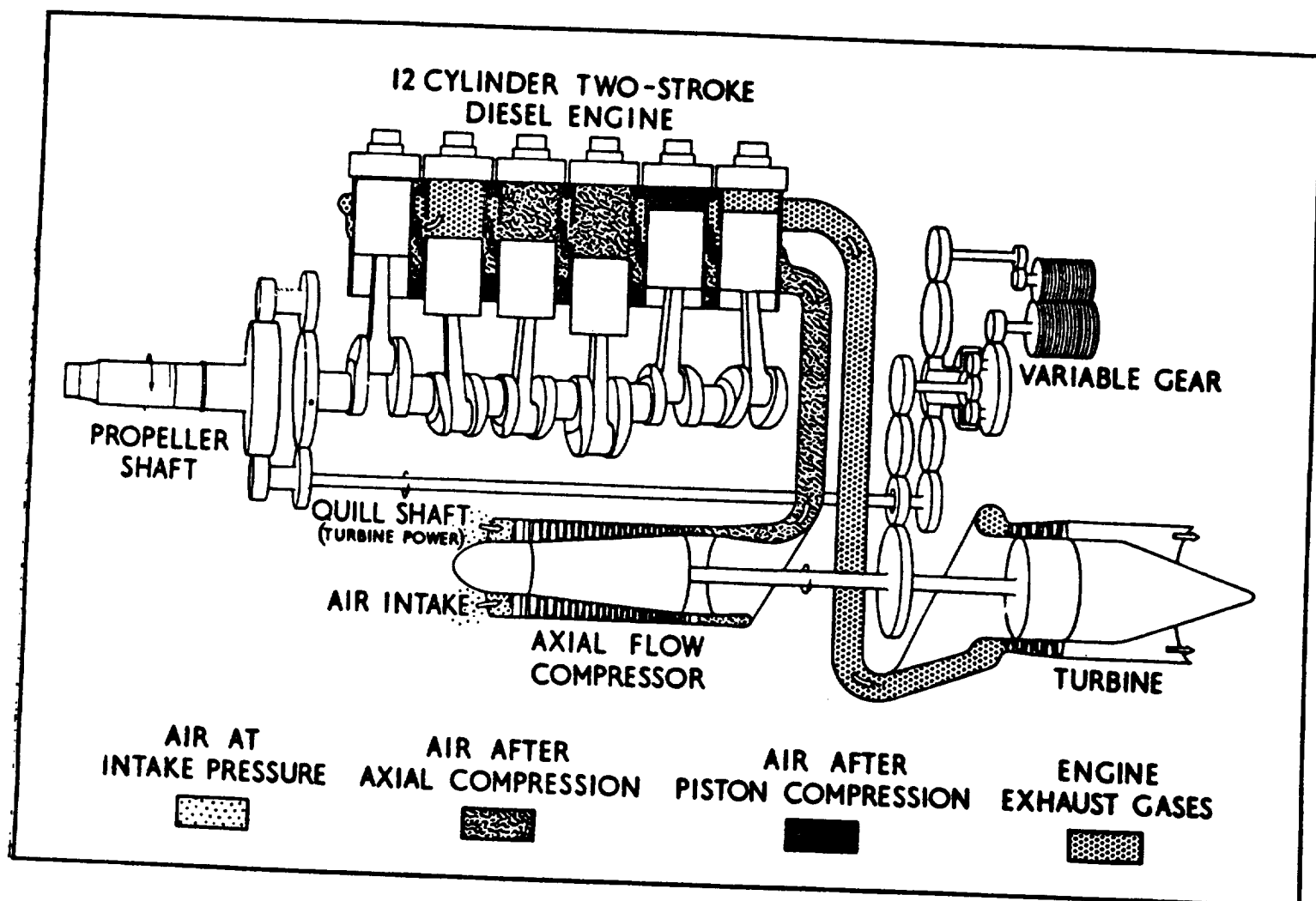


Figure 61. Diagram of Nomad Engine.

and exhaust ports. The arrangement of the cylinder is shown in Figure 62, which depicts the loop-scavenging gas flow and also the centrally located diesel fuel injector. The injection pumps, which are in blocks of six, are of normal "jerk-pump" design, specially developed to deal with the high outputs and speeds of operation required.

The pistons (Figure 63) have aluminum alloy bodies but are fitted with austenitic steel crowns designed to operate at 1100 to 1300F (593 to 704C) at full power. At this point, oil cooling is provided behind the piston rings to ensure minimum temperatures.

The wrist pin-connecting rod-crank pin bearing designs are quite innovative because of the unidirectional loading, which exists in a 2-stroke engine. Figure 64 shows that the connecting rod has half-bearings or "slipper" type construction at both the small and big ends with light straps as safety devices in the reverse-loading direction. A later development of this type of bearing is applied at the small end because the unidirectional (compressive) loading usually prevents separation of the bearing and journal, thereby preventing the formation of a substantive oil film between them. On the Nomad, this difficulty has been overcome in the manner illustrated in Figure 65.

The wrist pin bearing is divided lengthwise into three sections comprised of two outer bearings "X" and a center bearing "Y". The outer bearings are coaxial with each other but their centers are displaced transversely from the centerline of the connecting rod. The axis of the center bearing is similarly displaced on the opposite side of the connecting rod axis. Therefore, the three bearings constitute two bearings eccentric to one another, equally spaced [0.035 inch (0.9 mm)] about the axis of the connecting rod. The operation of this arrangement can best be understood by studying the exaggerated diagrams, B, C, and D in Figure 65, which show the rocking motion of the connecting rod that unloads and loads the segmented bearing.

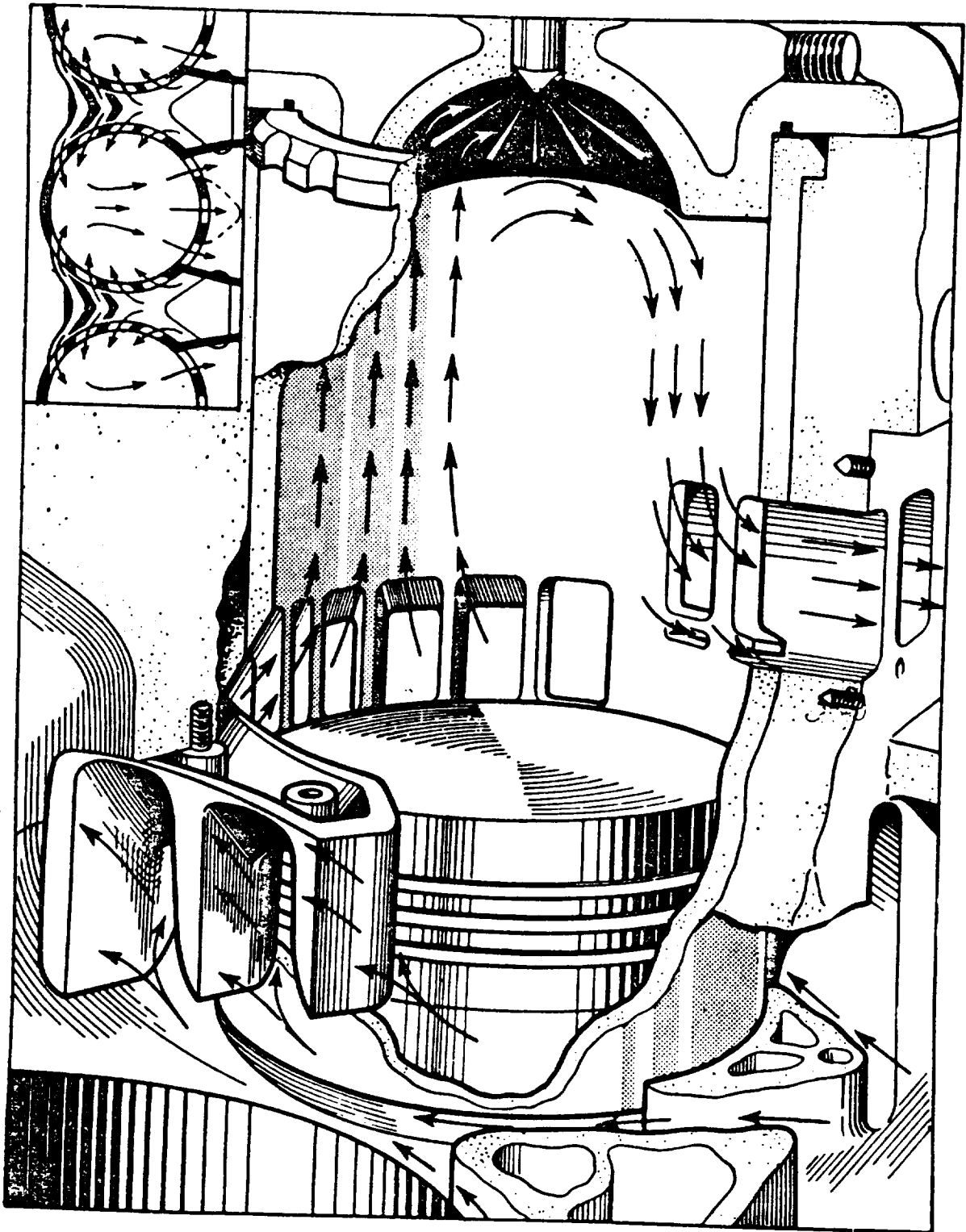
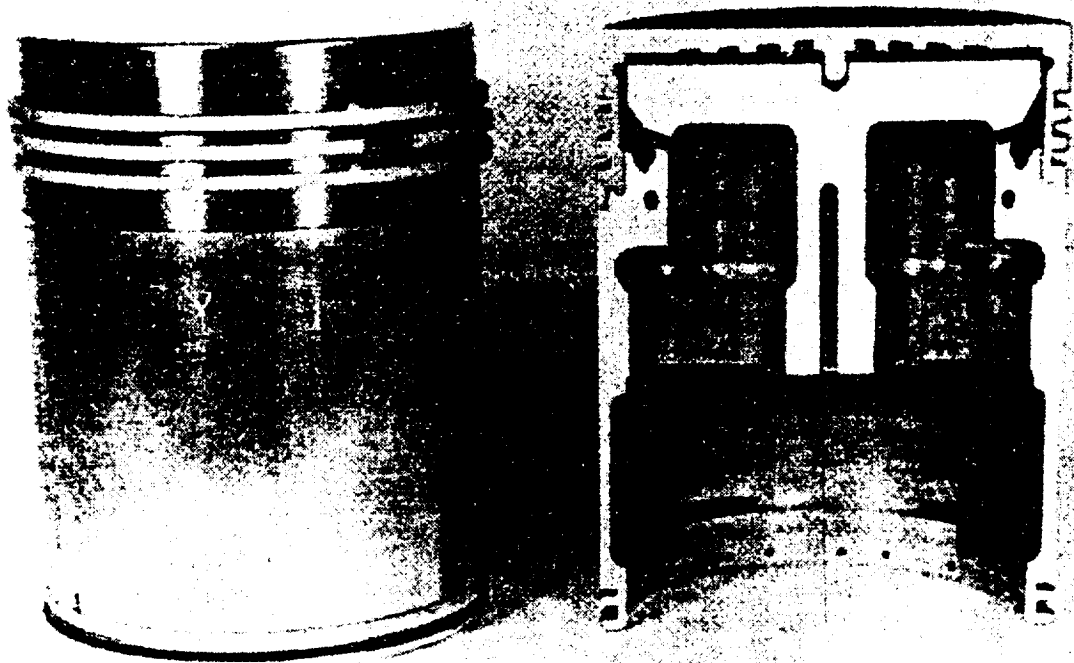


Figure 62. Arrangement of Engine Cylinder.

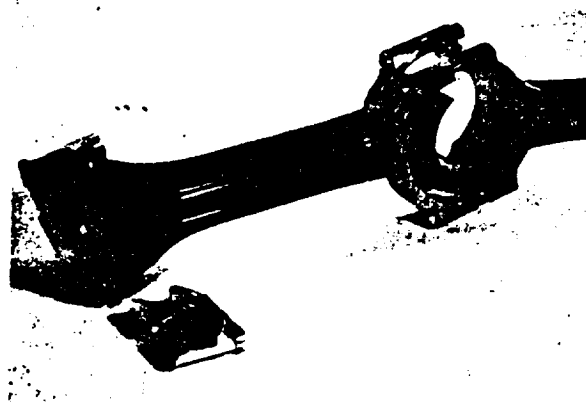
ORIGINAL PAGE  
BLACK AND WHITE PHOTOGRAPH



ORIGINAL PAGE IS  
OF POOR QUALITY

Figure 63. Arrangement of Piston.





ORIGINAL PAGE  
BLACK AND WHITE PHOTOGRAPH

**Figure 64. Arrangement of Connecting Rod.**

ORIGINAL PAGE IS  
OF POOR QUALITY,

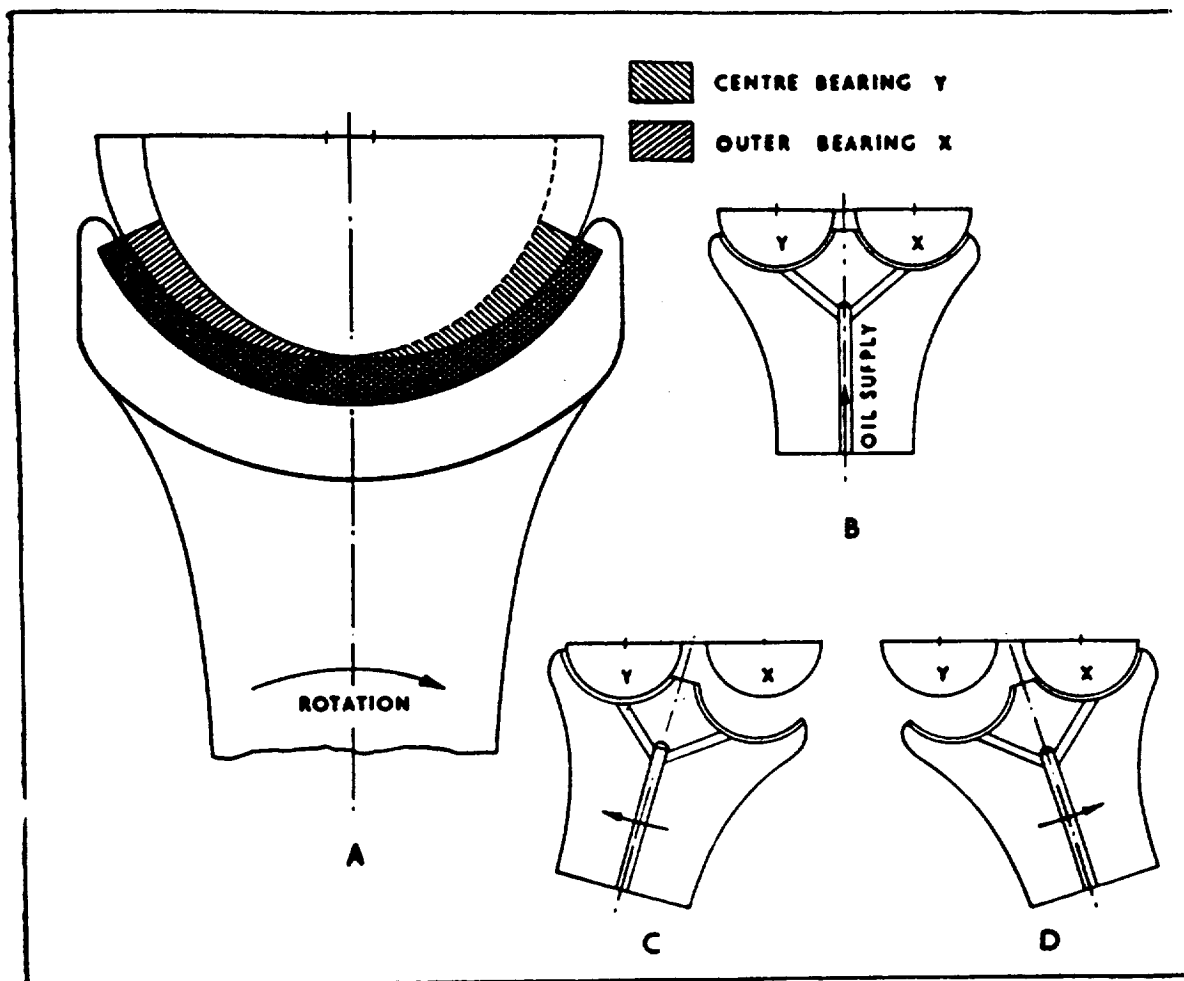


**Figure 65. Connecting-Rod Small-End Bearing.**

The axial compressor has 12 stages and operates at a maximum pressure ratio of 8.25/1 with an air mass flow of 13 lb/sec (5.9 kg/sec) and to extend operating range at the low-speed end, has adjustable inlet guide vanes. The adiabatic efficiency of the compressor at takeoff (sea-level static) is 85 percent and its peak efficiency is 87.5 percent.

The three-stage turbine is mounted coaxially with the compressor, and its blading is designed to extract maximum energy from the gases, rather than to obtain some jet thrust from the exhaust. The efficiency at takeoff (sea-level static) is 84 percent and 86 percent at the altitude cruise rating. Both compressor and turbine are connected into the rear gear casing by shafts having splines at each end to allow expansion effects.

The engine is equipped with an infinitely variable speed traction drive between the turbomachinery and the reciprocator. This device, also known as a Beier, consists of a pair of conical members that are end-loaded together. The gear ratio is varied by sliding one cone over the other. Actual details are shown in Figure 66, where a "pack" of disks with narrow conical rims are mounted on a central shaft and spring loaded to trap between them a series of coned disks carried on each of three planetary shafts and arranged to swing about a fulcrum to obtain changes in speed ratio. This arrangement provides a constant mesh system whose speed ratio may be changed while running.

The variable-speed drive efficiency ranges from 65 to 92 percent, being the greatest at high power. Only 30 percent (1000 shp [746 kW]) of the total engine power is transmitted through that part of the system where the speed-varying device is fitted. The arrangement of this complete system in the Nomad is shown in Figure 67.

A longitudinal section through the engine is shown in Figure 68, the layout following closely the diagrammatic arrangement of

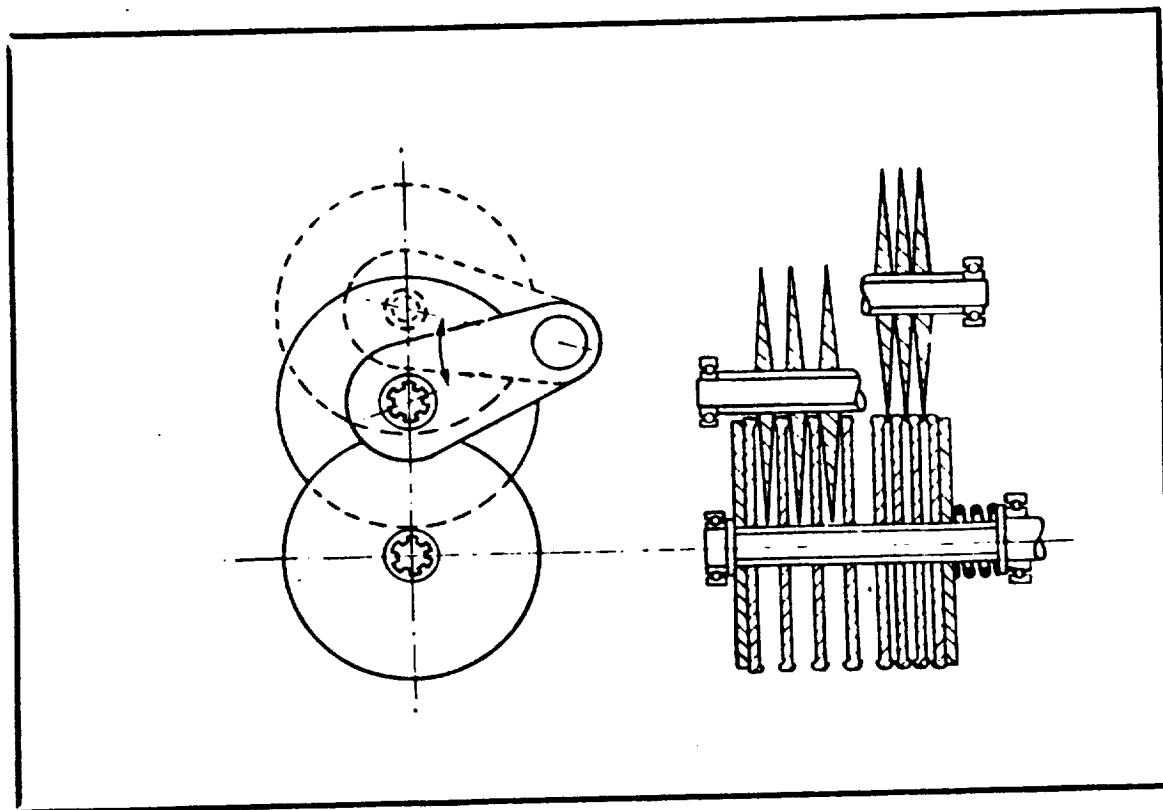


**Figure 66. Diagram Showing Operation of Variable Gear.**

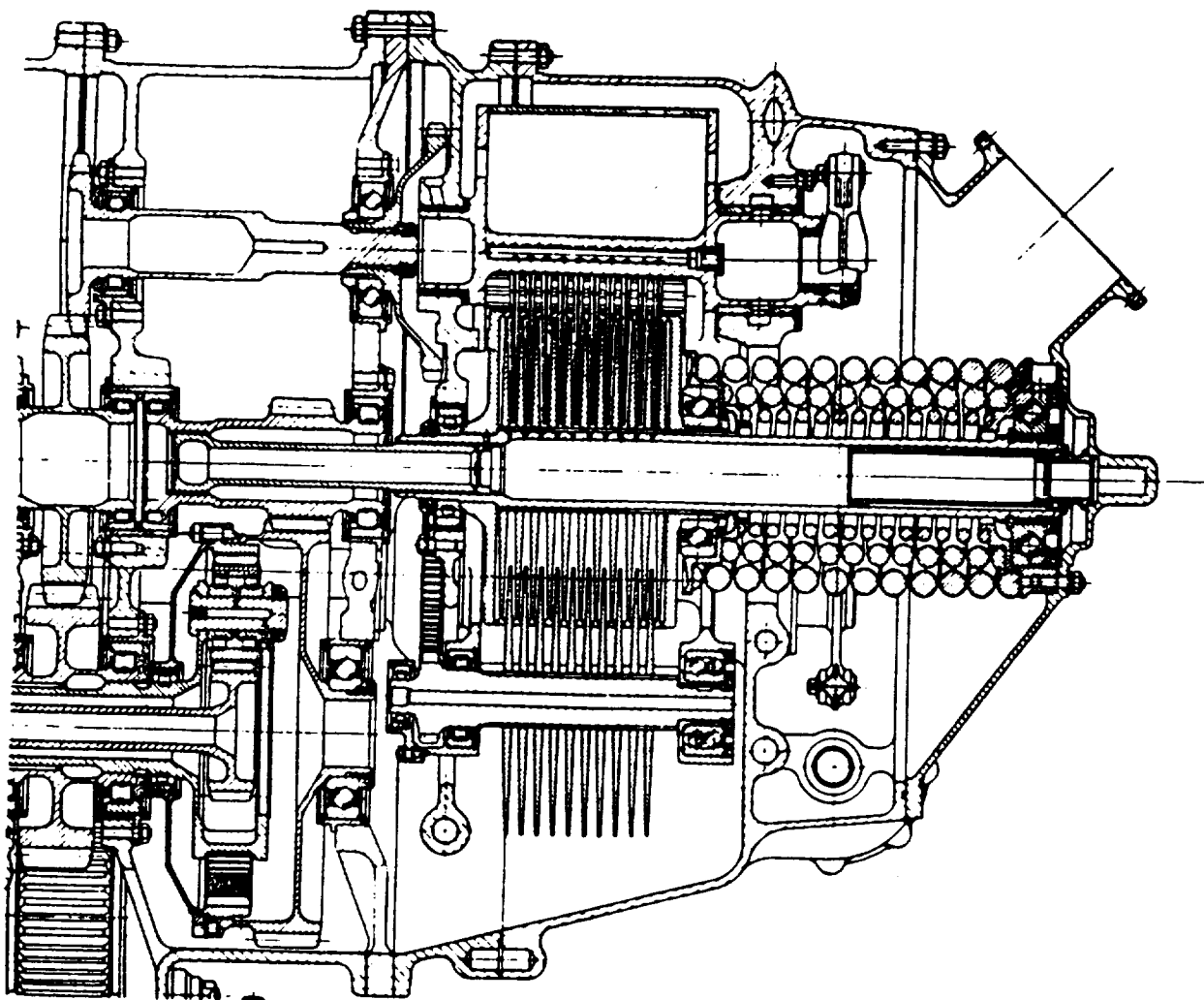


Figure 67. Variable Gear as Fitted to Engine.

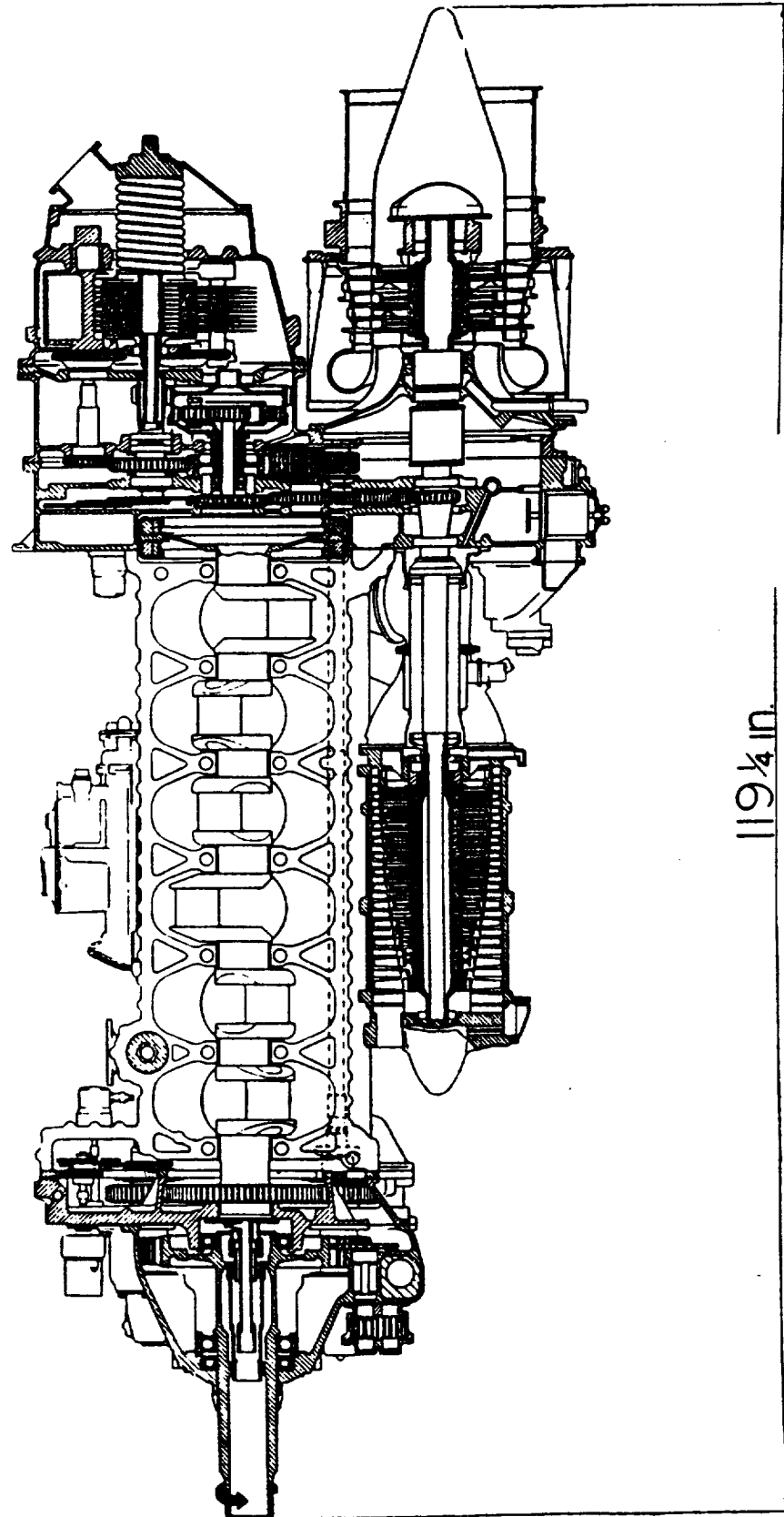


Figure 68. Longitudinal Section of Nomad Engine.

Figure 61. Figure 69 shows the engine cross section and clearly indicates the vertically divided magnesium crankcase and the aluminum cylinder blocks, which are bolted together by steel through bolts. It will be seen that dry liners are employed with the liners themselves being of chromium-copper material and chromium-plated in the bores. Figure 70 shows a cutaway drawing where the main features have been identified. A photograph from one side has been made (Figure 71) and shows that the engine is suspended from four pickup points. This arrangement is convenient for maximum accessibility, particularly to the compressor and turbine.

Engine starting is by electric motor. Since the compression ratio in the engine cylinders is insufficient to give self-ignition under these conditions, spark plugs are fitted in each cylinder head and are activated by a high-energy system. These plugs are used only for starting.

#### Engine Performance

The following details apply to the Napier Nomad:

|                              |                          |
|------------------------------|--------------------------|
| Bore x Stroke, in. (mm)      | 6 x 7.375<br>(152 x 187) |
| Number of Cylinders          | 12                       |
| Rated Speed, rpm             | 2050                     |
| Piston Speed, ft/min (m/sec) | 2520 (12.7)              |
| Net Dry Weight, lb (kg)      | 3580 (1624)              |

#### Take-Off Performance at Sea-Level, Static

|                  |                                  |             |
|------------------|----------------------------------|-------------|
| Dry:             | BHP, ehp (ekW)                   | 3155 (2339) |
|                  | BSFC, lb./ehp-hr,<br>(gm/ekW-hr) | 0.345 (207) |
| Water Injection: | BHP, ehp (ekW)                   | 3580 (2671) |
|                  | BSFC, lb/ehp-hr<br>(gm/ekW-hr)   | 0.336 (202) |

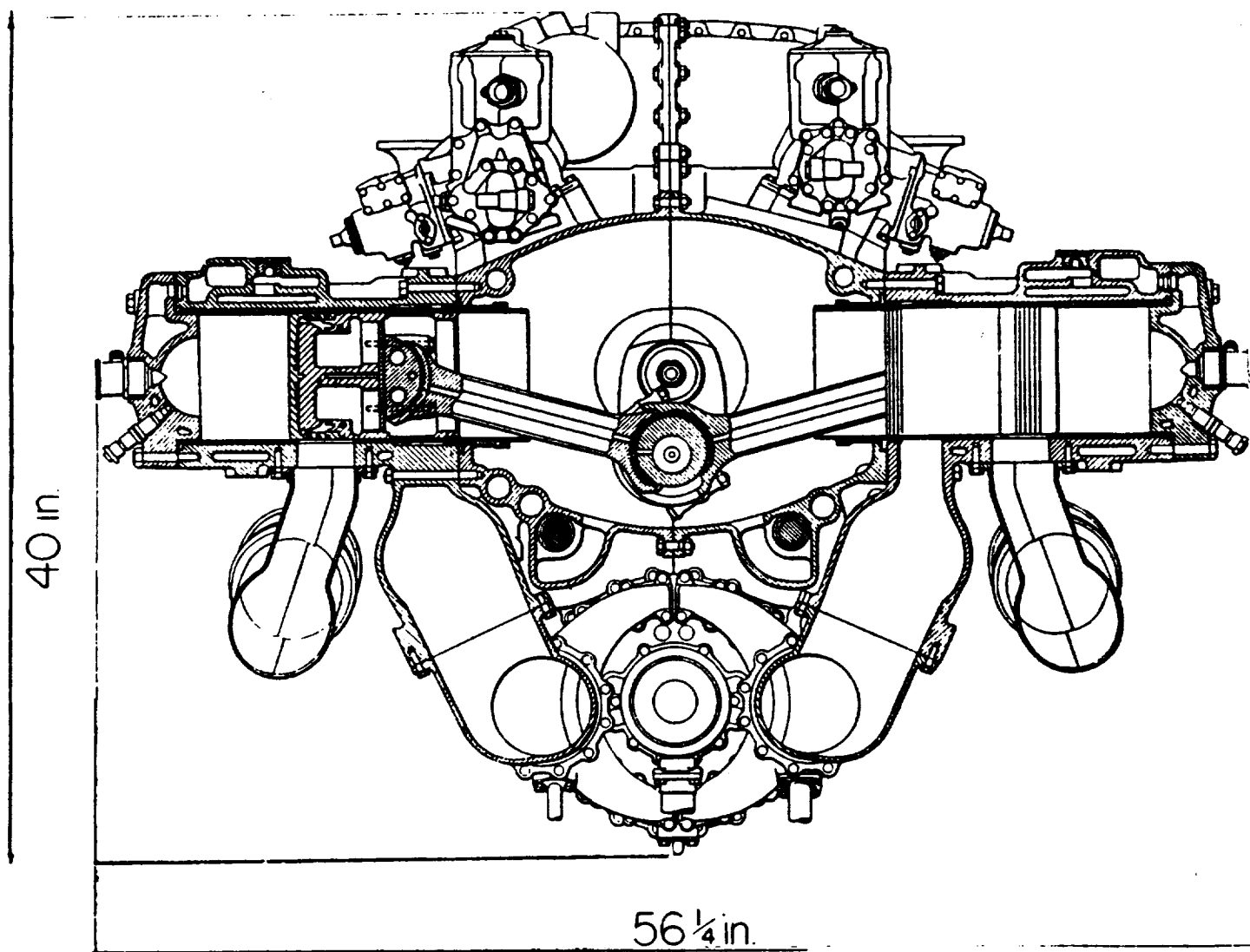


**Figure 69. Crosssection of Nomad Engine.**







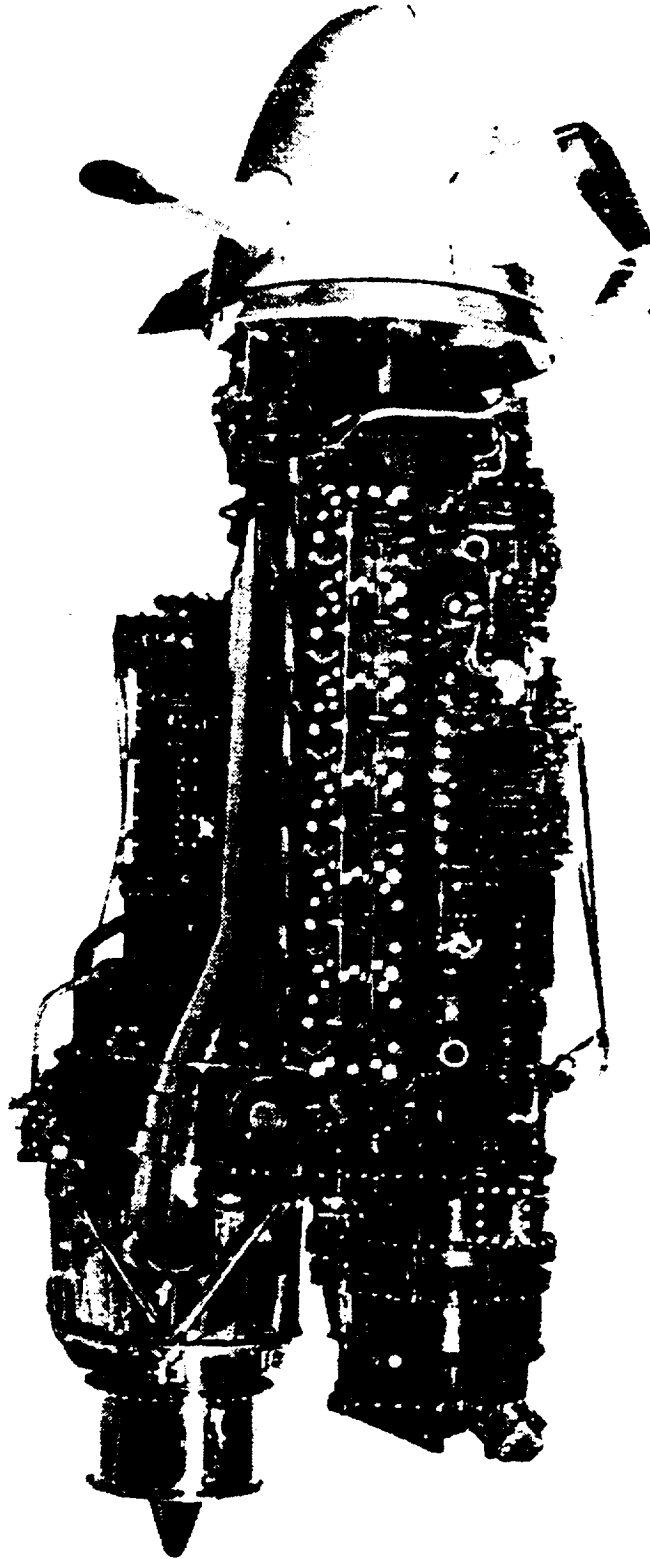


Figure 71. Side View of Nomad Engine.



Plus Auxiliary Combustion:

|                 |             |
|-----------------|-------------|
| BHP, ehp (ekW)  | 4100 (3059) |
| BSFC, lb/ehp-hr | 0.374(224)  |
| (gm/ekW-hr)     |             |

\*e = equivalent - includes reciprocator and turbine outputs plus jet thrust contribution.

The basic engine take-off performance includes 2745 bhp from the reciprocator and 390 hp, which is surplus from the turbine for a combined output of 3135 ehp.

The normal charge air temperature at takeoff is quite high [477F (247C)]. It is necessary to reduce this temperature if increased output is required. The use of aftercoolers would impose bulk, weight, and thermodynamic penalties on the system. However, the charge temperature can be reduced most conveniently, and density increased without energy loss by injecting water into the inlet manifolds. When this is done, a greater quantity of air can be packed into the engine cylinders and the power output still further increased. Using water injection in this way, the equivalent power of the engine is increased to 3580 hp (2671 kW).

Another possibility for increasing the maximum power output arises from the presence of excess air in the exhaust manifold between the engine and the turbine. At the expense of a slight increase in the turbine inlet temperature, a small quantity of additional fuel can be injected and burned at this point. This extra fuel would be burned at low expansion ratio and therefore at low efficiency, but the effect on the overall SFC is small. This system of combustion could be used in association with water injection, and for a turbine inlet temperature of 1377F (747C) the take-off power could be increased to 4100 hp (3059 kW). The take-off performances against altitude for the three conditions referred to are illustrated in Figure 72.

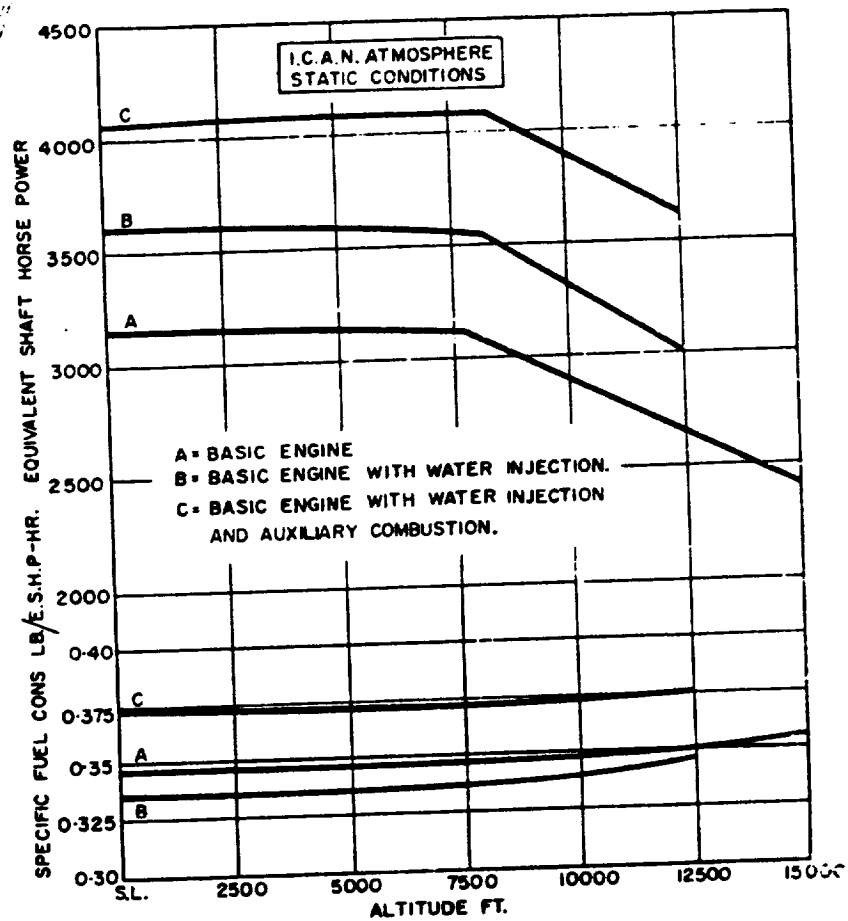


Figure 72. Takeoff Powers Against Altitude With Fuel Consumption.

The power split at which the engine is controlled over the speed range under sea-level static conditions is shown in Figure 73. The shape of this curve is devised to maintain optimum thermal efficiency and altitude performance over as wide a range as possible and also to suit control requirement of the propeller. Also, on the same diagram are the corresponding diesel, turbine, and compressor powers and at 1500 rpm, the turbine power exactly balances that absorbed by the compressor. At lower speeds, the power developed by the turbine is below that demanded by the compressor and this power deficiency has to be made up by the diesel engine. The engine rpm where balance occurs between the turbine and compressor powers varies with altitude and forward speed, but over the useful cruising range, the power transmitted through the infinitely variable gear is relatively small.

As seen in Figure 74, the shaft power at each engine crankshaft speed increases with altitude until a maximum is reached. The lower power ratings are able to be attained at almost 30,000 feet (9.14 km) before derating sets in. The reason for the power increase with altitude is that the infinitely variable gear set permits the turbomachinery to increase its speed with altitude to maintain the in-cylinder equivalence ratio. The reciprocator power is essentially constant (flat rated - refer to Figure 72) and the turbine power surplus is fed into the crankshaft to increase the overall equivalent shaft output. When the turbomachinery can no longer increase its speed due to thermal and rotational limitations to maintain charge density, the power lapse rate with increasing altitude is approximately 3 percent per thousand feet (0.3 km) takes over. The altitude cruising curves for both equivalent shaft horsepower and SFC are remarkable for their "flatness" across the range of altitude. In fact, due to the increased turbine thermodynamic performance and output, the BSFC decreases until the turbine speed limit is reached. The best fuel economy of

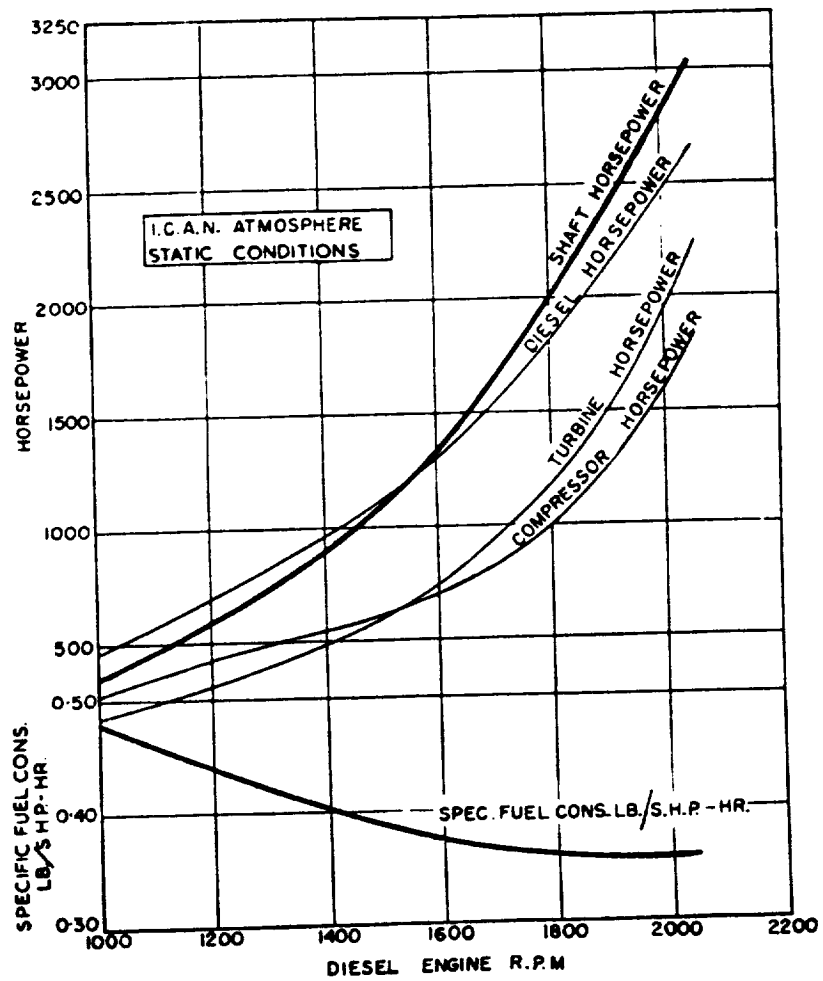


Figure 73. Sea-Level Static Interconnection Power Curve.



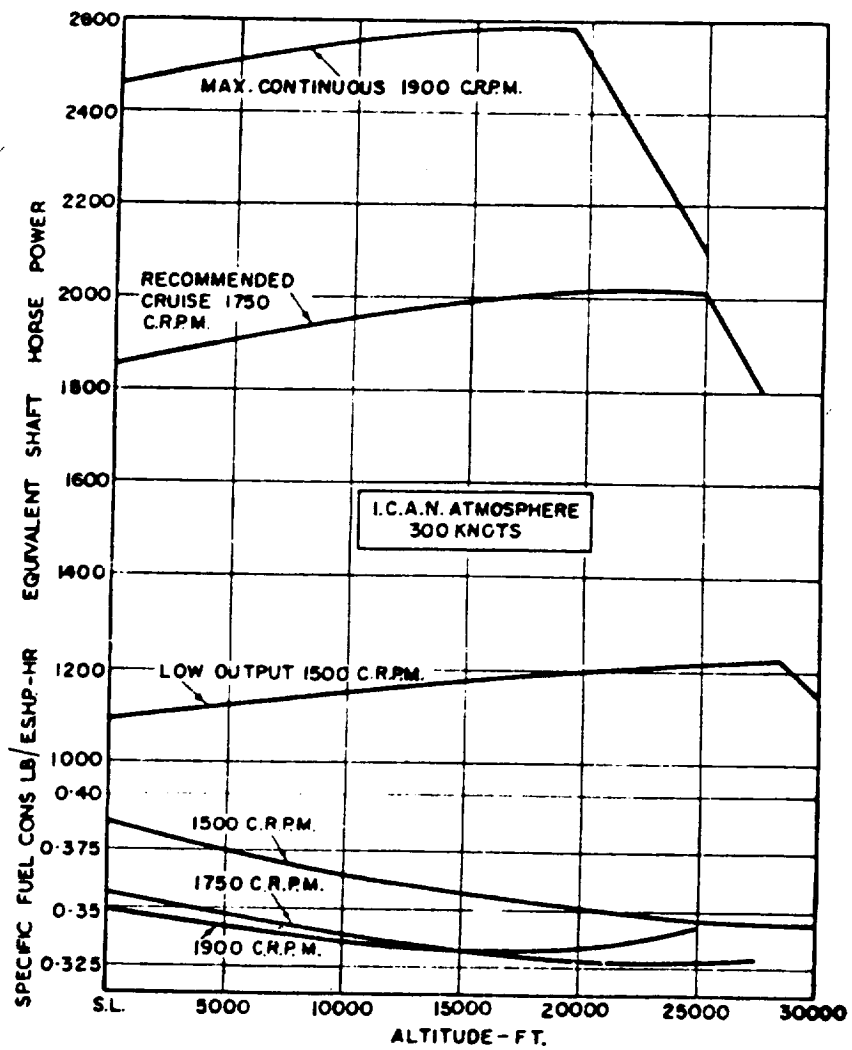
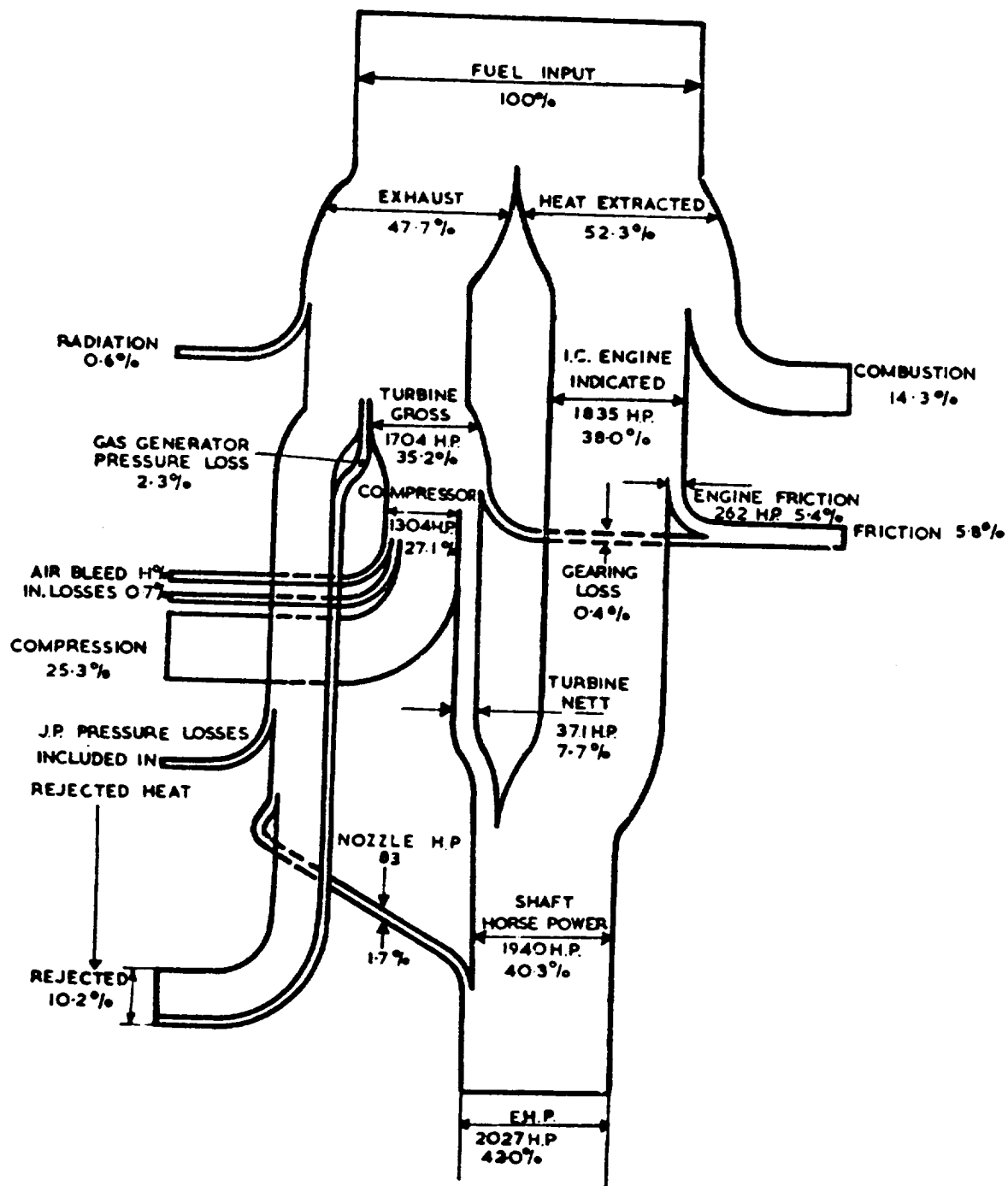


Figure 74. Altitude Cruising Curves with Fuel Consumptions.

0.326 lb per ehp/hr (195 gm ekW/hr) is achieved at the recommended cruising rating at 22,250 ft (6.78 km) where a power of 2027 ehp (1512 kW) is developed. A complete heat balance for this operating point is depicted in Figure 75 and from this it can be seen that a brake thermal efficiency of 42 percent is obtained, which is greater than that of any other engine (Circa 1954).

### Summary

The Napier Nomad Aircraft Diesel Engine was a highly efficient power producer, which came into being at an inopportune time. The combination of 10 to 20 cents per gallon fuel and the advent of large, relatively efficient turboprop engines were sufficient in 1955 to bring about the end of Nomad production. However, since 1973, fuel prices have increased to the \$1 to 2 dollar per gallon figure and the time for of the compound cycle engine for both airborne and ground power applications may have come again.



1750 C.R.P.M. 300 KNOTS. 22,250 FT P.5(A)3

Figure 75. Heat Balance Diagram.

## APPENDIX B

### METRIC CONVERSION FACTORS

| FROM:          | MULTIPLY BY: | TO:             | FROM:              | MULTIPLY BY: | TO:                 |
|----------------|--------------|-----------------|--------------------|--------------|---------------------|
| km             | 0.6214       | mi              | bar                | 100          | kPa                 |
| km             | 3281         | ft              | bar                | 1.01972      | kg/cm <sup>2</sup>  |
| m              | 3.281        | ft              | bar                | 14.50377     | psi                 |
| m              | 39.37        | in              | MPa                | 1000         | kPa                 |
| dm             | 3.937        | in              | MPa                | 10.1972      | kg/cm <sup>2</sup>  |
| mm             | 0.03937      | in              | MPa                | 145.0377     | psi                 |
| m <sup>3</sup> | 35.31        | ft <sup>3</sup> | kPa                | 0.14504      | psi                 |
| m <sup>3</sup> | 61,023       | in <sup>3</sup> | kg/cm <sup>2</sup> | 9.812        | N/cm <sup>2</sup>   |
| m <sup>3</sup> | 264.2        | gallons         | kg/cm <sup>2</sup> | 14.223       | psi                 |
| ℓ              | 0.0353       | ft <sup>3</sup> | N-m                | 0.10197      | kgm                 |
| ℓ              | 61.02        | in <sup>3</sup> | N-m                | 0.73759      | ft-lb               |
| ℓ              | 0.264        | g               | kgm                | 7.2333       | ft-lb               |
| m <sup>2</sup> | 10.76        | ft <sup>2</sup> | m <sup>3</sup> /kW | 26.331       | ft <sup>3</sup> /HP |
| metric ton     | 2.205        | lb              | m <sup>3</sup> /kg | 16.0165      | ft <sup>3</sup> /lb |
| kg             | 2.2046       | lb              | kW/                | 0.02198      | HP/in <sup>3</sup>  |
| MN             | 224,810      | lb              | kg/kW              | 1.644        | lb/HP               |
| kN             | 224.81       | lb              | kg/ℓ               | 0.03613      | lb/in <sup>3</sup>  |
| N              | 0.102        | kg              | kcal               | 3.9683       | BTU                 |
| N              | 0.22481      | lb              | kcal/kg            | 1.8          | BTU/lb              |
| °K             | 1.8          | °R              | kcal/kg-°C         | 1            | BTU/lb-°F           |
| °C             | 1.8°C + 32   | °F              | g/kWh              | 0.00164      | lb/HP-hr            |
| kW             | 1.341        | HP              |                    |              |                     |

## REFERENCES

1. E.A. Willis and W.T. Wintucky, "An Overview of NASA Intermittent Combustion Engine Research," AIAA-84-1393.
2. H. D. Wilsted, "Preliminary Survey of Possible Use of the Compound Adiabatic Diesel Engine For Helicopters," SAE820432.
3. H. Sammons and E. Chatterton, "Napier Nomad Aircraft Diesel Engine," SAE Transaction Vol. 63 1965.
4. J. Lueke and R. Spencer, "Advanced Cruise Missile Propulsion Concepts," AIAA-81-1714.
5. J.G. Castor, et. al., "Compound Cycle Turbofan Engine," AIAA-83-1338.
6. Compound Cycle Turbofan Engine Phase II Final Report "Development of Critical Technologies," AFWAL-TR-81-2142. Garrett Turbine Engine Company.
7. Janes, All the World's Aircraft, The McGraw-Hill Book Co., N.Y. 1945, p. 54d.
8. Walter Serecke, "Development and Operating Behavior of the Fire Ring as a Highly Loaded Piston's Seal Element," MTZ June, 1953 pp. 182-186 and November, 1953 pp. 333-337.
9. C.A. Rosen, "German Diesel Engine Development," SAE Quarterly Transactions 1947, Vol. 1, pp. 144-163.
10. Janes, All the World's Aircraft, The McGraw-Hill Book Co., N.Y. 1945, p. 58d.
11. D. Gerdon and J.M. Wetzler, "Allison V-1710 Compounded Engine," SAE Quarterly Transactions, Vol. 2, April 1948, pp. 329-338.
12. F.J. Wiegard and W.R. Eichberg, "Development of the Turbo-compound Engine," SAE Transaction, Vol. 62, 1954 pp. 265-279.
13. J.H. Pitchford, "The Future of the High-Speed Reciprocating Internal-Combustion Engine," Proc. Instn. Mech. Engrs., Vol. 174, 1960, pp. 1044-1051.
14. H. Sammons and E. Chatterton, "Napier Nomad Aircraft Diesel Engine," SAE Transactions, Vol. 63, 1955 pp. 107-131.

## REFERENCES (Contd)

15. E.E. Chatterton, "Compound Diesel Engines for Aircraft," Royal Aeronautical Society Journal, Vol. 58, No. 525, pp. 613-633.
16. P.H. Schweitzer, Scavenging of 2-Stroke Cycle Diesel Engines, The MacMillan Co., N.Y., 1949.
17. D.A. Richeson, et al., "Application of Air-to-Air Charge Cooling to the 2-Stroke Cycle Diesel Engine," SAE 850317.
18. W.D. Annand and T.H. Ma, "Instantaneous Heat Transfer Rates to the Cylinder Heat Surface of a Small Compression Ignition Engine," Proc. Inst. Mech. Engrs., Vol. 185, 1970/1971.
19. C.F. Taylor, "The Internal Combustion Engine in Theory and Practice," Vol. 1, p. 441.
20. R. Herschkron, et al., "Contingency Power Concepts for Helicopter Turboshaft Engine," American Helicopter Society Symposium, 1984 pp. 597-608.
21. P.H. Schweitzer, et al., "Fumigation Kills Smoke-Improves Diesel Performance," SAE Transactions Vol. 66, 1958, pp. 574-495.
22. N.J. Beck, et al., "Direct Digital Control of Electronic Unit Injectors," SAE 840273.
23. G. Sovran and E. Klomp, "Experimentally Determined Optimum Geometries for Rectilinear Diffusers with Rectangular, Conical or Annular Cross Sections," Research Publication GMR-511, Nov. 16, 1965.
24. N.A. Graham, "Bypass Lube Oil Filtration," SAE 860547.
25. J. Melchior and T. Andre-Talamon, "Hyperbar System of High Supercharging," SAE 740723.
26. H.G. Braendal, "Modern Ring Design for High Output Engines," 10th CIMAC Conference, 1973, Washington, D.C., discussion by Kent Thurston.
27. J.C. Hallinan, "Development of the Caterpillar 3500 Series Engines," ASME 83-DGEP-2.
28. M. Fellberg, J.W. Huber, and J.W. Duerr, "The Development of Detroit Diesel Allison's New Generation Series 53 Engines," SAE 850259.

## REFERENCES (Contd)

29. K. Okamura, et al., "Recent Developments of the Mitsubishi WZ High Speed Engine," 10th CIMAC Conference, 1973, Washington, D.C.
30. L.K. Setright, "Some Unusual Engines," p. 63, SAE-MEP-5, 1979.
31. W.R. Alexander, et al., "Improving Engine Durability via Filters and Lubricants," SAE 852125.
32. N.A. Graham, "Bypass Lube Oil Filtration," SAE 860547.
33. G.E. Thomas and R.M. Cuthbert, "Ingested Dust, Filters, and Diesel Engine Wear," SAE 680536.
34. F.A. Christiansen and P.I. Brown, "Military and Manufacturer Specification Oils - Their Evaluation and Significance," SAE 1962, Paper 573B.
35. J.E. Bush and A.L. London, "Cocktail Shaker Cooled Pistons and Valves," SAE Transactions, Vol. 74 1966 pp. 446-459 Discussion by J.M. Cherrie.
36. W.T. Lyn, "Optimization of Diesel Combustion Research," SAE 780942.
37. Alvon, "Napier Nomad," Flight, 30 April 1954, pp. 543-551.





7. STIMS 1X ACC# 9010397 IPS-FILE ADABAS # = 116856  
 FICHE AVAIL = OK HARD COPY AVL = OK COPYRIGHT = N  
 ORIG AGENCY = NASA RECEIPT TYPE = REG ACQUIS TYPE = REG  
 DOCUMENT CLASS= TRP ACCESS LEVEL = O ACCESS RESTR = UNRES  
 LIMITATION CAT= NONE DOCUMENT SEC = NC TITLE SECURITY= NC  
 SUBJECT CATGRY= O7 SPECIAL HANDL = PAGE COUNT = 00188  
 INC AUTHOR LST= N INC CNTRCT LST= N LANGUAGE = EN  
 COUNTRY ORIGIN= US COUNTRY FINANC= US ABSTRACT PREP = AUT  
 PUB DATE = 19870930 CORP SOURCE = GA706891

TITLE = Compound cycle engine for helicopter application

TITLE SUPP = Final Report  
 AUTHOR = CASTOR, JERE  
 AUTHOR = MARTIN, JOHN  
 AUTHOR = BRADLEY, CURTISS  
 CONTRACT NUM = NAS3-24346  
 CONTRACT NUM = DA PROJ. 1L1-6110-AH-45  
 REPORT NUM = NAS-CR-180824  
 REPORT NUM = NAS 1.26:180824  
 REPORT NUM = GTEC-21-5854-1  
 REPORT NUM = AVSCOM-TR-87-C-30  
 MAJOR TERMS = DIESEL ENGINES  
 MAJOR TERMS = ENGINE DESIGN  
 MAJOR TERMS = FUEL CONSUMPTION  
 MAJOR TERMS = GAS TURBINE ENGINES  
 MAJOR TERMS = HELICOPTERS  
 MAJOR TERMS = MILITARY HELICOPTERS  
 MAJOR TERMS = RANKINE CYCLE  
 MAJOR TERMS = THERMODYNAMICS  
 MAJOR TERMS = TURBOMACHINERY  
 MINOR TERMS = COMPRESSION RATIO  
 MINOR TERMS = FUEL TANKS  
 MINOR TERMS = HIGH SPEED  
 MINOR TERMS = WEIGHT ANALYSIS  
 ABST AUTHOR = Author  
 FORM OF INPUT = HC

ABSTRACT = The compound cycle engine (CCE) is a highly turbo charged, power-compounded, ultra-high-power-density, lightweight diesel engine. The turbomachinery is similar to a moderate-pressure-ratio, free-power-turbine gas turbine engine and the diesel core is high speed and a low compression ratio. This engine is considered a potential candidate for future military helicopter applications. Cycle thermodynamic specific fuel consumption (SFC) and engine weight analyses performed to establish general engine operating parameters and configurations are presented. An extensive performance and weight analysis based on a typical 2-hour helicopter (+30 minute reserve) mission determined final conceptual engine design. With this mission, CCE performance was compared to that of a contemporary gas turbine engine. The CCE had a 31 percent lower-fuel consumption and resulted in a 16 percent reduction in engine plus fuel and fuel tank weight. Design SFC of the CCE is 0.33 lb/hp-hr and installed wet weight is 0.43 lb/hp. The major technology development areas required for the CCE are identified and briefly



discussed.

\*\*\*\*\*

END OF ADABAS RECORD # 116856

\*\*\*\*\*

